



University of Calabria

Faculty of Pharmacy and Nutritional and Health Science
Department of Pharmaco-Biology

Ph.D. program in
“Cellular Biochemistry and Drug Activity in Oncology”
(XXII ciclo)
SSD BIO/10

Mechanisms of RA action in steroidogenic tissues and
pro-apoptotic effects of combined treatment of breast tumoral cell
lines with 9-cis retinoic acid and rosiglitazone

Ph.D. Director

Prof. Diego Sisci

Tutor

Dr. Daniela Bonofiglio

Graduate Student

Dr. Attilio Pingitore

INDEX

• ABSTRACT	1
• INTRODUCTION	2
• RESULTS AND DISCUSSION	12
▪ <i>All-trans retinoic acid binds and inhibits 2-oxoglutarate carrier</i>	12
▪ <i>Adrenal glands, as steroidogenic tissue, are affected by retinoylation reaction</i>	18
▪ <i>The activity of the adenine nucleotide translocator is affected by a component of the retinoylation buffer</i>	24
▪ <i>Combined low doses of PPARγ and RXR ligands trigger an intrinsic apoptotic pathway in human breast cancer cells</i>	33
• METHODS	41
• REFERENCES	47

ABSTRACT

Vitamin A (Retinol) plays a central role in many essential biological processes such as vision, immunity, reproduction, growth, development, control of cellular proliferation and differentiation. The main active forms of retinol, not primary involved in vision, are all-*trans* retinoic acid and 9-*cis* retinoic acid, both able to act at nuclear level by binding their receptors RAR and RXR and modulating many physiological processes. However, the nuclear action of vitamin A derivatives is not the only mechanism of retinoic acid (RA) acting on cells. RA is able to modify covalently proteins via a post-translational modification, named retinoylation that has been shown to occur at physiological concentration on pre-existing proteins and localized mainly in the mitochondrial compartment. The present study has been focused on the non genomic action of RA on steroidogenic tissues, testes and adrenal glands, giving further details on the ability of RA to influence protein activity and therefore cell physiology. In particular RA effects on mitochondria from the adrenal glands and the 2-oxoglutarate carrier protein from testes and TM-3 Leydig cell line were studied, providing new data on the peculiarity of steroidogenic tissues to incorporate RA at dietary levels and demonstrating how the shuttling of reducing equivalent across the mitochondrial membrane is influenced by RA treatment. Looking for the biochemical mechanism of RA action on the Adenine Nucleotide Translocator, that exchanges ATP for ADP between mitochondria and cytosol, for the first time, it was possible to demonstrate how the activity of this carrier protein is positively modulated by the Coenzyme A, a fundamental component of the retinoylating buffer. At pharmacological levels, retinoids are also active compounds in the treatment of cancer due to the capability to promote cell differentiation and their pro-apoptotic activity. In this latter concern, the mechanisms of nutraceutical concentration of 9-*cis* RA, together with nanomolar concentration of the selective PPAR γ ligand, rosiglitazone, to promote apoptosis in breast cancer cell lines, have been investigated. The data lay the basis for a potential use of the combined therapy with low doses of both BRL and 9-*cis* RA as novel therapeutic tool particularly for breast cancer patients who develop resistance to antiestrogen therapy.

INTRODUCTION

The retinol (Vitamin A) belongs to the “retinoids” family including both the compounds possessing one of the biological activities of the retinol (ROH) and the many synthetic analogues related structurally to the retinol, with or without biological activity. Provitamin A is the dietary source of retinol and is supplied as carotenoids (mainly β -carotene) in vegetables and preformed retinyl-esters (long chain fatty acids esters of retinol: palmitate, stearate, oleate, linoleate) in animal meat (Blomhoff 1994). Retinol plays a central role in many essential biological processes such as vision, immunity, reproduction, growth, development, control of cellular proliferation and differentiation. The main active forms of retinol are retinoic acids, except for vision and reproduction where retinal and retinol play important roles. Two vehicles are described for mammalian blood transport of retinoids. First the retinyl esters and carotenoids can be incorporated in intact or remnant chylomicrosomes or very low density lipoproteins (Debier and Larondelle, 2005). Second, the main form of retinol blood transport is the association with a specific binding protein (RBP), which is itself complexed with transthyretin (ratio 1 mol/1 mol). The constitution of this ternary complex prevents the glomerular filtration of the small RBP-retinol form (21KDa) and increases the affinity of RBP for retinol (Bellovino *et al.* 2003). A binding to other plasma proteins, such as albumin or lipocalins, is also described for retinol. Albumin could serve as transport for RA, which circulates in very small levels in the blood. The transfer of retinol to target cells involves a specific membrane-bound receptors (Sivaprasadarao *et al.*, 1998). It has been recently demonstrated that cellular retinol penetration is based on the interaction between the RBP-retinol complex and a membrane receptor STRA6. STRA6 is a multitransmembrane domain protein not homologous to any other proteins with known function. It functions as the high-affinity receptor for plasma retinol binding protein (RBP) and mediates cellular uptake of vitamin A from the vitamin A-RBP complex. It is widely expressed in embryonic development and in adult organ

systems. Consistent with the diverse roles of vitamin A and the wide tissue expression pattern of STRA6, mutations in STRA6 are associated with severe pathological phenotypes in humans (Kawaguchi *et al.*, 2007). The uptake of remnant chylomicrons and very low density lipoproteins containing retinyl esters and carotenoids is realized by target tissues using, respectively, the lipoprotein lipase and low density lipoproteins receptor pathways. Bound to albumin, RA can be transferred into the tissues by passive diffusion, with an efficiency of transfer, which is cell type and tissue specific. To be biologically active retinol must be first oxidized to retinaldehyde and then to RA. A large number of enzymes catalyzes the reversible oxidation of retinol to retinaldehyde: the alcohol dehydrogenases (ADH), the retinol dehydrogenases (RDH 1-3) of the microsomal fraction, *cis*-retinol:androgen dehydrogenase 1 and 2 (CRAD), retSDRs1–4, 9:11-*cis*-retinol dehydrogenase, and 17 β -hydroxysteroid dehydrogenase (17 β -HSD) types 6 and 9, and some members of the cytochrome P450 family (Napoli, 2001). Several enzymes are able to catalyze irreversibly the oxidation of retinaldehyde to RA: the retinaldehyde dehydrogenases (RALDH 1-4) are also member of the cytochrome P450 family (Liden and Eriksson, 2006). Specific isomerization reactions are also likely to occur within the cells, since there are at least two RA stereoisomers *in vivo* (*all-trans* and 9-*cis* RA) exhibiting distinct biochemical activities. The catabolism of *all-trans* and 9-*cis* RA is also an important mechanism for controlling RA levels in cells and tissues and is carried out by three specific members of cytochrome P450s, CYP26A1, B1, and C1. RA is catabolized to products such as 4-oxo-RA, 4-hydroxy-RA, 18-hydroxy-RA, and 5,18-epoxy-RA, which are finally excreted. These compounds can also undergo glucuronidation (Marill *et al.* 2003). The complex of microsomal UDP-glucuronosyl transferases (UGT; EC 2.4.1.17) of rat liver catalyzes the formation of retinoyl beta-glucuronide (RAG) from retinoic acid (RA) and retinyl beta-glucuronide (ROG) from retinol (ROL) in the presence of UDP-glucuronic acid (UDPGA). Rates of glucuronidation of retinoids clearly depend both on their isomeric states and on their chemical structures. Different UGT enzymes might well act on different geometric

isomers of RA (Genchi *et al.* 1996). Numerous reports have indicated that the biological activity of all-*trans* retinoyl-glucuronide (RAG) is similar to that of all-*trans*-retinoic acid (RA), but without the toxic side effects of RA. An alternative metabolic pathway was present for intracellular retinol: the formation and storage of retinyl esters. Indeed retinol may be esterified by two enzymes: the first is lecithin:retinol acyltransferase (LRAT), which catalyzes the transfer of a fatty acid from the snK1 position of phosphatidylcholine (PC) to retinol. The products of this reaction are 1-lyso-phosphatidylcholine (lyso-PC) and a retinyl ester, usually retinyl palmitate. The mRNA for LRAT has been cloned and shown to encode an integral-membrane protein of 230 residues. LRAT is present in multiple tissues including liver, small intestine, testis, mammary gland, and retinal pigment epithelium. Although LRAT preferentially esterifies all-*trans*-retinol (atROL) to yield all-*trans*-retinyl esters (atREs), it also utilizes 11-*cis*-retinol (11cROL) as a substrate to form 11-*cis*-retinyl esters (11cREs). The second retinyl-ester synthase is acyl CoA:retinol acyltransferase (ARAT), which uses a fatty-acyl coenzyme A, such as palmitoyl coenzyme A (palm CoA), as an acyl donor. ARAT has not been purified or cloned. Palm CoA-dependent retinyl-ester synthase activity has been observed in multiple tissues including liver, small intestine, mammary gland, epidermis, testis, and cone-dominant retinas. Palm CoA-dependent synthesis of retinyl esters has also been observed in retinal pigment epithelium. However, it has been suggested that in this tissue, the palm CoA stimulation effect is due to regeneration of PC from lyso-PC, and is thus mediated by LRAT. (Catherine *et al.*, 2006 and references therein). These esters are then stored in cytosolic lipid droplets. The mobilization of these retinyl esters and the release of retinol esters are realized by a retinyl ester hydrolase. Since retinol, retinaldehyde and RA are lipids they lack appreciable water solubility and consequently must be bound to protein within cells. Several intra-cellular binding proteins for retinol, retinaldehyde and RA have been identified and extensively characterized. They include cellular retinol-binding proteins (CRBP I and II) and cellular retinoic acid-binding protein (CRABP I and II). The CRBPI is a key protein

to regulate the metabolism of retinol by orientating to storage, export of retinol or conversion into RA (Ghyselinck *et al.*, 1999). Both the CRABPs bind RA controlling the intracellular levels of retinoids, acting as cofactors for RA-metabolizing enzymes, and/or participating in the cytoplasmic-nuclear transport of RA (Napoli, 1999; Ong, 1994). The 15.5 kDa protein, cellular RA binding protein has been shown to specifically bind RA with nanomolar affinities. There are several reports that suggest CRABP may protect the cell from the genomic action of RA by sequestering the compound and accelerating its catabolism. RA bound to CRABP has been demonstrated to be a substrate for oxidation by members of the P450 family. A potential key to attenuation of the RA signal may be found in the specific location of CRABP within the cell. Immunohistochemical experiments performed on tissue sections has revealed that this protein is restricted to the cytoplasmic compartment of cells, even though its size should enable free entry into the nucleus (In contrast, CRBP, a related protein of the same family, was shown to be present in both the cytoplasm and the nucleus, as expected for a protein of this size). This nuclear restriction might create a barrier that prevents RA from reaching the RARs in the nucleus. However, the mechanism(s) by which this restriction is accomplished has not been established. Moreover, Ruff and Ong demonstrated that CRABP is localized to the mitochondria of bovine adrenal gland. This association with the mitochondria effectively restricts it to the cytosolic compartment of the cell and suggests a role for mitochondria in retinoid metabolism (Ruff and Ong, 2000, and references therein). Although RA functions mainly by binding to nuclear receptor proteins, this is not the only mechanism of retinoids action on cells. Retinoic acid, is capable to modify covalently pre-existing proteins via a post-translational modification (PTM) termed retinoylation (acylation by RA of protein). Single PTMs are capable of regulating protein function, either through creating new protein binding sites, by abrogating protein-protein interactions, or through allosteric effects. However, many proteins are multiply modified, and a significant increase in information content would be obtained if PTMs acted combinatorially. There are several established principles

through which PTMs mediate crosstalk. In this context, crosstalk can be either positive or negative in nature. Positive crosstalk is defined as a situation in which one PTM serves as a signal for the addition or removal of a second PTM or for recognition by a binding protein that carries out a second modification. In the case of negative crosstalk, there can be direct competition for modification of a single residue in a protein, or indirect effects, wherein one modification masks the recognition site for a second PTM. Histone tails provide one of the most remarkable examples of PTM density and variety, with Lys acetylation, mono-, di-, or trimethylation, biotinylation, ubiquitylation, NEDDylation, SUMOylation; Arg methylation; Ser/Thr/Tyr phosphorylation; and Glu ADP ribosylation all occurring within 50–100 residues on the N-terminal and C-terminal tails of H2A, H2B, H3, and H4 (Bhaumik et al., 2007; Latham and Dent, 2007). These “marks” are proposed to represent a code that is read by a series of transcriptional regulators and chromatin modifiers that affect local chromatin structure, leading to activation or repression of adjacent transcription units. Although there is little direct information regarding which PTMs occur simultaneously on a single histone molecule, functional analysis of histone tail PTMs has revealed many examples of crosstalk between different PTMs. Nuclear coreceptors are another family of proteins in which PTM crosstalk is beginning to be uncovered (Lonard and O’Malley, 2007). About RA Acylation, via retinoylation RA is incorporated into proteins of cells in culture (Breitman and Takahashi, 1996; Takahashi and Breitman, 1989, 1990, 1994; Tournier *et al.*, 1996) and into proteins of rat tissues, both in vivo (Myhre *et al.*, 1996) and in vitro (Genchi and Olson, 2001; Myhre *et al.*, 1998; Renstrom and DeLuca, 1989). The retinoylation reaction involves the intermediate formation of retinoyl-CoA (Wada *et al.*, 2001) and subsequent transfer and covalent binding of the retinoyl moiety to protein(s) (Renstrom and DeLuca, 1989). The covalent linkage between RA and protein(s) is a thioester bond (Genchi and Olson, 2001; Myhre *et al.*, 1996). Retinoylated proteins that have been identified so far include cyclic AMP-binding proteins, vimentin, the cytokeratins, some nuclear proteins and a component of the mitochondrial carrier family (Breitman

and Takahashi, 1996; Takahashi and Breitman, 1989, 1990, 1994; Tournier *et al.*, 1996, Cione *et al.* 2009). Several types of lipid modifications have received considerable attention over the last few years. It has been demonstrated that palmitic, myristic, acetic and phosphoric acids, as well as isoprenes farnesol and geranylgeranol, bind to a number of proteins (Schultz *et al.*, 1988; Towler *et al.*, 1988). Retinoylation is one of these covalent modification reactions occurring on proteins. Biochemical similarities exist between retinoylation and acylation (i.e., palmitoylation and myristoylation). In these processes, RA, MA, and PA covalently bind to preformed protein via a thioester bond after the intermediate formation of acyl-CoA and retinoyl-CoA (Renstrom and DeLuca, 1989; Wada *et al.*, 2001). Such covalent modification reactions regulate the interactions of the proteins with cellular membranes, as well as the interactions with other proteins. Physiologically, retinoids, bound to proteins or lipoproteins in the extracellular fluids, are taken up by cell surface receptors, are transferred into the cytoplasm and subsequently bound to intracellular proteins (Blomhoff *et al.*, 1991). Therefore, retinoids do not normally equilibrate in phospholipids of cellular membranes. Retinoylation appear to be tissue specific: steroidogenic tissues (adrenal glands and testes) resulted to be the most active tissues in incorporating RA with significant differences in the necessity of ATP among the two tissues (Cione and Genchi, 2004; Pingitore *et al.* 2009). In general it is known that RA is essential for the normal growth of testes (Chaudhary *et al.*, 1989). The steroid biosynthesis is very active into testes mitochondria and moreover is stimulated also by RA (Tucci *et al.*, 2008); therefore this so active testes mitochondrial process of retinoylation should be bound to steroidogenesis. The retinoylation reaction of rat testes mitochondrial proteins occurred in the presence of ATP, CoASH, and Mg^{++} . Either the omission of ATP and/or CoASH in the incubation buffer or the omission of Mg^{++} , or its substitution with Ca^{++} reduced the radioactivity bound to the mitochondrial proteins in considerable manner. Moreover the retinoylation reaction exhibited substrate specificity. In fact the reaction occurred only in the presence of ATP, ADP (50% of

the control), and GTP (30% of the control). In testes derived cell lines, RA was able to bind pre-existing protein and RA supplementation was able to stimulate testosterone biosynthesis in these cells in the same doses where the retinoylation reaction was found to be enhanced suggesting a putative role in testicular steroidogenesis. RA in mouse testes is present constitutively at a concentration of 7–14 pmol/g or approximately 7–14 nM (Deltour et al. 1997; Kane et al. 2005). At nuclear level it is well known that RA functions by binding to ligand-inducible transcription factors (nuclear receptor proteins belonging to the steroid/thyroid hormone receptor superfamily) that activate or repress the transcription of downstream target genes (Chambon, 1996; Soprano and Soprano, 2003). Six nuclear receptors, termed RAR α , RAR β , RAR γ , RXR α , RXR β and RXR γ , encoded by different genes, have been demonstrated to mediate the actions of RA. The natural metabolite all-*trans* RA (atRA) and 9-*cis* RA are high affinity ligands for RARs, whereas 9-*cis* RA, phytanic acid, docosahexanoic acid, and unsaturated fatty acids, have been suggested to bind RXRs. These proteins, as heterodimers (RAR/RXR) or homodimers (RXR/RXR), function to regulate transcription by binding to DNA sequences located within the promoter of target genes called retinoic acid response elements (RARE) or retinoid X response elements (RXRE), respectively. RAREs consist of direct repeats of the consensus half-site sequence AGGTCA separated most commonly by five nucleotides (DR-5) while RXREs are typically direct repeats of AGGTCA with one nucleotide spacing (DR-1). The RAR/RXR heterodimer binds to the RARE with RXR occupying the 5' upstream half-site and RAR occupying the 3' downstream half-site. atRA and 13-*cis* RA bind to and transactivate only RXR/RAR complexes, while 9-*cis* RA interacts with both RXR/RAR heterodimers and RXR/RXR homodimers. RXR/RAR dimers are believed to be nonpermissive complexes, in which RXRs act as silent partner. In other words, when the cognate ligand is bound to the RAR moiety, the RXR counterparts loses the ability to bind its corresponding ligand (Mangelsdorf and Evans, 1995; Mangelsdorf *et al.* 1993). In basal conditions, the RXR/RAR heterodimer is bound to the cognate DNA sequence

(RARE) and interacts with a multiprotein complex known as the corepressor (Wei, 2004; Weston *et al.* 2003). The corepressor (RIP140 receptor interacting protein 140) contains protein endowed with the histone deacetylase (HDAC) and DNA-methylating activity that concur to keep the surrounding chromatin structure in a “closed” state, effectively suppressing the transcriptional activity of RNA polymerase II. On ligand binding the corepressor is released from the RXR/RAR dimer and substituted by the “coactivator”, which consists of a multiprotein complex with histone acetylase and demethylase activity (Westin *et al.* , 2000; Xu *et al.*, 1999a) opening the chromatin structure and favouring transcription. The activity of the RXR/RAR dimer is also controlled by a number of accessory signals in which phosphorylation events stand out (Gianni *et al.* 2002, 2006) A further layer of control is represented by the rate of proteolytic degradation of the RXR/RAR dimer and the various components of the corepressor and coactivator complexes (Gianni *et al.* 2006). Little is known about the RXR/RXR pathway which is far less studied than the RXR/RAR counterpart. Retinoids are promising agents in the chemoprevention and treatment of the neoplastic disease. Fenretinide, a synthetic retinoid, has shown efficacy in the secondary chemoprevention of breast cancer (Veronesi *et al.* 1999). Indeed, this class of agents finds clinical application or is proposed also in the treatment of various neoplastic diseases, among which, acute promyelocytic leukemia (APL) is the most prominent example. The observation that atRA induces remission in APL through a mechanism of action that is distinct from cytotoxicity, is regarded as a milestone in the history of medicine (Huang *et al.* 1988). The retinoid is the first and only example of clinically successful cytodifferentiating agent. Cytodifferentiation is a particularly attractive modality of treatment and differentiating agents promise to be less toxic and more specific than conventional chemotherapy. Currently, the promise of differentiation therapy is only partially met and a more general use of atRA and other retinoids as differentiating agents in oncology is hampered by a number of problems including natural and acquired resistance as well as local and systemic toxicity. Therefore, retinoids are

often used as part of a combined therapy. *atRA* and derivatives modulate the activity of numerous genes and intracellular pathways. On the other hand, the activity of nuclear RARs is controlled by various signals, including different types of kinase cascades. Often the cross talk between *atRA*-dependent and other intracellular pathways modulates the cytodifferentiating activity of the retinoid. The knowledge on the molecular mechanism underlying this cross talk has increased tremendously over the course of the last few years. In cell cultures, the cytodifferentiating activity of retinoids is almost invariably accompanied by growth inhibition and the two processes are difficult to dissociate (Gianni *et al.* 2000). On the other hand, retinoid-dependent cytodifferentiation is not necessarily associated with cell death or apoptosis. Indeed, classical retinoids are relatively weak apoptotic agents and, in some cases, they even exert a pro-survival action (Lomo *et al.* 1998). These aspects of retinoids pharmacology need to be considered when discussing the use of such agents in oncology. An antiproliferative effect superimposed to cytodifferentiation is highly desirable, whereas an antiapoptotic action should be avoided. A generalized use of retinoids in oncology is hampered by a number of unresolved problems including natural and induced resistance as well as toxicity issues are of particular evidence, given the fact that differentiation therapy with retinoids requires prolonged administration of the agents. Chronic exposure to retinoids is accompanied by serious effects at the level of central nervous and hepatic systems, as well as the well-known teratogenic problems associated with the administration of these compounds. Clearly these problems call for strategies aimed at increasing the efficacy and the therapeutic index of retinoids developing novel, more powerful and less toxic synthetic retinoids and identifying non-retinoid agents capable of potentiating the pharmacological activity of retinoids without affecting their toxicity. This second approach is based on the experimental evidence that the nuclear receptor pathway interacts with numerous other intracellular pathways, some of which are of obvious significance from a therapeutic point of view. Retinoids have been proposed in the adjuvant treatment of breast carcinoma for their ability to inhibit growth and

induce morphological or phenotypic deifferentiation of breast carcinoma cell lines (Paik *et al.* 2003; Yang *et al.*, 2002) and most of the studies have focused on the antiproliferative activity of retinoids (del Rincon *et al.* 2003). It is generally accepted that breast cancer cells express RAR α , RAR γ and RXR α but also Peroxisome Proliferator-Activated Receptor gamma (PPAR γ) that can regulate cell proliferation, differentiation and survival (Lemberger *et. Al.*, 1996; Lefebvre *et al.* 2006). PPAR γ functions as a transcription factor by heterodimerizing with RXR, after which this complex binds to specific DNA sequence elements called Peroxisome Proliferator Response Elements (PPREs). PPREs are direct repeats of the consensus sequesnce with a spacing of one nucleotide (AGGTCA-N-AGGTCA) (Palmer *et al.* 1995). The heterodimer PPAR/RXR activated with their ligands, can bind to PPREs in promoter regions of target genes recruiting coactivator or corepressor to this complex to modulate gene expression (DiRenzo *et al.* 1997; McJerney *et al.* 1998; Yuan *et al.* 1998). Previous data show that PPAR γ , poorly expressed in normal breast epithelial cells (Elstenr *et al.*, 1998), is present at higher levels in breast cancer cells (Tontonoz, P., *et al.* 1994) and its synthetic ligands, such as thiazolidinediones (TZDs), induce growth arrest and differentiation in breast carcinoma cells *in vitro* and in animal models (Mueller *et al.*, 1998; Suh *et al.*, 1999).

RESULTS AND DISCUSSION

All-trans retinoic acid binds and inhibits 2-oxoglutarate carrier

Previously it was demonstrated that mitochondria from rat testes (Genchi and Olson, 2001; Cione and Genchi, 2004) and TM-3 cells (Cione *et al.*, 2005) were extremely active in incorporating retinoic acid. Moreover, it was highlighted how the retinoylation reaction and testosterone biosynthesis are positively correlated when Leydig cell cultures are incubated with atRA at 100 nM (Tucci *et al.*, 2008). As the biosynthetic steps that lead to testosterone production are mainly NADH/NADPH dependent, the 2-Oxoglutarate carrier (OGC) activity from mitochondria extracted both from whole rat testes and Leydig TM-3 cells, was chosen as the experimental target for its involvement in the malate-and aspartate oxoglutarate–isocitrate shuttle to provide for the necessary exchange of reducing equivalents between the mitochondria and the cytosol. The efforts were focused on the OGC from rat testes as the retinoylation process is more efficient in this tissue and testosterone production in TM-3 positively correlates to atRA supplementation. In addition, the strong inhibitory effect of 2-cyano-4-hydroxycinnamate (an inhibitor of OGC) but not 1,2,3-benzotricarboxylate (an inhibitor of citrate carrier) on the retinoylation processes (as highlighted in **Table 1**) was the start point for further investigation in this work. 2-cyano-4-hydroxycinnamate shows 45% inhibition when used at a concentration of 5 Mm, whilst, at the same concentration 1,2,3-benzotricarboxylate has a very weak effect (12% inhibition). In proteoliposomes OGC has been shown to exist as a homodimer and to function according to a sequential antiport mechanism, catalyzing the transport of 2-oxoglutarate in electroneutral exchange for some other dicarboxylates to which malate is bound with the highest affinity. These results have been interpreted by assuming two separate and coordinated substrate translocation pathways, one in each monomer.

Carrier Inhibitors on Retinoylation Reaction	pmol/mg ptn x 90 minutes	SEM	n	% Inhibition
Control	21,47	2,44	23	
Mersaly1 1 mM	1,84	0,09	5	91,43
NEM 5 mM	2,47	0,28	5	88,49
2-Cyano-4-hydroxycinnamate 5mM	11,90	1,23	3	44,58
1,2,3-Benzenetricarboxylate 5mM	18,93	1,99	3	11,83

Table 1. Effect of Mitochondrial Carrier Inhibitors on Retinoylation Reaction.

Mitochondria from testes were incubated 90 minutes in a buffer as described in Materials and Methods with $^3\text{HatRA}$, 100 nM final concentration, at 37 °C. Then the reaction was stopped with TCA and the radioactivity detected in a liquid scintillation counter. Results are presented as Mean \pm SEM of three independent experiments. **P < 0.01 compared to the control. 1,2,3-Benzenetricarboxylate P > 0.05

Our results showed that transport activity of OGC from rat testes mitochondria was strongly influenced by the sulphhydryl group reagent N-ethyl-maleimide (NEM) and atRA. NEM, at 5 mM, markedly reduced the OGC activity by 47%. A similar inhibition of 51% was highlighted for 100 nM atRA, and when the two compounds are co-incubated the activity was reduced to 49%, equal to RA alone as shown in **Fig. 1A**. In humans, cows and rats there is only one gene encoding OGC: according to the amino acid sequence the bovine OGC protein contains three cysteines: Cys184 located in TMS IV and Cys221 and Cys224 in TMS V. Mercurials and maleimides interact only with Cys184 of the purified and reconstituted OGC, as Cys221 and Cys224 are linked by a disulphide bridge (Palmieri, 2004). Therefore we propose that atRA, via retinoylation reaction, could bind the OGC on the same residue (Cys184), as the inhibitory effect of atRA is still the same when NEM is present concomitantly as shown in Fig. 1A, leading us to hypothesize the existence of a putative amino acid sequence related to the atRA binding site in OGC. For what concerns OGC and its involvement in testosterone biosynthesis, the first enzymatic step is to convert cholesterol in pregnenolone: the reaction occurs in the mitochondrial matrix and

requires reducing equivalents mainly as NADPH; conversely the role of the OGC is to carry out reducing equivalents from the mitochondria to the cytoplasm. Previously it was demonstrated that there is a positive correlation between retinoylation reaction and testosterone biosynthesis (Tucci *et al.*, 2008): the action of RA to slow down the OGC transport activity is in agreement with the testosterone synthetic process as reducing equivalents are more necessary to convert cholesterol in the matrix rather than in the cytoplasm (Stocco, 2001). At the same time the retinoylation reaction is tightly dependent on the pH: in fact the inhibitory effect of atRA on OGC is lost when the pH is higher than 7.5 (**Fig. 1B**) as predicted by the general condition of retinoylation described by Cione and Genchi (2004). To gain insight into the interaction of atRA and OGC two separate assays could have been performed: the first through photolabeled testes mitochondrial protein with $^3\text{HatRA}$, because atRA binds covalently to proteins under UV light exposure (Bernstein *et al.*, 2005), and the second via retinoylation reaction with $^3\text{HatRA}$ (Takahashi and Breitman, 1990). Performing the latter we observed how the $^3\text{HatRA}$ binding to a 31.5 KDa protein was prevented by 2-oxoglutarate, the specific OGC substrate (**Fig. 1C**). Fluorography of the electrophoresed proteins revealed the labeling of very few mitochondrial proteins. Indeed it was observed that the labeling of the 31.5-kDa protein was prevented when 2-oxo-glutarate, the specific OGC substrate, was added demonstrating that OGC was labeled by $^3\text{HatRA}$. It is presumed that the binding is covalent on the basis of the work of Takahashi and Breitman (1989). Under normal conditions, atRA is present in the testes at nanomolar concentrations (Kane *et al.*, 2008). Our results show that, only in mitochondria derived from the Leydig TM-3 cell line, does atRA have effects on OGC at concentration of 10 nM and in a stronger manner inhibit the OGC activity at a concentration of 100 nM: OGC activity decreased to 54% of control values with 10 nM atRA and 38% of control values when atRA was used at a concentration of 100 nM (**Fig. 1D**). Interestingly, the concentrations of atRA required for producing this effect in steroidogenic cells are lower than those required with mitochondria isolated from the whole organ,

supporting the above-mentioned view that steroidogenic cells can be more sensitive to atRA than isolated mitochondria as no effect was highlighted at 10 nM of atRA on OGC extracted from whole tissue (**Fig. 1E**). In addition 13-*cis* RA has been shown as a competitive inhibitor of atRA in the retinoylation process ($K_i = 13.50$ nM) (Cione and Genchi, 2004). In this case 13-*cis* RA exerts its effects of reducing OGC transport activity on mitochondria from whole tissue at a lower concentration than atRA (**Fig. 1F**): 10 nM 13-*cis* RA was more active in inhibiting OGC activity than atRA, most likely thanks to the altered conformation of this isomer that may allow it to better interact with OGC both in mitochondria from cultured cells or whole tissue (**Fig. 1G**). Our study, along with others (Notario *et al.*, 2001; Rial *et al.*, 1999; Radomska-Pandya *et al.*, 2000), suggests that specific interactions among retinoids and non-nuclear receptor proteins, such as PKC, ANT and OGC, which are different from nuclear receptors, take place. Thus, the extra-nuclear action of retinoids seems to be a more general and important phenomena leading to both physiological and also pharmacological relevance.

It is known that retinoids play an essential role in spermatogenesis in rodents. In fact, a vitamin A-deficient diet causes the cessation of spermatogenesis, loss of mature germ cells and a reduction in testosterone level in mice and rat testes (Wolbach and Howe, 1925; Appling and Chytil, 1981). There is argument in favour of biological action of atRA through OGC binding and inhibition. AtRA does not exist in the cell in free form but is bound to proteins such as cellular retinoic acid binding protein (CRABP). The unexpected discovery of the existence of a CRABP associated with mitochondria that binds and keeps retinoic acid in the organelle has been described (Ruff and Ong, 2000). CRABP had been studied for 25 years and has always been presented as a soluble, presumably cytosolic, protein and mitochondria had not previously been considered to have any role in RA function or metabolism. The only demonstrated function for CRABP is to bind RA. Since this protein is associated with mitochondria, this implies that mitochondria participate in RA management. This mitochondrial CRABP could explain how retinoic acids could concentrate and

regulate OGC in the mitochondrial compartment in vivo. The influence of atRA on OGC via retinoylation might therefore be another level of control in steroidogenesis.

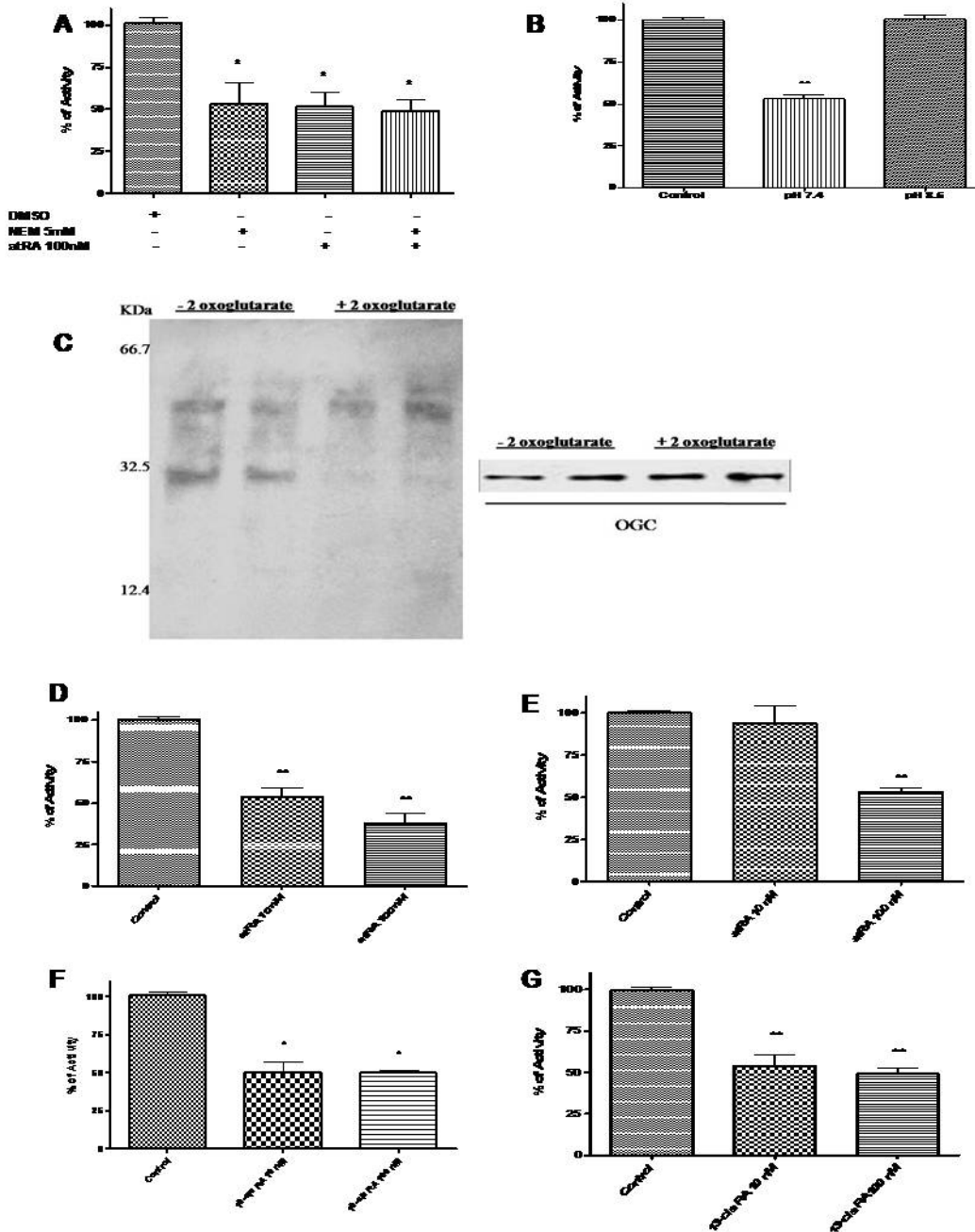


Figure 1. Mitochondria from testes were incubated for 90 minutes, at 37 °C, in buffer with: (A) ATP, CoA (control) supplemented with atRA, 100 nM final concentration and atRA + NEM 5mM and (B) ATP, CoA and atRA 100nM at different pH values. (C) Testes mitochondrial protein labeled with ³HatRA by retinoylation process as described in Materials and Methods. In fluorography, the lanes 1 and 2 correspond to 20 µg of mitochondrial testes protein labeled with ³HatRA. In lanes 3 and 4 10 mM of α -ketoglutarate was added to 20 µg of mitochondrial testes protein together with ³HatRA. OGC presence was verified by immunoblotting. (D) OGC activity from TM-3 cell line after atRA supplementation (E) Effect on OGC activity of different concentrations of atRA in mitochondria from testes incubated at 37 °C for 90 min. Effect of on OGC after treatment of mitochondria from TM-3 (F) and testes (G) with 13-*cis* RA. OGC was extracted as described in Materials and Methods. After extraction and reconstitution into liposomes the exchange activity was assayed by adding ¹⁴C 2-oxo-glutarate 0.1 mM. Results are presented as Mean \pm SEM of three independent experiments. * P< 0.05 . **P<0.01

Adrenal glands, as steroidogenic tissue, are affected by retinoylation reaction

Adrenal glands and gonads synthesize and secrete steroid hormones in response to pituitary hormones such as corticotrophin (ACTH) or luteotropin (LH) (Waterman, 1994; Saez, 1994). The binding of these peptide hormones to their cognate receptors is coupled to the formation of cAMP and activation of the protein kinase A signaling pathway (Richards and Hedin, 1988; Waterman and Bischof, 1997). In particular, adrenal glands are *vital* to health and have an important role in development and reproduction (Harvey and Everett, 2003). The adrenal glands serve a number of important purposes. They help to regulate glucose levels through cortisol, also known for their natural anti-inflammatory activity, and supply the organisms with sex hormones. Among them the dehydroepiandrosterone (DHEA) can be converted into sex hormones, including estrone and testosterone. In this latter concern, it is known that retinoids are important in maintaining testes function and testosterone production is found to be positively correlated to retinoylation in Leydig cells (Tucci *et al.*, 2007). Therefore we aimed to examine the retinoylation process (as post-translational modification) on adrenal glands mitochondria to better understand whether the physiological role of retinoylation process is steroidogenic tissues dependent as the adrenal glands are the second main steroidogenic tissue in males. In the mitochondrial compartment of adrenal glands, after 90 minutes at 37°C, the value of ³HRA incorporated reached that one of testes (Cione and Genchi, 2004), in the standard assay, with no need of ATP supplementation in the incubation buffer (**Fig. 2A**). In addition, the concentration of CoA required for the retinoylation process in adrenal glands mitochondria in the absence of ATP, was lower than testes, as shown in (**Fig. 2B-C**). The retinoylation extent (about 20 pmol/mg protein, 90 min) for adrenal glands mitochondria is time dependent: the incorporation rate was essentially linear for 20 minutes but then fell off at 30 to 90 minutes, decreasing at 150. In adrenal glands, the process reaches the maximum value found for testes mitochondria (Cione and Genchi, 2004) after the same incubation time (90 minutes), without any need of ATP supplementation in the incubation buffer (**Fig. 2D**). As happened for

testes, among the cellular sub-fractions mitochondria were 2.5-fold more active than adrenal glands homogenate (**Table 2**), providing a further evidence of a mitochondrial localization of the retinoylation system in steroidogenic tissues. Indeed, all fractions other than the mitochondria showed relative activities lower than that of the homogenate. In addition endogenous ATP quantification in both mitochondrial preparations showed a very significant difference between testes and adrenal glands: the great difference in the endogenous ATP levels between the two organs, 13×10^{-3} M for adrenal glands and 52×10^{-9} M for testes, is the explanation because no extra ATP is required for the retinoylation reaction to occur (**Table 3**). In our case, the Arrhenius plot of the retinoylation process showed that changes exist in the functioning of the transferring of the retinoyl moiety to the protein(s) between adrenal glands and testes: the adrenal glands activation energy was found equal to 19.36 KJ/mol in contrast with the 43.5 KJ/mol value determined for testes (Cione and Genchi, 2004). Most likely our retinoylated protein(s), such as the enzymatic complex that allows the transfer of the retinoyl moiety, is (are) embedded within the inner membrane and/or is localized on both side of the membrane because the retinoylation does not require external ATP supplementation to occur. A further evidence of it comes from Genchi and Olson (2001) as mitoplasts from testes are still labelled with 3HRA. Several proteins in Leydig cells are regulated by a cAMP-dependent pathway and are involved in steroidogenesis; first of all, cytochrome P450_{scc} (side chain cleavage) (Mellon and Vaisse, 1989) that catalyzes the conversion of cholesterol to pregnenolone. In our experimental procedures the aminoglutethimide (3-(4-aminophenyl)-3-ethyl-piperidine-2,6-dione), a specific inhibitor of cytochrome P450_{scc}, has no effect on the retinoylation process in both testes and adrenal glands mitochondria giving us the proof that this enzyme is not involved in the retinoylation process as shown in **Fig. 2E**. The membrane lipid composition, the degree of unsaturation and the length of the fatty acid chains play important roles in determining the influence of membranes lipids with respect to the specific enzyme activities in the mitochondria. Analyzing the composition of the

mitochondrial membranes of the two organs important differences in fatty acid composition were detected. Significant changes were measured in the ratio of total saturated/unsaturated fatty acids between the two tissues as shown in **Table 4** and **Fig. 2 (F-M)**. A lower percentage of myristic acid (14:0) (**Fig. 2F**) 10-fold less in testes as well as stearic acid (18:0) about 7-fold less were found in the testes mitochondrial membranes than adrenal gland as shown in **Fig. 2G**. In addition, about 3-fold higher amount of palmitic acid (16:0) was found only in testes mitochondria (**Fig. 2H**). **Fig. 2 (I-M)** shows the differences of unsaturated fatty acid composition. A much lower percentage of docosapentaenoic acid (DPA, C22:5 ω 6) about 60-fold less and a lower percentage of docosahexaenoic acid (DHA, C22:6 ω 3) about 10-fold less were found in the adrenal glands membranes of mitochondria compared to testes as shown in **Fig. 2L**. In addition, about 30% higher amount of arachidonic acid (ARA, C20:4 ω 6) was found in adrenal gland mitochondria (**Fig. 2M**). Due to the important physiological functions of arachidonic acid that serve to maintain membrane content and can permit the activity of enzymes of the respiratory chain (Vázquez-Memije *et al.*, 2005) the same statement could not be valid the retinoylation process as the differences could contribute to the enhanced incorporation of RA. Therefore, about 2-fold changes in the ratio of total saturated/unsaturated fatty acids between the two tissues lead us to suppose a relationship through fatty acids and retinoylation process (**Table 4**). In conclusion RA action by retinoylation process on protein(s) of rat adrenal glands and testes mitochondria is steroidogenic tissue dependent; cytochrome P450_{scc} is not affected by the process and probably docosapentaenoic acid (DPA, C22:5 ω 6) should play a fundamental role to allow the transfer of the retinoyl moiety. However, since adrenal glands are arguably the neglected organ in endocrine toxicology (Harvey *et al.*, 2007), it can't be excluded that perhaps the retinoylation process is toxic/protective for that organ.

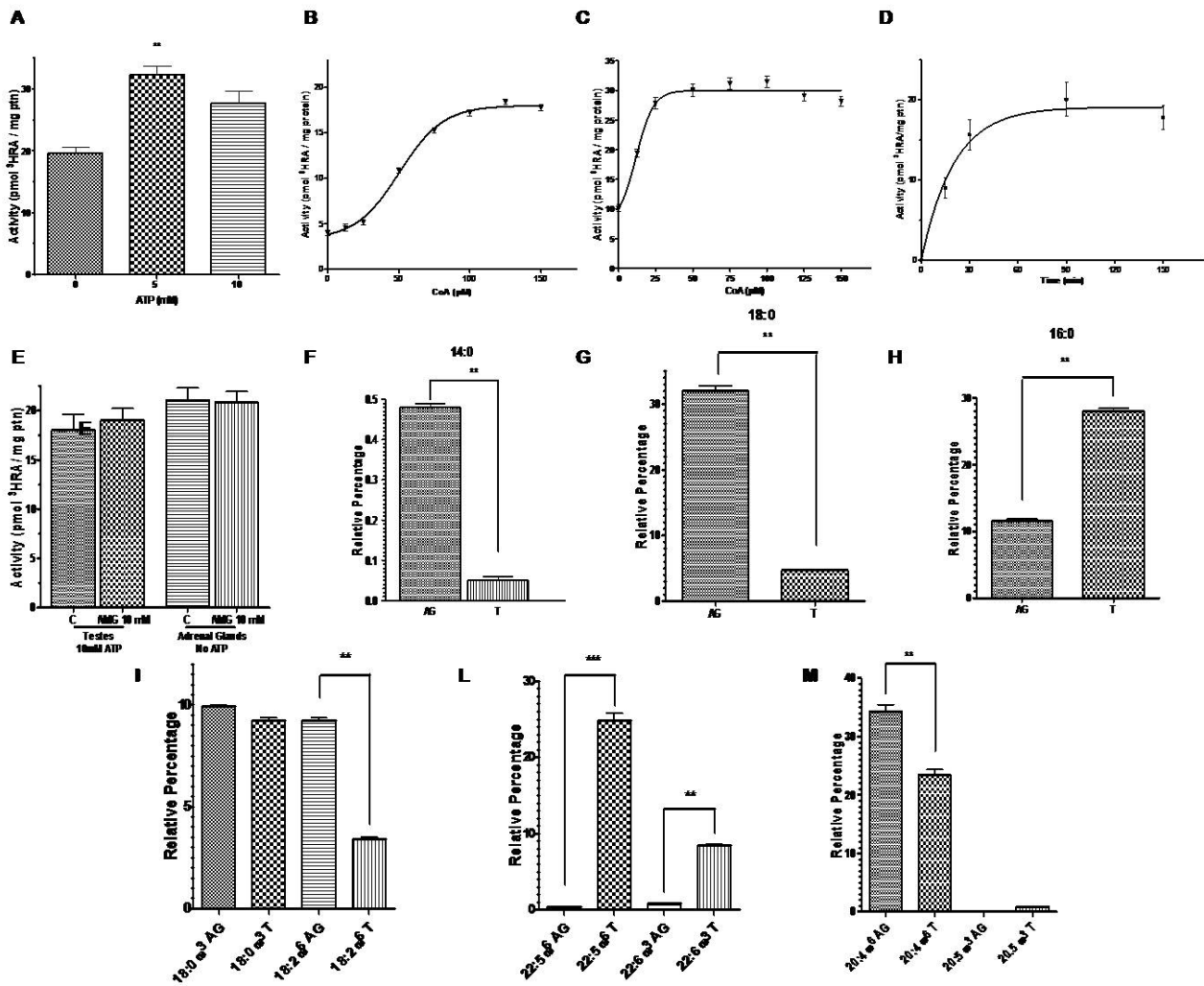


Figure 2. (A) Incorporation of [³H]RA (100 nM) into proteins via Retinoylation reaction on rat adrenal glands mitochondria at 37°C for 90 min in the absence and in the presence of 5 and 10 mM ATP. Retinoylation activity of mitochondria from rat testes (B) and adrenal glands (C) plotted as function of indicated CoA concentrations under the standard conditions for 90 min at 37°C, with 10 mM (B) and 5 mM ATP (C) respectively. (D) Time-dependent incorporation of [³H]RA (100 nM) into protein from rat adrenal glands mitochondria, incubated under standard assay conditions but without ATP at 37°C for the times indicated. (E) Mitochondria were incubated with 10 mM AMG in the presence of 10 mM ATP (testes) and in the absence of ATP (adrenal glands). Saturated (F-H) and unsaturated (I-M) fatty acids composition (mol %) and of rat mitochondrial membrane phospholipids from adrenal glands and testes determined by gas-liquid chromatography as Muci et al (20); other conditions as in Table 4;

Table 2. Retinoylation reaction on adrenal glands cellular sub-fractions
 Incorporation of [³H]RA (100 nM) into proteins by cellular fractions of adrenal glands in duplicate, incubated in a buffer without ATP for 90 min at 37°C, as described in Materials and Methods

Incorporation of ³H-retinoic acid (90 minutes)	
Cell fraction	Incorporated radioactivity (pmoles/mg protein)
Homogenate	8.32 - 8.09
Nuclei	6.89 - 6.53
Mitochondria	21.05 - 20.45
Microsomes	3.49 - 3.80
Cytosol	1.49 - 2.36

Table 3. Mitochondrial ATP quantification

Content of ATP in adrenal glands and testes mitochondria determined as in Material and Methods

Mitochondrial ATP Quantification (mol/L)	
Adrenal Glands	1.3×10^{-2}
Testes	5.2×10^{-8}

Table 4. Fatty Acid composition (mol %) of rat mitochondrial membrane phospholipids from adrenal glands and testes.

The fatty acid composition of adrenal glands and testes mitochondrial membranes was determined by gas-liquid chromatography as Muci et al (20). The data are the mean \pm S.D. of three independent determinations. Σ saturated = sum of saturated fatty acids; Σ unsaturated = sum of unsaturated fatty acids.

Fatty Acid composition (relative percentage)		
FA	Adrenal Glands	Testes
14:0	0.48 \pm 0.01	0
16:0	11.52 \pm 0.35	28 \pm 0.41
18:0	31.96 \pm 0.85	4.7 \pm 0.14
18:1 ω 9	9.94 \pm 0.02	6.2 \pm 0.19
18:2 ω 6	9.25 \pm 0.11	3.4 \pm 0.10
20:4 ω 6	34.30 \pm 1.12	23.4 \pm 0.96
20:5 ω 3	n.d	0.9 \pm 0.01
22:5 ω 6	0.38 \pm 0.04	24.8 \pm 0.94
22:6 ω 3	0.80 \pm 0.06	8.4 \pm 0.13
Σ saturated	44.11 \pm 1.19	32.7 \pm 1.02
Σ unsaturated	55.82 \pm 1.17	67.1 \pm 1.29
Σ sat/ Σ unsat.	0.79 \pm 0.03	0.49 \pm 0.01

The activity of the adenine nucleotide translocator is affected by a component of the retinoylation buffer.

Indeed, the OGC is not the only mitochondrial carrier protein influenced by the atRA. A previous study by Notario *et al.* (2001) demonstrated how micromolar concentrations of atRA are capable to bind the Adenine Nucleotide Translocator (ANT) via photo-labelling and inhibit its activity. The ANT translocator exchanges ADP/ATP across the inner mitochondrial membrane. Discovered about four decades ago (Bruni *et al.*, 1964; Pfaff *et al.*, 1965), ANT is a well-studied protein (Klingenberg, 1989; Fiore *et al.* 1998) due to its abundance, its sensitivity to transport inhibitors and the robustness of the reconstitution method of transport activity in liposomes (Klingenberg, 1985). Consisting of two identical subunits of about 32 kDa, the ANT is present in two distinct conformational states, namely the cytosolic (c) and the matrix (m) states. The inhibitors carboxyatractyloside (CATR) and atractyloside (ATR) bind to c-state, while bongkreikic acid (BKA) binds to the m-state (Klingenberg *et al.*, 1983). It is also assumed that the ANT is the rate-limiting step in energy metabolism (Heldt and Klingenberg, 1968). It has been demonstrated that Mg^{2+} inhibits the ADP/ATP exchange and Mg^{2+} -nucleotides are not recognized by the ANT carrier in reconstituted proteoliposomes (Brandolin *et al.*, 1980; Brandolin *et al.*, 1981). To provide insight to the biochemical mechanism of atRA we studied the ANT exchange activity under retinoylating conditions (Genchi and Olson, 2001; Cione and Genchi, 2004). Instead of confirming the negative regulation of the ATP/ADP exchange (Notario *et al.*, 2003) we found a positive modulation of the ANT activity due to the presence of Coenzyme A (CoA) in the buffer rather than RA. CoA is an enzyme cofactor in various reactions: it functions as an acyl group carrier and carbonyl activating group in numerous reactions central to cellular metabolism, and provides the 4- phosphopantetheine prosthetic group to proteins that play key roles in fatty acid, polyketide and non-ribosomal peptide biosynthesis. As acetyl-CoA, it is essential to the citric acid cycle, to the synthesis and oxidation of ketone bodies and to cholesterol synthesis. The importance of CoA is reflected in conserved

biosynthetic pathway across animals, plants and micro-organisms (Genschel, 2004). Palmitoyl-CoA and long chain acyl-CoA have been shown as potent inhibitors of the ATP/ADP exchange, when added to a suspension of liposomes reconstituted with ANT from rat or bovine heart or liver mitochondria, while CoA and palmitic acid have no effects (Brandolin et al., 1980; Woldegiorgis et al., 1981; Ruoho et al., 1989; Faergeman and Knudsen, 1997). The role of the ANT in energy-linked respiration is an important factor in assessing the potential significance of the acyl-CoA esters as inhibitors and implies that the ANT carrier, like other rate-limiting enzymes, must be carefully regulated. In order to better understand whether CoA is involved in ANT interaction, we used a novel experimental model that pre-incubates mitochondria in an isotonic buffer to mimic the cellular milieu rather than pre-loading vesicles with CoA or simultaneous addition of CoA with ADP or ATP. It seems reasonable to consider the possibility that the CoA might represent a natural ligand of the translocator; fatty acyl-esters share a common structural backbone with the ANT substrates. Therefore, we studied the activity of ANT after pre-incubation of isolated liver mitochondria into Tris-HCl buffer, pH 7.4, supplied with ATP-Mg²⁺ and CoA. Our results indicate that CoA is responsible for an enhanced transport activity of the ANT carrier protein suggesting a new role of CoA in energy-requiring processes. The ANT represents the most abundant protein of the inner mitochondrial membrane, spans the inner mitochondrial membrane and allows the exchange of cytosolic ADP for mitochondrial ATP. In all the transport assays performed, the liposomal reconstituted system consisted of partially purified protein. In order to study whether CoA has any influence on the ANT, we used liver mitochondria in isotonic Tris-HCl buffer, pH 7.4, supplied with ATP-Mg²⁺ and CoA as experimental model. The [³H]ATP/ATP exchange was carried out at 25°C and the transport activity of ANT versus mitochondria pre-incubation time with or without CoA is shown in **Fig. 3A**. In the first section of the graph (0-30 minutes), there's a linear behaviour with slopes of 0.6 and 2.0, respectively for control and CoA incubation. In the second section (30-90 minutes), CoA pre-incubation shows a 3.8 fold greater increase in activity compared

to control. Both CoA pre-incubated and control samples reach maximum activity at 90 minutes, that remains constant till 150 minutes. Therefore a pre-incubation time of 90 minutes was selected for all subsequent studies. In order to study how different concentrations of CoA affect the ANT activity, mitochondria were pre-incubated with the coenzyme in a range of 0-150 μM . The treatment induced activation of the ANT in a dose-dependent manner as shown in **Fig. 3B**. Linear regression analysis resulted in a R^2 value of 0.8951. To obtain K_m and V_{max} values with or without CoA, the dependence of the [^3H]ATP/ATP exchange rate on ATP concentration at 25°C was studied increasing the concentration of external [^3H]ATP (in a range of 0-500 μM), while the internal concentration of ATP was constant at 20 mM. Michaelis-Menten equation was used to interpolate our data. In control experiments, K_m and V_{max} were $22.19 \pm 0.98 \mu\text{M}$ and $155 \pm 1.9 \text{ nmol ATP/mg protein/min}$; while with CoA, K_m and V_{max} were $22.85 \pm 2.52 \mu\text{M}$ and $673.3 \pm 20.74 \text{ nmol ATP/mg protein/min}$, respectively (**Fig. 3C**). 3D imaging shows that the interaction between CoA and ANT is located within the cavity (**Fig. 3D**) and molecular docking revealed that the R80, D135, D232 and R235 residues are all involved in the interaction between CoA and ATP on ANT protein (**Table 5**). All the above-mentioned amino acids are tightly conserved among species, including humans, and are key positions for CATR interaction resulting in inhibitory effects (Pebay-Peroula et al., 2003). To investigate the influence of CoA on the inhibitory effect of CATR on ANT activity, we used 150 μM CoA as described and a range of CATR concentrations from 0 to 10 μM preloaded into liposomes. The most prominent effect occurs at 0.1 μM CATR, where the transport activity of the control was less inhibited compared to the CoA treatment (**Fig. 3E**). At 0.1 μM of inhibitor the ANT transport activity of the CoA treated mitochondria was reduced of a further 20% compared to the control (60% and 80% of relative exchange activity, respectively). No significant differences were evident at 0.5 and 1 μM CATR, while a slight influence of CoA could be observed at 2 and 10 μM CATR. IC_{50} resulted changed with a value of $0.198 \pm 0.011 \mu\text{M}$ for control and $0.142 \pm 0.012 \mu\text{M}$ for CoA treated samples. In order to evaluate the dependence

of the observed CoA-induced activation on a specific ANT isoform, mitochondria prepared from different tissues were tested. ANT1 is mainly expressed in heart and skeletal muscle and ANT2 is expressed in tissues able to undergo proliferation, such as liver, while ANT3 is expressed ubiquitously. The highest transport activation was found in heart (6.7 activation fold), followed by liver (3.4 activation fold), and skeleton muscle (2.9 activation fold), while the lowest enhancement of transport activity was detected in brain (2.5 activation fold), as shown in **Table 6**. To assess any modification on the protein between CoA treated and untreated samples, 2D electrophoresis of purified ANT were run on 18% AA/bisAA gel, resulting in a slightly shift towards the positive side of the IPG strip after CoA treatment (**Fig. 3F-G**). The demonstration that ADP and ATP are the actual substrates for the ANT comes from experiments carried out either with isolated mitochondria or after incorporation of the purified carrier into liposomes where the effectors were pre-loaded into the vesicles or added simultaneously with the substrates when starting the exchange. In our case, pre-incubation of mitochondria into an isotonic buffer supplemented with CoA led to completely unique results, which are opposite to the general behaviour provided by the literature (Brandolin et al., 1980; Woldegiorgis et al., 1981; Ruoho et al., 1989; Faergeman and Knudsen, 1997). When mitochondria are pre-incubated at 37°C, the exchange activity of ANT during the first 30 minutes is almost equal to zero in control sample (20.0 ± 4.5 nmol/mg protein/10 min) and three times higher (60.0 ± 6.3 nmol/mg protein/10 min), when CoA is present (**Fig. 3A**), suggesting that the relationship between ANT and CoA should be enzyme related. Activity increases rapidly between 30 and 90 min for CoA-treated (10.2 fold) and control mitochondria (8.25 fold) further supporting an enzymatic ANT/CoA relationship. The increase in control activity is probably due to endogenous mitochondrial CoA. Both CoA-treated and control reach maximum activity at 90 minutes (615.0 ± 16.1 nmol/mg protein/10 min and 165.0 ± 13.0 nmol/mg protein/10 min, respectively) leading to the maximum difference in CoA-mediated ANT exchange activity over control. In the 90 minutes period both curves are sigmoidal

with the CoA-mediated activity curve 3~4-fold greater than the control curve additionally supporting a possible enzymatic mechanism. Hence, the incubation time of 90 minutes, the first point of maximum activity, was chosen for subsequent experiments. Once the system overcomes the lag phase (0-30 minutes) ANT activity is directly proportional to CoA concentration in the range 0-150 μM as shown in **Fig. 3B**. Kinetic properties of ANT were modified in the presence of CoA (**Fig. 3C**). V_{max} , determined in the presence of CoA was more than fourfold greater than control. No differences in K_m were observed in the presence of CoA. Enhanced V_{max} indicates a positive modulation of the carrier, suggesting that ANT could be poised to exchange when both anabolic and catabolic CoA-mediated biochemical events, requiring more energy to be transferred from the mitochondrial matrix to the cytoplasm, take place in the cell. Partial purification of ANT by chromatographic passage through an HTP column does not decrease the transport activity of the CoA treated samples. CoA mediated enhancement of ANT transport activity is observed in HTP eluates and in crude Triton X-100 extracts (with 4 and 9 nmol ATP /mg protein /10 min for mitochondria pre-incubated in control buffer, and control buffer plus 150 μM CoA, respectively). Exchange activity of freshly prepared mitochondria, in the presence of CoA was almost tenfold higher than the control (1412.2 ± 52.8 nmol ATP/mg protein/10min versus 153.7 ± 13.5 nmol ATP/mg protein/10 min). Moreover, because the K_m value is not affected by the CoA treatment, it is reasonable to affirm that the ATP binding site on ANT is not involved in the CoA interaction. In order to identify the region involved in the CoA-ANT interaction, we performed a molecular docking simulation. Results of the molecular docking simulation indicate that R80, D135, D232 and R235 are all involved in the interaction with CoA as shown in **Table 5** and **Fig. 3D**. In addition the ATP binds to the same region and the same amino acids that are also responsible for CATR interaction (Pebay-Peroula et al., 2003). As these simulated results are in contrast with the ones provided by the kinetic profile, we investigated the influence of CoA on CATR effect. The stronger inhibition given at 0.1 μM (20% more than control) is reflected in a change in the IC_{50} value upon CoA

pre-incubation. High concentration of CATR resulted in similar inhibition between control and CoA-treated due to the excess of inhibitor (**Fig. 3E**). This result, together with the unchanged K_m suggests that the binding site of CoA is different than that given for ATP/CATR. Stronger inhibition of ANT activity by CATR in the presence of CoA implies that the inhibitor interacts more easily with ANT when mitochondria are pre-incubated with CoA. According to Pebay-Peroula et al. (2003) and our molecular docking simulations, ATP and CATR share three residues of interaction on the ANT. Thus in absence of CATR, CoA effect would largely be on ATP. This supposition that CoA would facilitate interaction with ATP is consistent with the experimental data shown here: i.e. that ANT exchanges more ATP in presence of CoA. Therefore we can assert that the CoA binds to ANT independently from the ATP/CATR binding site and CoA interaction with the ANT protein leads to an increase in the transport activity as well as an increase in sensitivity to the CATR inhibitor and/or interaction with ATP. CoA shows a homology motif with the ADP both in the structure and in the net superficial charge. Therefore a contact between the protein and the CoA could be justified according to a proximity approach. The segment spanning residues I311-K318, corresponding to the C-terminal end of the carrier, was also identified as an ADP binding site able to induce a conformational change of the dimeric structure (Dianoux et al., 2000). As CoA does not prevent ATP and CATR from binding ANT, we can hypothesize that the CoA interacts with the accessory site rather than the one localized in the cavity. Subsequently, an interaction between the –SH group of the β -mercaptoethylamine and the neighbour region could take place. More likely, a covalent bond between the –SH group and an acid residue on the portion of the ANT that spans the intermembrane space could be responsible of a “key mechanism” that leads to structure modification of the carrier. Alternately, because CoA is strictly close to the ANT loops and helices, due to the charge pairing attractions, an enzyme, possibly bound to the outer side of the inner membrane, could provide the necessary enzymatic activity to conjugate the –SH of the CoA with the carrier protein. Based on current data, a CoA derivative or a CoA induced

mechanisms cannot be excluded. As shown in **Fig. 3F** and **3G**, a shift in one of the bands attributed to the ANT is highlighted. Upon visualization with silver stain technique, two spots, at about 64 KDa and 32 KDa respectively, appear on both gels that can be easily identified as a dimeric and monomeric form of the ANT, whose molecular weight is known to be 31.7 KDa. The purity of the protein sample is guaranteed by the isolation procedure and chromatographic passages on HTP first and Matrex Gel Blue B thereafter, verified with an increase in the specificity of the exchange activity (data not shown). According to its chemical properties, the ANT is localized around pH 10 on the IPG strip (**Fig. 3F**): a shift towards the more positive side of the isoelectrofocusing strip upon incubation of rat liver mitochondria with CoA has been detected (**Fig. 3G**). This shift is most likely due to a modification of the charges on the carrier protein surface, as a result of treatment with CoA. Although all the ANT isoforms share at least 90% nucleotide sequence identity, they have been implicated differently in several cellular functions (Battini et al., 1987; Neckelmann et al., 1987; Cozens et al., 1989; Stepien et al., 1992; Doerner et al., 1997). We now add the possibility that all the isoforms are similarly involved in the export functions (**Table 6**). ANT is a portion of ATP synthasome (Chen et al., 2004) and the ANT complex is involved in multiple diseases affecting both humans and animals in which ANT activity is disrupted. Among these, heart diseases, mitochondrial diseases, osteoporosis, macromolecular degeneration, immune deficiency, cystic fibrosis, type II diabetes, ulcers, nephro-toxicity, hearing loss, skin disorders, and cancer are found (Klingenberg, 1989; Dahout-Gonzalez et al., 2005). A new emerging class of drugs, named mitocans, are activators of either VADC or ANT and could be used as promising alternative cancer therapeutics (Ralph et al., 2006). Our findings could provide a novel therapeutic approach for treatment of all the above mentioned diseases, or just lay the fundamentals for further discoveries in biochemistry. Additionally, in the literature it is indicated the inhibition of key enzymes in metabolism by long chain acyl-CoA esters, besides the ADP/ATP translocator (Woldegiorgis et al., 1981). Our report that the exchange of ADP/ATP

across the mitochondrial membranes is enhanced by CoA may provide insight into these enzymatic mechanisms influenced by CoA and suggest unique interactions and/or structural modifications may exist.

Table 5. Molecular Docking of CoA and ATP interactions with ANT amino acid residues. With the program *Patch-Doc*® twelve simulations have been carried out and the percentage of interactions of the binding region of the BTADT1-CATR complex respect to the binding region of the RnADT1-CoA and RnADT1-ATP complexes are expressed as Very High Frequency (VHF, 12/12), High Frequency (HF, 10/12), Low Frequency (LF, 5/12) and Not Available (NA).

<i>Amino acid residues</i>	<i>Molecular Docking Simulation</i>	
	CoA	ATP
R80	HF	HF ¹
D95	LF	NA
D135	HF	NA
D232	VHF	HF
R235	VHF	VHF
R236	VHF	VHF

Table 6. Exchange activity of ANT isolated from mitochondria of various tissues after pre-incubation, with or without CoA.

Mitochondria were pre-incubated for 90 minutes at 37°C in 50 mM sucrose, 100 mM Tris-HCl, 10 mM ATP, 27 mM MgCl₂, pH 7.4 (control buffer) and in the same buffer supplemented with 150 μM CoA. ANT was isolated and partially purified. The exchange activities (nmol/mg protein /10 min) were determined as in Material and Methods. The activation fold was calculated as the ratio between the exchange activity of ANT from mitochondria pre-incubated in control buffer plus 150μM CoA and control buffer. Results are expressed as Mean ± SEM of 5 independent experiments.

<i>Tissue</i>	<i>Exchange Activity (nmol ATP/mg ptn/10min)</i>		<i>Activation Fold</i>
	- CoA	+ CoA	
Liver	151.3 ± 2.6	512.2 ± 40.8	3.4
Heart	77.7 ± 4.6	519.0 ± 7.7	6.7
Skeleton muscle	75.0 ± 2.9	220.2 ± 11.5	2.9
Brain	7.7 ± 1.1	19.6 ± 2.1	2.5

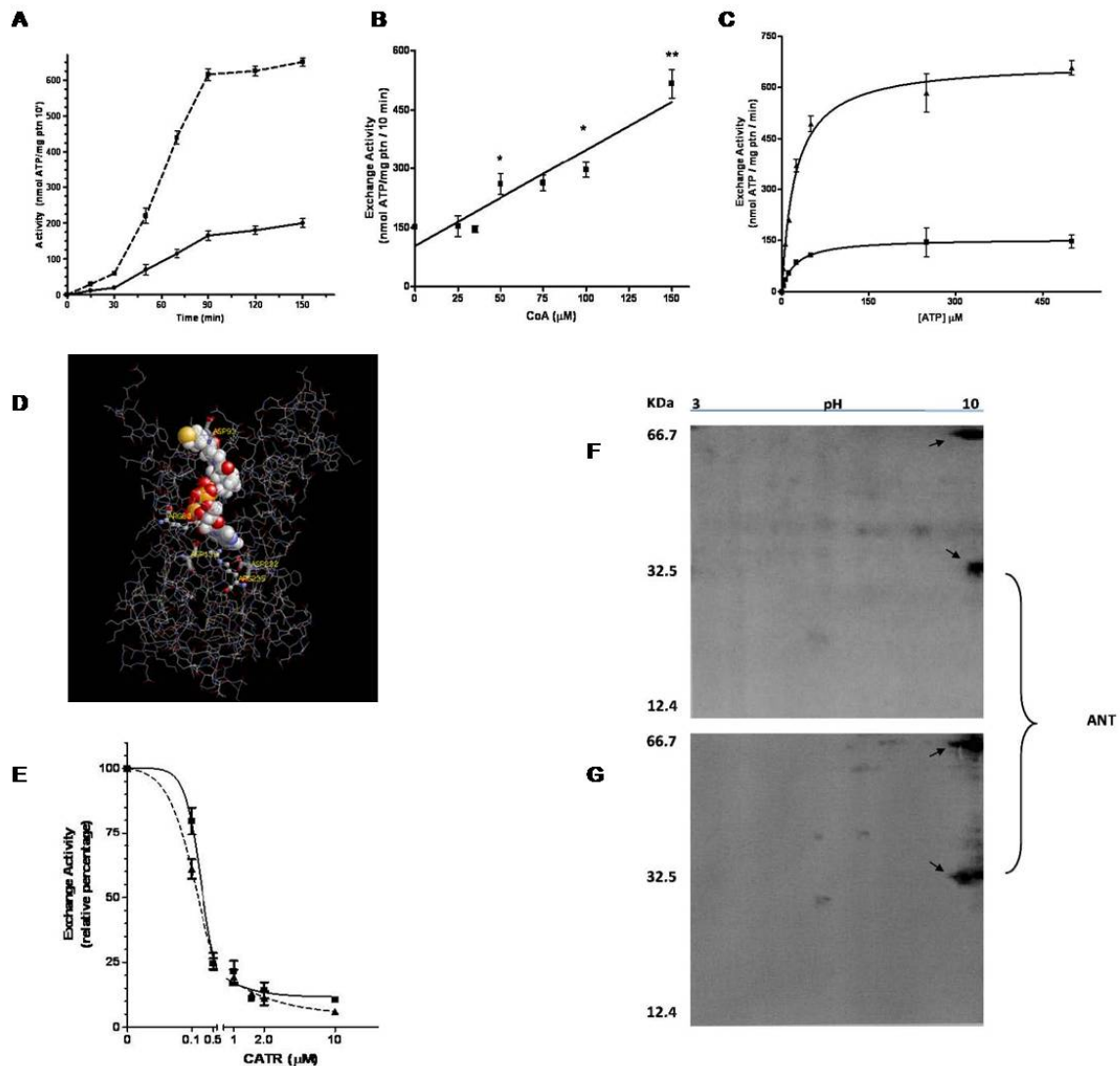


Figure . (A) Exchange activity of ANT from rat liver mitochondria pre-incubated in 50 mM sucrose, 100 mM Tris-HCl, 10 mM ATP, 27 mM MgCl₂, pH 7.4 (control buffer ■) and in the same buffer supplemented with 150 μM CoA (▲) at 37 °C, for the indicated time points. The exchange activity was assayed at 25°C for 10 minutes as described in Materials and Methods. (B) Effect of CoA concentration on the ANT exchange activity. (C) Michaelis-Menten kinetic profile of rat liver mitochondria pre-incubated in 50 mM sucrose, 100 mM Tris-HCl, 10 mM ATP, 27 mM MgCl₂, pH 7.4 (control buffer ■) and in the same buffer supplemented with 150 μM CoA (▲) at 37 °C. The exchange activity was assayed for one minute with [³H]ATP, added at concentrations from 0 to 500 μM, at 25°C. (D) 3D Imaging of Interaction between CoA and ANT. The 3D structure of the ANT carrier was calculated through homology modelling parameters by Swiss-PDB Viewer software. The template structure is the bovine heart ANT. The final structure was minimized through the GROMOS96 process implemented in the Swiss-PDB Viewer to reduce steric/binding perturbation. Molecular-docking simulations were performed on the on-line <http://bioinfo3d.cs.tau.ac.il/PatchDock/index.html> server PatchDock and the structures were visualized and analyzed with PyMol software. (E) Inhibition effect of CATR on ANT from mitochondria incubated for 90 minutes in 50 mM sucrose, 100 mM Tris-HCl, 10 mM ATP, 27 mM MgCl₂, pH 7.4 (control buffer ■) and in the same buffer plus 150 μM CoA (▲). Other experimental procedures as in (B) except that proteoliposomes were pre-loaded with CATR at the indicated concentrations. After isoelectrofocusing and SDS PAGE, of totally purified ANT protein, upon visualization with Silver Stain method, two main spots are highlighted at 64 KDa and 32 KDa both in control (F), and in CoA treated mitochondria(G). Images were acquired in electronic format scanning the gels with a Canonscan Lite 100 scanner, in greyscale with a resolution of 600 DPI.

Combined low doses of PPAR γ and RXR ligands trigger an intrinsic apoptotic pathway in human breast cancer cells.

Recently, studies in human cultured breast cancer cells have shown how the TZD, Rosiglitazone (BRL), promotes antiproliferative effects and activates different molecular pathways leading to distinct apoptotic processes (Bonofiglio *et al.* 2005, 2006, 2008). Apoptosis, the genetically controlled and programmed death leading to cellular self-elimination, can be initiated by two major routes: the intrinsic and extrinsic pathways. The intrinsic pathway is triggered in response to a variety of apoptotic stimuli that produce damage within the cell, including anticancer agents, oxidative damage and UV irradiation, and is mediated through the mitochondria. The extrinsic pathway is activated by extracellular ligands able to induce oligomerization of death receptors, such as Fas, followed by the formation of the death-inducing signaling complex, after which the caspases cascade can be activated. Previous data show that the combination of PPAR γ ligand with either ATRA or 9-*cis*-retinoic acid (9RA) can induce apoptosis in some breast cancer cells (Elstner *et al.* 2002). Furthermore, Elstner *et al.* demonstrated that the combination of these drugs at micromolar concentrations reduced tumor mass without any toxic effects in mice (Elstner *et al.* 1998). The ability of PPAR γ ligands to induce differentiation and apoptosis in a variety of cancer cell types, as in human lung (Tsubouchi *et al.*, 2000), colon (Kitamura *et al.* 1999) and breast (Mueller *et al.* 1998) has been exploited in experimental cancer therapies (Roberts-Thomson, 2000). PPAR γ agonist administration in liposarcoma patients resulted in histologic and biochemical differentiation markers *in vivo* (Demetri *et al.* 1999). However, a pilot study of short-term therapy with PPAR γ ligand Rosiglitazone in early-stage breast cancer patients does not elicit significant effects on tumor cell proliferation, although the changes observed in PPAR γ expression may be relevant to breast cancer progression (Yee *et al.* 2007). However, in humans PPAR γ agonists at high doses exert many side effects including weight gain due to increased adiposity, edema, hemodilution, and plasma-volume expansion, which preclude their clinical application in patients with heart

failure (Arakawa *et al.*, 2004; Rangwala and Lazar, 2004; Staels, 2005). On the other hand, the natural ligand for RXR, 9RA (Leblanc and Stunnenberg, 1995) has been effective *in vitro* against many types of cancer, including breast tumor (Crouch *et al.*, 1991; Delia *et al.*, 1993; Rubin *et al.*, 1994; Sun *et al.*, 1997; Wu *et al.*, 1997). Recently, RXR-selective ligands were discovered to inhibit proliferation of ATRA-resistant breast cancer cells *in vitro* and caused regression of the disease in animal models (Bishoff *et al.*, 1998). The undesirable effects of RXR-specific ligands on hypertriglyceridemia and suppression of the thyroid hormone axis have been also reported (Pinaire and Reifel-Miller, 2007). The additive antitumoral effects of PPAR γ and RXR agonists, both at elevated doses, have been shown in human breast cancer cells (Elstner *et al.* 2002; Grommes *et al.*, 2004 and references therein). However, high doses of both ligands have remarkable side effects in humans such as, weight gain and plasma volume expansion for PPAR γ ligands (Arakawa *et al.*, 2004; Rangwala and Lazar, 2004; Staels, 2005) and hypertriglyceridemia and suppression of the thyroid hormone axis for RXR ligands (Pinaire and Reifel-Miller, 2007). Thus, in the present study it has been demonstrated that nanomolar concentrations of BRL and 9RA in combination do not induce noticeable influences in cell vitality on normal breast epithelial cells, whereas they exert significant antiproliferative effects on breast cancer cells. The molecular mechanism by which combined treatment with BRL and 9RA at nanomolar doses triggers apoptotic events in breast cancer cells, have been elucidated, suggesting potential therapeutical uses for these compounds. To investigate whether low doses of combined agents are able to inhibit cell growth, the capability of 100 nM BRL and 50 nM 9RA to affect normal and malignant breast cell lines was first assessed. We observed that treatment with BRL alone does not elicit any significant effect on cell viability in all breast cell lines tested, while 9RA alone reduces cell vitality only in T47-D cells (**Fig. 4A**). In the presence of both ligands cell viability is strongly reduced in all breast cancer cells: MCF-7, its variant MCF-7TR1, SKBR-3 and T-47D, while MCF-10 normal breast epithelial cells are completely unaffected (**Fig. 4A**). To evaluate the effectiveness of both ligands in the

presence of serum, we performed MTT assay in MCF7 cells treated with low doses of BRL and 9RA in SFM as well as in 5% CT-FBS (**Fig. 4B**). The molecular mechanism underlying these effects has been elucidated in MCF-7 cells in which an upregulation of tumor suppressor gene p53 has been observed. A significant increase in p53 and p21^{WAF1/Cip1} content was observed by Western Blot only upon combined treatment after 24 and 36 h (**Fig. 4C**). Furthermore, we showed an upregulation of p53 and p21^{WAF1/Cip1} mRNA levels induced by BRL plus 9RA after 12 and 24 h (**Fig. 4D**). To investigate whether low doses of BRL and 9RA are able to transactivate the p53 promoter gene, we transiently transfected MCF-7 cells with a luciferase reporter construct (named p53-1) containing the upstream region of the p53 gene spanning from -1800 to +12 (**Fig. 4E**). Treatment for 24 h with 100 nM BRL or 50 nM 9RA did not induce luciferase expression, whereas the presence of both ligands increased in the transactivation of p53-1 promoter (**Fig. 4F**). To identify the region within the p53 promoter responsible for its transactivation, we used constructs with deletions to different binding sites such as CTF-1, nuclear factor-Y (NF-Y), NF κ B and GC sites (**Fig. 4E**). In transfection experiments performed using the mutants p53-6 and p53-13 encoding the regions from -106 to +12 and from -106 to -40, respectively, the responsiveness to BRL plus 9RA was still observed (**Fig. 4F**). In contrast, a construct with a deletion in the NF κ B domain (p53-14) encoding the sequence from -106 to -49, the transactivation of p53 by both ligands was absent (**Fig. 4F**), suggesting that NF κ B site is required for p53 transcriptional activity. To gain further insight into the involvement of NF κ B site in the p53 transcriptional response to BRL plus 9RA, we performed electrophoretic mobility shift assay experiments using synthetic oligodeoxyribonucleotides corresponding to the NF κ B sequence within p53 promoter. We observed the formation of a specific DNA binding complex in nuclear extracts from MCF-7 cells (**Fig. 5A**, lane 1), where specificity is supported by the abrogation of the complex by 100-fold molar excess of unlabeled probe (**Fig. 5A**, lane 2). BRL treatment induced a slightly increase in the specific band (**Fig. 5A**, lane 3), while no changes were observed on 9RA exposure (**Fig. 5A**,

lane 4). The combined treatment increased the DNA binding complex (**Fig. 5A**, lane 5), which was immunodepleted and supershifted using anti-PPAR γ (**Fig. 5A**, lane 6) or anti-RXR α (**Fig. 5A**, lane 7) antibodies. These data indicate that heterodimer PPAR γ /RXR α binds to NF κ B site located in the promoter of p53 *in vitro*. The interaction of both nuclear receptors with the p53 promoter was further elucidated by chromatin immunoprecipitation assays. Using anti-PPAR γ and anti-RXR α antibodies, protein-chromatin complexes were immunoprecipitated from MCF-7 cells treated with 100nM BRL and 50nM 9RA. PCR was used to determine the recruitment of PPAR γ and RXR α to the p53 region containing the NF κ B sequence. The results indicated that either PPAR γ or RXR α was constitutively bound to the p53 promoter in untreated cells and this recruitment was increased on BRL plus 9RA exposure (**Fig. 5B**). Similarly an augmented RNA-Pol II recruitment was obtained by immunoprecipitating cells with an ANTI-RNA-Pol II antibody indicating that a positive regulation of p53 transcription activity was induced by combined treatment (**Fig. 5B**). The role of p53 signaling in the intrinsic apoptotic cascades involves a mitochondria-dependent process, which results in cytochrome *C* release and activation of caspase-9. Because disruption of mitochondrial integrity is one of the early events leading to apoptosis, we assessed whether BRL plus 9RA could affect the function of mitochondria by analyzing membrane potential with a mitochondria fluorescent dye JC-1 (Cossarizza *et al.*, 1997; Smiley *et al.*, 1991). In non-apoptotic cells (control) the intact mitochondrial membrane potential allows the accumulation of lipophilic dye in aggregated form in mitochondria which display red fluorescence. MCF-7 cells treated with 100 nM BRL or 50 nM 9RA exhibit red fluorescence indicating intact mitochondrial membrane potential (data not shown). Cells treated with both ligands exhibit green fluorescence indicating disrupted mitochondrial membrane potential where JC-1 cannot accumulate within the mitochondria, but instead remains as a monomer in the cytoplasm (**Fig. 5C**). Changes in mitochondrial membrane permeability, an important step in the induction of cellular apoptosis, is concomitant with collapse of the electrochemical gradient across the mitochondrial

membrane through the formation of pores in the mitochondria leading to the release of cytochrome *C* into the cytoplasm, and subsequently with cleavage of procaspase-9. This cascade of events, featuring the mitochondria-mediated death pathway, were detected in BRL plus 9RA-treated MCF-7 cells. Concomitantly, cytochrome *C* release from mitochondria into the cytosol, a critical step in the apoptotic cascade, was demonstrated after combined treatment (**Fig. 5D**). BRL and 9RA at nanomolar concentration did not induce any effects on caspase-9 separately, but activation was observed in the presence of both compounds (**Table 7A**). No effects were elicited by either the combined or the separate treatment on caspase-8 activation, a marker of extrinsic apoptotic pathway (**Table 7B**). The activation of caspase 9, in the presence of no changes in the biological activity of caspase 8, support that in our experimental model only the intrinsic apoptotic pathway is the effector of the combined treatment with the two ligands. Since inter-nucleosomal DNA degradation is considered a diagnostic hallmark of cells undergoing apoptosis, we studied DNA fragmentation under BRL plus 9RA treatment in MCF-7 cells, observing that the induced apoptosis was prevented by either the specific antagonist of PPAR γ GW9662 (GW) or by AS/p53, which is able to abolish p53 expression (**Fig. 5E**). Finally, we examined in three additional human breast malignant cell lines: MCF-7 TR1, SKBR-3 and T-47D the capability of low doses of a PPAR γ and an RXR ligand to trigger apoptosis. DNA fragmentation assay showed that only in the presence of combined treatment did cells undergo apoptosis in a p53-mediated manner (**Fig. 5F**), implicating a general mechanism in breast carcinoma. The crucial role of p53 gene in mediating apoptosis supported by the evidence that the effects on the apoptotic cascade were abrogated in the presence of AS/p53 in all breast cancer cell lines tested, including tamoxifen resistant breast cancer cells. In tamoxifen resistant breast cancer cells, other authors have observed that EGFR, IGF-1R and c-Src signaling are constitutively activated and responsible for a more aggressive phenotype consistent with an increased motility and invasiveness (Knowlden *et al.*, 2003; Jones *et al.*, 2004; Hiscox *et al.*, 2005). This gives emphasis to the potential use of the combined therapy with low

doses of both BRL and 9RA as novel therapeutic tool particularly for breast cancer patients who develop resistance to antiestrogen therapy.

Table 7. Activation of caspases in MCF-7 cells. Cells were stimulated for 48 h in presence of BRL 100nM, 9RA 50nM alone or in combination. The activation of caspase 9 (A) and caspase 8 (B) was analysed by Flow Cytometry Assay. Data were presented as mean \pm S.D. of triplicate experiments. * $p < 0.05$ combined-treated vs untreated cells.

A

Caspase 9	% of Activation	SD
control	14,16	$\pm 2,565$
BRL100nM	17,23	$\pm 1,678$
9RA50nM	18,14	$\pm 0,986$
BRL+9RA	33,88 *	$\pm 5,216$

B

Caspase 8	% of Activation	SD
control	9,20	$\pm 1,430$
BRL100nM	8,12	$\pm 1,583$
9RA50nM	7,90	$\pm 0,886$
BRL+9RA	10,56	$\pm 2,160$

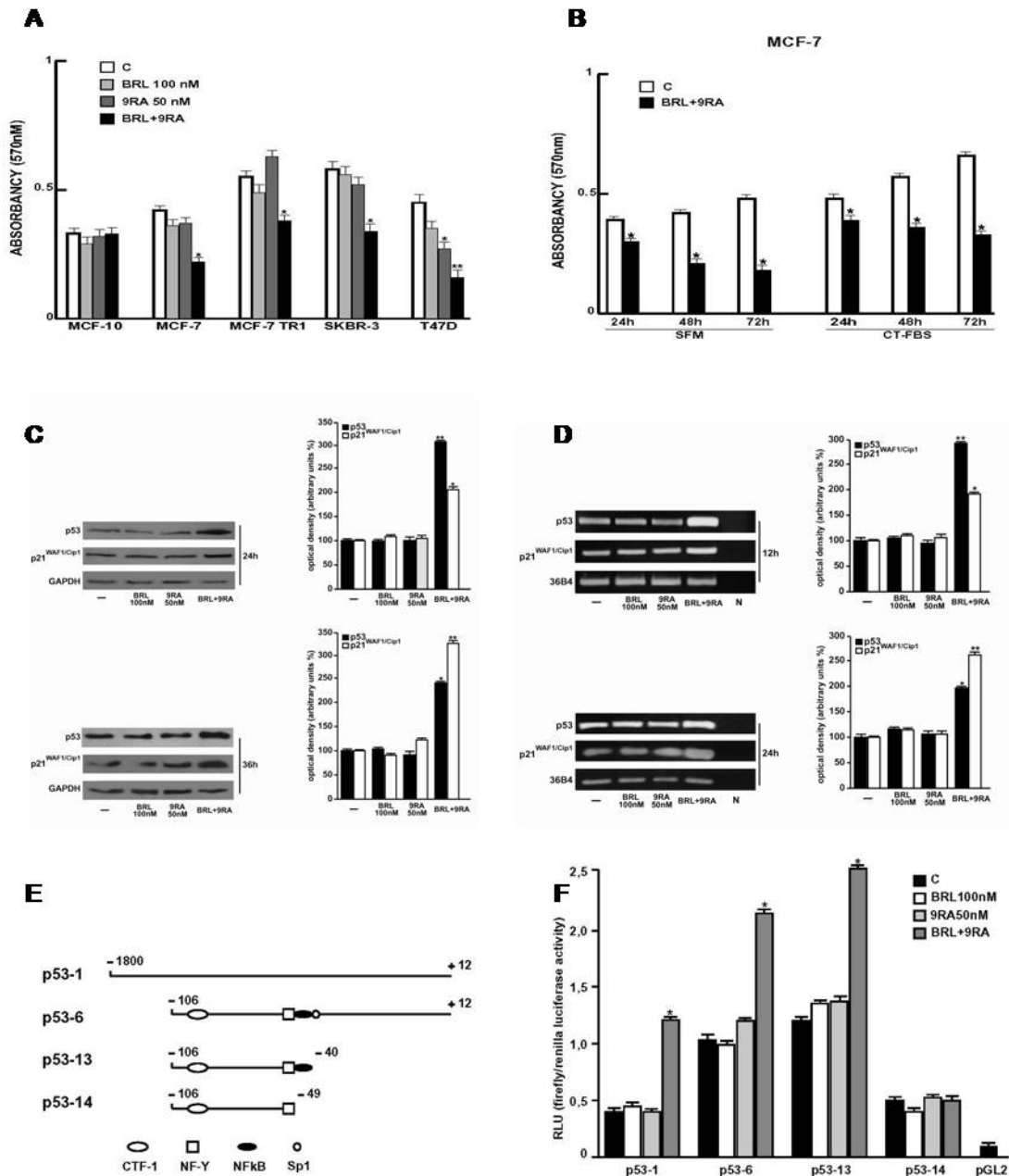


Figure 4.(A) Breast cells were treated for 48 h in SFM in the presence of BRL 100nM or/and 9RA 50nM. Cell vitality was measured by MTT assay. Data were presented as mean \pm S.D. of three independent experiments done in triplicate. (B) MCF7 cells were treated for 24, 48 and 72 h with BRL 100nM and 9RA 50nM in the presence of SFM and 5% CT-FBS. * $p < 0.05$ and ** $p < 0.01$ treated vs untreated cells. (C) Immunoblots of p53 and p21^{WAF1/Cip1} from extracts of MCF-7 cell treated with BRL 100nM and 9RA 50nM alone or in combination for 24 and 36 h. GAPDH was used as loading control. The side panels show the quantitative representation of data (mean \pm S.D.) of three independent experiments after densitometry. (D) p53 and p21^{WAF1/Cip1} mRNA expression in MCF-7 cells treated as in A for 12 and 24 h. The side panels show the quantitative representation of data (mean \pm S.D.) of three independent experiments after densitometry and correction for 36B4 expression. * $p < 0.05$ and ** $p < 0.01$ combined-treated vs untreated cells. N: RNA sample without the addition of reverse transcriptase (negative control). (E) Schematic map of the p53 promoter fragments used in this study. (F) MCF-7 cells were transiently transfected with p53 gene promoter-luc reporter constructs (p53-1, p53-6, p53-13, p53-14) and treated for 24 h with BRL 100nM and 9RA 50nM alone or in combination. The luciferase activities were normalized to the Renilla luciferase as internal transfection control and data were reported as RLU values. Columns are mean \pm S.D. of three independent experiments performed in triplicate. * $p < 0.05$ combined-treated vs untreated cells. pGL2: basal activity measured in cells transfected with pGL2 basal vector; RLU, Relative Light Units. CTF-1, CCAAT-binding transcription factor-1; NF-Y, nuclear factor-Y; NFkB, nuclear factor kB.

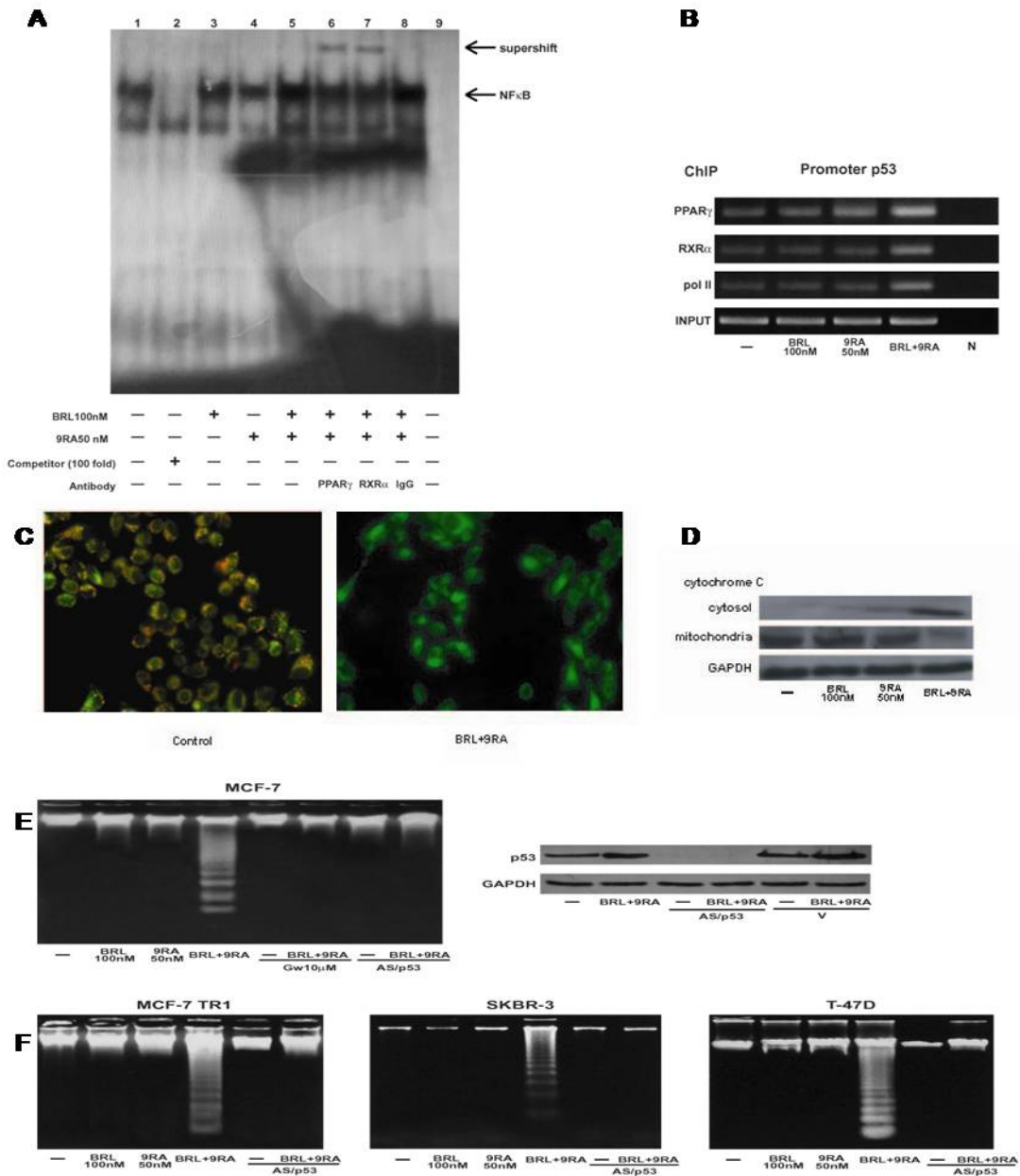


Figure 5. (A) Nuclear extracts from MCF-7 cells (lane 1) were incubated with a double-stranded NF κ B consensus sequence probe labeled with [32 P] and subjected to electrophoresis in a 6% polyacrylamide gel. Competition experiments were done, adding as competitor a 100-fold molar excess of unlabeled probe (lane 2). Nuclear extracts from MCF-7 were treated with 100nM BRL (lane 3), 50nM 9RA (lane 4) and in combination (lane 5). Anti-PPAR γ (lane 6), anti-RXR α (lane 7) and IgG (lane 8) antibodies were incubated. Lane 9 contains probe alone. (B) MCF-7 cells were treated for 1 h with 100nM BRL and/or 50nM 9RA as indicated, and then cross-linked with formaldehyde and lysed. The soluble chromatin was immunoprecipitated with anti-PPAR γ , anti-RXR α and anti-RNA Pol II antibodies. The immunocomplexes were reverse cross-linked, and DNA was recovered by phenol/chloroform extraction and ethanol precipitation. The p53 promoter sequence containing NF κ B was detected by PCR with specific primers. To control input DNA, p53 promoter was amplified from 30 μ l of initial preparations of soluble chromatin (before immunoprecipitations). N: negative control provided by PCR amplification without DNA sample. (C) MCF-7 cells were treated with 100nM BRL plus 50nM 9RA for 48 h and then used fluorescent microscopy to analyze the results of JC-1 (5,5',6,6'-tetrachloro-1,1',3,3'-tetraethylbenzimidazolylcarbocyanine iodide) kit. In control non-apoptotic cells, the dye stains the mitochondria red. In treated apoptotic cells, JC-1 remains in the cytoplasm in a green fluorescent form. (D) MCF-7 cells were treated for 48 h with BRL 100nM and/or 9RA50nM. GAPDH was used as loading control. (E) DNA laddering was performed in MCF-7 cells transfected and treated as indicated for 56 h. One of three similar experiments is presented. The side panel shows the immunoblot of p53 from MCF-7 cells transfected with an expression plasmid encoding for p53 antisense (AS/p53) or empty vector (v) and treated with 100nM BRL plus 50nM 9RA for 56 h. GAPDH was used as loading control. (F) DNA laddering was performed in MCF-7 TR1, SKBR-3, T47-D cells transfected with AS/p53 or empty vector (v) and treated as indicated. One of three similar experiments is presented.

METHODS

Isolation of mitochondria from tissues. Male Wistar rats (250-300 g) were euthanized, according to practice procedures approved by the ethical committee, and tissues were immediately removed. The tissue(s) object of study was first minced and then homogenized in 10 volumes of 250 mM sucrose, 10 mM Tris-HCl, 1 mM EDTA, pH 7.4, by use of a Potter-Elvehjem Teflon homogenizer and the mitochondria were isolated by differential centrifugation as described by Genchi et al. (1996). Mitochondria were then resuspended in sucrose-Tris-EDTA buffer to provide a protein concentration of 15-18 mg/mL. These suspensions were either immediately used or frozen at -70°C. Protein concentration was measured by the Lowry procedure (Lowry et al., 1951) with bovine serum albumin (BSA) as reference standard. The purity of the mitochondrial preparation was checked by assaying marker enzymes for lysosomes, peroxisomes and plasma membranes.

Incubation of mitochondria and extraction of the 2-oxoglutarate carrier (OGC). atRA or ³HatRA were dissolved in ethanol and 3 µL of the solution was added to the tissue preparation (0.5 mg protein), and incubated in the presence of 10 mM ATP, 150 µM CoA, 27 mM MgCl₂, 50 mM sucrose, and 100 mM Tris, pH 7.4, in a total volume of 0.5 ml at 37°C for 90 min. The inhibitors were added together with ³HatRA. The mitochondrial suspensions were centrifuged and protein extracted in 3% Triton X-114, 20 mM Na₂SO₄, 1 mM EDTA, 10 mM Pipes, pH 7.0, and after 10 minutes on ice, the mixture was centrifuged at 13000 rpm for 5 minutes.

Incorporation of radioactive RA in mitochondria from adrenal glands and testes. [³H]RA or RA were dissolved in ethanol under yellow safe-light. The concentration of RA was spectrophotometrically determined, the ethanol was evaporated under nitrogen, and the dry residue resuspended in dimethylsulfoxide (DMSO). The RA solution was diluted into the retinoylation buffer such that the final concentration of DMSO was no higher than 0.5%. The buffers were 5mM ATP, 50 µM CoA, 27 mM MgCl₂, 50 mM sucrose, 100 mM Tris, pH 7.4 for adrenal glands mitochondrial preparation, and 10 mM ATP, 150 µM CoA, 27 mM MgCl₂, 50 mM sucrose, 100 mM Tris, pH 7.4 for testes mitochondria and the incubation was carried out at 37°C for 90 minutes in a final ratio of 1 mg protein / 1 ml (see Fig.1 and 2 and Results). The reaction was stopped by adding TCA at a final concentration of 5%. The mixture was centrifuged in an Eppendorf centrifuge at 13,000rpm for 10 min, and the precipitate was extracted seven times with 0.5 ml CHCl₃:MeOH (2:1) containing 0.005% BHT. The pellet was solubilised in 0.2 ml 1% SDS, 40 mM Tris, 2 mM EDTA, pH 7.5, at 50 °C and counted in a TriCarb 2100TR liquid scintillation counter (Packard). The counting efficiency was about 70%.

Pre-incubation of mitochondria and purification of Adenine Nucleotide Translocator. Mitochondria (20 mg protein) were pre-incubated in a buffer of 10 mM ATP, 150 µM CoA, 27 mM MgCl₂, 50 mM sucrose, and 100 mM Tris, pH 7.4, in a final volume of 20 mL at 37°C for 90 min. Then the suspension was centrifuged in a Sorvall centrifuge at 13,000 x g for 10 min. The mitochondrial pellet was solubilized in 300µL 3% Triton X-100 (w/v), 20 mM Na₂SO₄, 1 mM EDTA, and 10 mM Pipes, pH 7.0. After 15 min at 4 °C, the mixture was centrifuged at 13,000 x g for 10 min and then 225 µL of Triton X-100 extract supplemented with 1 mg of cardiolipin were applied to 600 mg dry hydroxylapatite (HTP) column and eluted at 4°C with the same buffer until the first milliliter was collected (partial purification). 2 mL of HTP eluates were pooled together and applied to a pasteur pipette filled with 1mL of Matrex Gel Blue B pre-equilibrated with 4 mL 8M Urea, 4 mL of water and 4 mL of Triton X-100 buffer (0.1% Triton X-100, 20mM Na₂SO₄, 1mM EDTA and 5mM PIPES, pH 7.0) each in sequence. The resin was then eluted with 4 mL of 0.1% Triton X-100 buffer followed by two additions of 800µL of 6mg/mL asolectin in 0.1% Triton X-100 buffer, the latter of which allows the recovery of the total purified ANT. The purity of the sample was verified via SDS PAGE and Coomassie staining (data not shown). Protein concentration was determined by the Lowry method modified for the presence of Triton (Dulley and Grieve, 1975).

Reconstitution into liposomes and Determination of OGC transport Activity. 20 µg of protein from the triton X-114 extract of mitochondria were added to 100 µL of sonicated phospholipids (10% w/v), 100 µL of 10% Triton X-114 in Pipes 10 mM, 40µL of Malate 200 mM, 230 µL Pipes 10 mM pH 7.0 in a final volume of 700 µL and were applied to an Amberlite XAD-2 column in agreement with Palmieri [21]. All the operations were carried out at room temperature. In order to determine the OGC transport activity, the external malate was removed by passing 650 µL of

the proteoliposomal suspension through a Sephadex G-75 column preequilibrated with 50 mM NaCl and 10 mM Pipes, pH 7.0. The first 600 μL of the slightly turbid eluate, containing the proteoliposomes, were collected, transferred to 1.5 mL microcentrifuge tubes (150 μL each), and used for transport measurements by the inhibitor stop method. Transport was carried out at 25 °C by adding 0.1 mM [^{14}C] 2-oxoglutarate and stopped after 10 minutes by the addition of 20 mM pyridoxal 5'-phosphate. In control samples, the pyridoxal 5'-phosphate was added together with the labeled substrate at time zero. To remove the external radioactivity, each sample was passed through a Sephadex G-75 column (0.5x8cm). The liposomes, eluted with 50 mM NaCl, were collected in 4 mL of scintillation cocktail and counted using a Tricarb 2100 TR scintillation counter with a counting efficiency of about 70-73 %. The exchange activity was evaluated as the difference between the experimental and the control values as previously published by Bisaccia et al.

Testes mitochondria labeling with $^3\text{HatRA}$ and Western Blot analysis of OGC. Direct labeling with $^3\text{HatRA}$ was performed according to a method described previously. Under yellow safe-light, 5 $\mu\text{Ci}/5 \mu\text{L}$ of $^3\text{HatRA}$ (40–60 Ci/mmol) in ethanol (1 $\mu\text{Ci}/\mu\text{L}$) were added to 1.5 mL glass microcentrifuge tubes for each sample tested. After the ethanol was removed under nitrogen, 20 μg of Triton extract of testes mitochondrial protein were added to each tube, and the final volume was adjusted to 10 μL with incubation buffer, pH 7.4, for a final concentration of 10 μM $^3\text{HatRA}$, while 2-oxo-glutarate was added at a final concentration of 10 mM. The samples were incubated at 37°C and shaken for 90 minutes under yellow light, after which 10 μL of SDS-polyacrylamide gel electrophoresis sample buffer was added, the samples boiled and then loaded to run with standard SDS-polyacrylamide gel electrophoresis techniques. The gel was stained with Coomassie Brilliant Blue, soaked in Amplify (Amersham Biosciences) and then used for fluorography at - 80°C for 30 days. In order to verify the presence of the OGC protein, western blot analyses was performed using overnight rabbit monoclonal antibody to OGC at 4° C (1:500 dilution in TBST). Next day the membrane was incubated for 1 h at room temperature with horseradish peroxidase-conjugate antibodies to rabbit immunoglobulin G (1:2000 dilutions) and the immune complex was detected with chemiluminescence reagents (ECL).

Reconstitution of the ADP/ATP carrier in liposomes and transport measurements. 20 μg of protein from the HTP eluate were added to 100 μL of sonicated phospholipids (10% w/v), 100 μL of 10% Triton X-114 in 10 mM Pipes, 70 μL of 200 mM ATP, 230 μL of 10 mM Pipes, pH 7.0, in a final volume of 700 μL . This mixture was applied to an Amberlite XAD-2 column for 15 times in agreement with Palmieri and Klingenberg(1979). All the operations were carried out at room temperature. External substrates were removed by a passage of the Amberlite XAD-2 eluate through a Sephadex G-75 column (0.75 cm x 15 cm) pre-equilibrated with 50 mM NaCl and 10 mM Pipes, pH 7.0. The eluted proteoliposomes were split in 150 μL aliquots and assayed at 25°C for the transport measurements by the inhibitor stop method (Palmieri and Klingenberg, 1979), using 0.1 mM [^3H]ATP to start the exchange and 20 mM pyridoxal 5'-phosphate to stop it after 10 minutes. At time zero, the inhibitor and [^3H]ATP were added to the control sample. A further passage through a Sephadex G-75 column (0.5 cm x 8cm), eluting with 50 mM NaCl, allowed the removal of the external radioactivity. The proteoliposome fractions containing [^3H]ATP were collected in 4 ml of scintillation cocktail. The experimental values were corrected by subtracting the respective control. A Tricarb 2100 TR scintillation counter was used and the counting efficiency was about 70-73 %. To obtain K_m and V_{max} data, the exchange was performed as described above, stopping the process after 1 minute. The kinetic values were calculated by GraphPad® Prism 4 software. When CATR was used, liposomes were preloaded with the inhibitor during the reconstitution passage.

Isoelectrofocusing and SDS PAGE. 9 volumes of ice cold acetone were added to an equivalent volume of 20 μg of Matrex Gel Blue B eluted protein followed with two washes in the same solvent to allow precipitation of the protein and further removal of interfering substances (like salts and detergent). The pellet was then solubilized in 150 μL rehydration buffer [128 μL 1.1X Zoom 2D protein solubilizer (Invitrogen), 0.7 μL 2M DTT, 0.5 % ampholytes, trace of Bromophenol Blue, deionized water to 150 μL]. A 3-10 IPG strip (Invitrogen) was then carefully covered with the buffer paying attention to provide a homogeneous distribution of the sample under the strip with no formation of air bubbles, according with the *ZOOM IPG Runner System* protocols provided by the manufacturer, and left overnight at room temperature. Isoelectrofocusing (IEF) was performed following 3 steps: 175 V, 15 min; 175-2000 V ramp, 45 min; 2000 V, 30 min. Prior to perform the SDS PAGE separation the strip was removed from the IEF chamber, washed with milli-Q distilled water, equilibrated and alkylated with 223 mg iodoacetamide in 10mL of equilibration buffer at room temperature. The proteins were resolved into a 18% acrylamide gel with a ratio acrylamide:bisacrylamide of 30:0.2, and visualized with silver stain method.

Alignment of ANT and molecular docking simulations. The 3D structure of the ANT carrier was calculated through homology modelling parameters by Swiss-PDB Viewer software (Guex and Peitch, 1997). The bovine heart ANT, whose crystalline structure has been resolved with a 2.2 Å resolution, was used as template structure (Pebay-Peyroula et al., 2003). In order to reduce steric or/and binding perturbations, the final structure was minimized through the GROMOS96 process (Van Gusteren et al, 2004) implemented in the Swiss-PDB Viewer. Molecular-docking simulations were performed using the on-line server PatchDock (Sandak et al., 2002, Schneidman-Duhovny et. Al., 2002) available at <http://bioinfo3d.cs.tau.ac.il/PatchDock/index.html> and the structures were visualized and analyzed with PyMol software (DeLano, 2002).

TM-3 Cell Cultures. Leydig (TM-3) cell line derived from testes of immature BALB/c mice, was generously donated by Dr. S. Andò (University of Calabria), and cultured in DMEM/F12 medium supplemented with 10% FCS, 2 mM glutamine, 1% of a stock solution containing 10,000 IU/mL penicillin and 10,000 µg/mL streptomycin and were grown on 90 mm plastic tissue culture dishes in a humidified atmosphere of 5% CO₂ in air at 37 °C. Cells from exponentially growing stock cultures were removed from the plate with trypsin (0.05% w/v) and EDTA (0.02% w/v). Cell number was estimated with a Burker camera and cell viability by trypan blue dye exclusion. The medium was changed twice weekly. TM-3 cells were subcultured when confluent.

TM-3 cells treated with atRA and Mitochondrial Isolation. TM-3 cells growing exponentially were removed by trypsin/EDTA, harvested by centrifugation and resuspended at 1x10⁶ cells/mL in DMEM/F12 medium supplemented with serum. The next day the medium was removed and replaced with serum-free DMEM/F12. The cells were incubated at 37 °C in a humidified atmosphere of 5% CO₂ in air for 24 h in the presence of 10 or 100 nM atRA dissolved in DMSO and diluted into the growth medium such that the final DMSO concentration was no higher than 0.01%. After the above mentioned treatments, TM-3 cells were collected by trypsinization and isolated by centrifugation at 1,200×g for 5 min at 4°C. The pellet was solubilized in 180 µL RIPA buffer. After the addition of 20 µL of 0.1% digitonin, the cells were incubated for 15 min at 4°C and mitochondria were isolated by differential centrifugation at 4°C.

Breast cancer cell cultures. Wild-type human breast cancer MCF-7 cells were grown in DMEM-F12 plus glutamax containing 5% new-born calf serum (Invitrogen, Milan, Italy) and 1 mg/ml penicillin-streptomycin. MCF-7 tamoxifen resistant (MCF-7TR1) breast cancer cells were generated in Dr. Fuqua's laboratory similar to that described by Herman (21) maintaining cells in MEM with 10% foetal bovine serum (FBS) (Invitrogen), 6 ng/ml insulin, penicillin (100 units/ml), streptomycin (100 µg/ml) and adding 4-hydroxytamoxifen in 10-fold increasing concentrations every weeks (from 10⁻⁹ to 10⁻⁶ final). Cells were thereafter routinely maintained with 1µM 4-hydroxytamoxifen. SKBR-3 breast cancer cells were grown in DMEM without red phenol, plus glutamax containing 10% FBS and 1 mg/ml penicillin-streptomycin. T-47D breast cancer cells were grown in RPMI 1640 with glutamax containing 10% FBS, 1mM sodium pyruvate, 10mM HEPES, 2,5g/L glucose, 0,2 U/ml insulin and 1 mg/ml penicillin-streptomycin. MCF-10 normal breast epithelial cells were grown in DMEM-F12 plus glutamax containing 5% horse serum (Sigma), 1 mg/ml penicillin-streptomycin, 0,5 µg/ml hydrocortisone and 10 µg/ml insulin.

Plasmids. The p53 promoter-luciferase plasmids, kindly provided by Dr. Stephen H. Safe (Texas A&M University, College Station, TX, USA), were generated from the human p53 gene promoter as follows: p53-1 (containing the -1800 to +12 region), p53-6 (containing the -106 to +12 region), p53-13 (containing the -106 to -40 region) and p53-14 (containing the -106 to -49 region) (20). As an internal transfection control, we cotransfected the plasmid pRL-CMV (Promega Corp., Milan, Italy) that expresses Renilla luciferase enzymatically distinguishable from firefly luciferase by the strong cytomegalovirus enhancer promoter. The pGL3 vector containing three copies of a PPRE sequence upstream of the minimal thymidine kinase promoter ligated to a luciferase reporter gene (3XPPRE-TK-pGL3) was a gift from Dr. R. Evans (The Salk Institute, San Diego, CA, USA). The p53 antisense plasmid (AS/p53) was kindly provided from Dr. Moshe Oren (Weizmann Institute of Science, Rehovot, Israel).

MTT Assay. Cell viability was determined with the MTT assay (22). Cells (2x10⁵ cells/ml) were grown in 6 well plates and exposed to BRL 100nM, 9RA 50nM alone or in combination in serum free medium (SFM) and in 5% charcoal treated (CT)-FBS. 100 µl of MTT (5mg/ml) were added to each well, and the plates were incubated for 4 h at 37 °C. Then, 1 ml 0.04N HCl in isopropanol was added to solubilise the cells. The absorbance was measured with the Ultraspec 2100 Pro-spectrophotometer (Amersham-Biosciences, Milan, Italy) at a test wavelength of 570 nm with a

reference wavelength of 690 nm. The optical density (O.D.) was calculated as the difference between the two absorbencies.

Immunoblotting. Cells were grown in 10cm dishes to 70–80% confluence and exposed to treatments in SFM as indicated. Cells were then harvested in cold phosphate-buffered saline (PBS) and resuspended in lysis buffer containing 20mM HEPES (pH 8), 0.1mM EGTA, 5mM MgCl₂, 0.5M NaCl, 20% glycerol, 1% Triton, and inhibitors (0.1mM sodium orthovanadate, 1% phenylmethylsulfonylfluoride (PMSF), 20mg/ml aprotinin). Protein concentration was determined by Bio-Rad Protein Assay (Bio-Rad Laboratories, Hercules, CA USA). A 40µg portion of protein lysates was used for Western blotting (WB), resolved on a 10% SDS-polyacrylamide gel, transferred to a nitrocellulose membrane, and probed with an antibody directed against the p53, p21^{WAF1/Cip1} (Santa Cruz Biotechnology, CA USA). As internal control, all membranes were subsequently stripped (0.2 M glycine, pH 2.6, for 30 min at room temperature) of the first antibody and reprobed with anti-GAPDH antibody (Santa Cruz Biotechnology). The antigen-antibody complex was detected by incubation of the membranes for 1 h at room temperature with peroxidase-coupled goat antimouse or antirabbit IgG and revealed using the enhanced chemiluminescence system (Amersham Pharmacia, Buckinghamshire UK). Blots were then exposed to film (Kodak film, Sigma). The intensity of bands representing relevant proteins was measured by Scion Image laser densitometry scanning program.

RT-PCR Assay. MCF-7 cells were grown in 10cm dishes to 70–80% confluence and exposed to treatments in SFM as indicated. Total cellular RNA was extracted using TRIZOL reagent (Invitrogen) as suggested by the manufacturer. The purity and integrity were checked spectroscopically and by gel electrophoresis before carrying out the analytical procedures. Two micrograms of total RNA were reverse transcribed in a final volume of 20 µl using a RETROscript kit as suggested by the manufacturer (Promega). The cDNAs obtained were amplified by PCR using the following primers: 5'-GTGGAAGGAAATTTGCGTGT-3' (p53 forward) and 5'-CCAGTGTGATGATGGTGAGG-3' (p53 reverse), 5'-GCTTCATGCCAGCTACTTCC-3' (p21 forward) and 5'-CTGTGCTCACTTCAGGGTCA-3' (p21 reverse), 5'-CTCAACATCTCCCCCTTCTC-3' (36B4 forward) and 5'-CAAATCCCATATCCTCGTCC-3' (36B4 reverse) to yield, respectively, products of 190 bp with 18 cycles, 270 bp with 18 cycles, and 408 bp with 12 cycles. To check for the presence of DNA contamination, a reverse transcription PCR was performed on 2 µg of total RNA without Monoley murine leukemia virus reverse transcriptase (the negative control). The results obtained as optical density arbitrary values were transformed to percentage of the control taking the samples from untreated cells as 100%.

Transfection Assay. MCF-7 cells were transferred into 24 well plates with 500µl of regular growth medium/well the day before transfection. The medium was replaced with SFM on the day of transfection, which was performed using Fugene 6 reagent as recommended by the manufacturer (Roche Diagnostics, Mannheim, Germany) with a mixture containing 0.5µg of promoter-luc or reporter-luc plasmid and 5ng of pRL-CMV. After transfection for 24 h, treatments were added in SFM as indicated, and cells were incubated for an additional 24 h. Firefly and Renilla luciferase activities were measured using the Dual Luciferase Kit (Promega). The firefly luciferase values of each sample were normalized by Renilla luciferase activity, and data were reported as Relative Light Units. MCF-7 cells plated into 10cm dishes were transfected with 5µg of AS/p53 using Fugene 6 reagent as recommended by the manufacturer (Roche Diagnostics). The activity of AS/p53 was verified using Western blot to detect changes in p53 protein levels. Empty vector was used to ensure that DNA concentrations were constant in each transfection.

EMSA. Nuclear extracts from MCF-7 cells were prepared as previously described (23). Briefly, MCF-7 cells plated into 10cm dishes were grown to 70–80% confluence, shifted to SFM for 24 h, and then treated with 100nM BRL, 50nM 9RA alone and in combination for 6 h. Thereafter, cells were scraped into 1.5ml of cold PBS, pelleted for 10 sec and resuspended in 400µl cold buffer A (10mM HEPES-KOH, pH 7.9, at 4 °C, 1.5mM MgCl₂, 10mM KCl, 0.5mM dithiothreitol, 0.2mM PMSF, 1mM leupeptin) by flicking the tube. Cells were allowed to swell on ice for 10 min and then vortexed for 10 sec. Samples were then centrifuged for 10 sec and the supernatant fraction was discarded. The pellet was resuspended in 50µl of cold Buffer B (20mM HEPES-KOH, pH 7.9; 25% glycerol; 1.5mM MgCl₂; 420mM NaCl; 0.2mM EDTA; 0.5mM dithiothreitol; 0.2mM PMSF; 1mM leupeptin) and incubated in ice for 20 min for high-salt extraction. Cellular debris was removed by centrifugation for 2 min at 4 °C, and the supernatant fraction (containing DNA-binding proteins) was stored at -70 °C. The probe was generated by annealing single-stranded oligonucleotides and labeled with [³²P]ATP (Amersham Pharmacia) and T4 polynucleotide kinase (Promega) and then purified using Sephadex G50 spin columns (Amersham Pharmacia). The DNA sequence of the NFκB located within p53 promoter as probe is 5'-AGT TGA GGG GAC TTT CCC AGG C-3' (Sigma Genosys, Cambridge, UK). The protein-binding

reactions were carried out in 20 μ l of buffer [20mM HEPES (pH 8.0), 1mM EDTA, 50mM KCl, 10mM dithiothreitol, 10% glycerol, 1mg/ml BSA, 50 μ g/ml polydeoxyinosinic deoxycytidylic acid] with 50,000 cpm of labeled probe, 20 μ g of MCF7 nuclear protein, and 5 μ g of polydeoxyinosinic deoxycytidylic acid. The mixtures were incubated at room temperature for 20 min in the presence or absence of unlabeled competitor oligonucleotides. For the experiments involving anti-PPAR γ and anti-RXR α antibodies (Santa Cruz Biotechnology), the reaction mixture was incubated with these antibodies at 4 °C for 30 min before addition of labeled probe. The entire reaction mixture was electrophoresed through a 6% polyacrylamide gel in 0.25X Tris borate-EDTA for 3 h at 150 V. Gel was dried and subjected to autoradiography at -70 °C.

ChIP Assay. MCF-7 cells were grown in 10cm dishes to 50–60% confluence, shifted to SFM for 24 h, and then treated for 1 h as indicated. Thereafter, cells were washed twice with PBS and cross-linked with 1% formaldehyde at 37 °C for 10 min. Next, cells were washed twice with PBS at 4 °C, collected and resuspended in 200 μ l of lysis buffer (1% SDS; 10mM EDTA; 50 mM Tris-HCl, pH 8.1), and left on ice for 10 min. Then, cells were sonicated four times for 10 sec at 30% of maximal power (Vibra Cell 500 W; Sonics and Materials, Inc., Newtown, CT) and collected by centrifugation at 4 °C for 10 min at 14,000 rpm. The supernatants were diluted in 1.3 ml of immunoprecipitation buffer (0.01% SDS; 1.1% Triton X-100; 1.2mM EDTA; 16.7mM Tris-HCl, pH 8.1; 16.7mM NaCl) followed by immunoclearing with 60 μ l of sonicated salmon sperm DNA/protein A agarose (DBA Srl, Milan, Italy) for 1 h at 4 °C. The precleared chromatin was immunoprecipitated with anti-PPAR γ , anti-RXR α or anti-RNA Pol II antibodies (Santa Cruz Biotechnology). At this point, 60 μ l salmon sperm DNA/protein A agarose was added, and precipitation was further continued for 2 h at 4 °C. After pelleting, precipitates were washed sequentially for 5 min with the following buffers: Wash A [0.1% SDS, 1% Triton X-100, 2mM EDTA, 20mM Tris-HCl (pH 8.1), 150mM NaCl], Wash B [0.1% SDS, 1% Triton X-100, 2mM EDTA, 20mM Tris-HCl (pH 8.1), 500mM NaCl], and Wash C [0.25M LiCl, 1% NP-40, 1% sodium deoxycholate, 1mM EDTA, 10mM Tris-HCl (pH 8.1)], and then twice with TE buffer (10mM Tris, 1mM EDTA). The immunocomplexes were eluted with elution buffer (1% SDS, 0.1 M NaHCO₃). The eluates were reverse cross-linked by heating at 65 °C and digested with proteinase K (0.5mg/ml) at 45 °C for 1 h. DNA was obtained by phenol-chloroform-isoamyl alcohol extraction. Two microliters of 10mg/ml yeast tRNA (Sigma) were added to each sample, and DNA was precipitated with 95% ethanol for 24 h at -20 °C and then washed with 70% ethanol and resuspended in 20 μ l of TE buffer. A 5 μ l volume of each sample was used for PCR with primers flanking a sequence present in the p53 promoter: 5'-CTGAGAGCAAACGCAAAG-3' (forward) and 5'-CAGCCCGAACGCAAAGTGTC-3' (reverse) containing the κ B site from -254 to -42 region. The PCR conditions for the p53 promoter fragments were, 45 sec at 94 °C, 40 sec at 57 °C, 90 sec at 72 °C. The amplification products obtained in 30 cycles were analyzed in a 2% agarose gel and visualized by ethidium bromide staining. The negative control was provided by PCR amplification without a DNA sample. The specificity of reactions was ensured using normal mouse and rabbit IgG (Santa Cruz Biotechnology).

JC-1 Mitochondrial Membrane Potential Detection Assay. The loss of mitochondrial membrane potential was monitored with the dye 5,5',6,6'-tetra-chloro-1,1',3,3'-tetraethylbenzimidazolyl-carbocyanine iodide (JC-1) (Biotium, Hayward, USA). In healthy cells, the dye stains the mitochondria bright red. The negative charge established by the intact mitochondrial membrane potential allows the lipophilic dye, bearing a delocalized positive charge, to enter the mitochondrial matrix where it aggregates and gives red fluorescence. In apoptotic cells, the mitochondrial membrane potential collapses, and the JC-1 cannot accumulate within the mitochondria, it remains in the cytoplasm in a green fluorescent monomeric form (24). MCF-7 cells were grown in 10cm dishes and treated with 100 nM BRL and/or 50 nM 9RA for 48 hours, then cells were trypsinized, washed in ice-cold PBS, and incubated with 10mM JC-1 at 37 °C in a 5% CO₂ incubator for 20 min in darkness. Subsequently, cells were washed twice with PBS and analyzed by fluorescence microscopy. The red form has absorption/emission maxima of 585/590 nm. The green monomeric form has absorption/emission maxima of 510/527 nm. Both healthy and apoptotic cells can be visualized by fluorescence microscopy using a wide band-pass filter suitable for detection of fluorescein and rhodamine emission spectra.

Cytochrome C Detection. Cytochrome C was detected by western blotting in mitochondrial and cytoplasmic fractions. Cells were harvested by centrifugation at 2,500 rpm for 10 min at 4 °C. The pellets were suspended in 36 μ l RIPA buffer plus 10 μ g/ml aprotinin, 50mM PMSF and 50mM sodium orthovanadate and then 4 μ l of 0.1% digitonine were added. Cells were incubated for 15 min at 4 °C and centrifuged at 12,000 rpm for 30 min at 4 °C. The resulting mitochondrial pellet was resuspended in 3% Triton X-100, 20mM Na₂SO₄, 10mM PIPES and 1mM EDTA, pH 7.2, and centrifuged at 12,000 rpm for 10 min at 4 °C. Proteins of the mitochondrial and cytosolic fractions were determined by Bio-Rad Protein Assay (Bio-Rad Laboratories). Equal amounts of protein (40 μ g) were resolved by 15% SDS-PAGE

and electrotransferred to nitrocellulose membranes and probed with an antibody directed against the cytochrome C (Santa Cruz Biotechnology). Then, membranes were subjected to the same procedures described for immunoblotting.

Flow Cytometry Assay. MCF-7 cells (1×10^6 cells/well) were grown in 6 well plates and shifted to SFM for 24 h before adding treatments for 48 h. Thereafter, cells were trypsinized, centrifuged at 3,000 rpm for 3 min, washed with PBS. Addition of 0.5 μ l of FITC antibodies anti-caspase 9 and anti-caspase 8 (Calbiochem, Milan, Italy) in all samples was performed and then incubated for 45 min in at 37 °C. Cells were centrifuged at 3,000 rpm for 5 min, the pellets were washed with 300 μ l of wash buffer and centrifuged. The last passage was repeated twice, the supernatant removed, and cells dissolved in 300 μ l of wash buffer. Finally, cells were analyzed with the FACScan (Becton Dickinson and Co., Franklin Lakes, NJ).

DNA Fragmentation. DNA fragmentation was determined by gel electrophoresis. MCF-7 cells were grown in 10cm dishes to 70% confluence and exposed to treatments. After 56 h cells were collected and washed with PBS and pelleted at 1,800 rpm for 5 min. The samples were resuspended in 0.5ml of extraction buffer (50mM Tris-HCl, pH 8; 10mM EDTA, 0.5% SDS) for 20 min in rotation at 4 °C. DNA was extracted with phenol-chloroform three times and once with chloroform. The aqueous phase was used to precipitate nucleic acids with 0.1 volumes of 3M sodium acetate and 2.5 volumes cold ethanol overnight at -20 °C. The DNA pellet was resuspended in 15 μ l of H₂O treated with RNase A for 30 min at 37 °C. The absorbance of the DNA solution at 260 and 280 nm was determined by spectrophotometry. The extracted DNA (40 μ g/lane) was subjected to electrophoresis on 1.5% agarose gels. The gels were stained with ethidium bromide and then photographed.

Statistical Analysis. Statistical analysis was performed using one way ANOVA followed by Newman-Keuls testing to determine differences in means or Dunnett's Multiple Comparison test. $P < 0.05$ was considered as statistically significant. Differences were considered significant at values of * $P < 0.05$, ** $P < 0.01$.

Aknowledgements

Prof. S. Andò for providing TM-3 cell line.

Prof. F. Palmieri for donating the OGC antibody.

Prof. M. Przyblyski for IsoElectroFocusing hints and for his laboratory support.

Dr. Stephen H. Safe (Texas A&M University, College Station, TX, USA), for kindly providing the p53 promoter-luciferase plasmids. Dr. S.A. Fuqua for providing MCF-7 TR cell line.

Dr. R. Evans (The Salk Institute, San Diego, CA, USA) for the gift of the pGL3 vector containing three copies of a PPRE sequence upstream of the minimal thymidine kinase promoter ligated to a luciferase reporter gene (3XPPRE-TK-pGL3).

The p53 antisense plasmid (AS/p53) was kindly provided by from Dr. Moshe Oren (Weizmann Institute of Science, Rehovot, Israel).

REFERENCES

- Appling, D.R., Chytil, F. (1981) Evidence of a role for retinoic acid (vitamin A-acid) in the maintenance of testosterone production in male rats, *Endocrinology* 108; 2120–2124.
- Arakawa, K., Ishihara, T., Aoto, M., Inamasu, M. Kitamura, K., and Saito A.: An antidiabetic thiazolidinedione induces eccentric cardiac hypertrophy by cardiac volume overload in rats. *Clin Exp Pharmacol Physiol* 2004, 31:8–13
- Battini, R., Ferrari, S., Kaczmarek, L., Calabretta, B., Chen, S., Baserga, B. Molecular cloning of a cDNA for a human ADP/ATP carrier which is growth regulated. *J Biol Chem* 1987;262: 4355–4359
- Bellovino, D., Apreda, M., Gagnoli, S., Massimi, M., and Gaetani, S. (2003). Vitamin A transport: in vitro models for the study of RBP secretion. *Mol. Aspects Med.* 24, 411-420
- Bhaumik, S.R., Smith, E., and Shilatifard, A. (2007). Covalent modifications of histones during development and disease pathogenesis. *Nat. Struct. Mol. Biol.* 14, 1008–1016
- Bishoff E.D., Gottardis, M.M., Moon, T.E., Heyman, R.A., Lamph, W.W.(1998) Beyond tamoxifen: the retinoid X receptor selective ligand LGD1069 (TARGRETIN) causes complete regression of mammary carcinoma. *Cancer Res* 1998, 58:479-484
- Blomhoff, R. (1994) Transport and metabolism of Vitamin A. *Nutr. Rev.* 52, 13-23
- Bonofiglio, D., Aquila, S., Catalano, S., Gabriele, S., Belmonte, M., Middea, E., Qi, H., Morelli, C., Gentile, M., Maggiolini, M., Andò, S. (2006) Peroxisome proliferator-activated receptor-gamma activates p53 gene promoter binding to the nuclear factor-kappaB sequence in human MCF7 breast cancer cells. *Mol Endocrinol* 20:3083-3092
- Bonofiglio, D., Gabriele, S., Aquila, S., Catalano, S., Gentile, M., Middea, E., Giordano, F., Andò, S. (2005) Estrogen Receptor alpha binds to Peroxisome Proliferator-Activated Receptor (PPAR) Response Element and negatively interferes with PPAR gamma signalling in breast cancer cells. *Clin Cancer Res* 11:6139-6147
- Bonofiglio, D., Gabriele, S., Aquila, S., Qi, H., Belmonte, M., Catalano, S., Andò, S. (2008) Peroxisome proliferator-activated receptor gamma activates fas ligand gene promoter inducing apoptosis in human breast cancer cells. *Breast Cancer Res Treat* Feb 22
- Brandolin, G., Doussiere, J., Gulik, A., Gulik-Krzywicki, T., Lauquin, G.J.M., Vignais, P.V. (1980) Kinetic, binding and ultrastructural properties of the beef heart adenine nucleotide carrier protein after incorporation into phospholipid vesicles. *Biochim Biophys Acta* 592:592-614
- Brandolin, G., Dupont, Y., Vignais, P.V. (1981) Substrate-induced fluorescence change of the isolated ADP/ATP carrier protein in solution. *Biochem Biophys Research Commun* 98:28-35
- Breitman, T. R., and Takahashi, N. (1996). *Biochem. Soc. Trans.* 24, 723–727.
- Bruni, A., Luciani, S., Contessa, A.R.(1964) Inhibition by atractyloside of the binding of adenine nucleotides of rat liver mitochondria. *Nature* 201:1219-1220
- Chambon, P. (1996). A decade of molecular biology of retinoic acid receptors. *FASEB J.* 10, 940-954.
- Chaudhary, L. R., Huston, J. C., and Stocco, D. M. (1989). *Biochem.Biophys. Res. Commun.* 158, 400–406.
- Chen, C., Ko, Y., Delannoy, M., Ludtke, S.J., Chiu, W., Pedersen, P.L. (2004) Mitochondrial ATP Synthasome Three-dimensional structure by electron microscopy of the ATP synthase in complex formation with the carrier for Pi and ADP/ATP. *J Biol Chem* 279:31761-31768
- Chung, S.W., Kang, B.Y., Kim, S.H., Pak, Y.K., Cho, D., Trinchieri, G., Kim, T.S. (2000) Oxidized low density lipoprotein inhibits interleukin-12 production in lipopolysaccharide-activated mouse macrophages via

- direct interactions between peroxisome proliferator-activated receptor- γ and nuclear factor κ B. *J Biol Chem* 275:32681–32687
- Cossarizza, A., Baccarani-Contri, M., Kalashnikova, G., Franceschi, C. (1993) A new method for the cytofluorimetric analysis of mitochondrial membrane potential using the J-aggregate forming lipophilic cation 5,5',6,6'-tetrachloro-1,1',3,3' tetraethylbenzimidazolylcarbo-cyanine iodide (JC-1). *Biochem Biophys Res Commun* 197: 40-45
 - Couturier, C., Brouillet, A., Couriaud, C., Koumanov, K., Bereziat, G., Andreani, M. (1999) Interleukin 1beta induces type II-secreted phospholipase A2 gene in vascular smooth muscle cells by a nuclear factor κ B and peroxisome proliferator-activated receptor-mediated process. *J Biol Chem*, 274:23085–23093
 - Cozens, A.L., Runswick, M.J., Walker, J.E. (1989) DNA sequences of two expressed nuclear genes for human mitochondrial ADP/ATP translocase. *J Mol Biol* 206:261–280
 - Crouch, G.D., and Helman, L.J. (1991) All-trans retinoic acid inhibits the growth of human rhabdomyosarcoma cell lines. *Cancer Res* 51:4882-4887
 - Dahout-Gonzalez, C., Nury, H., Trézéguet, V., Lauquin, G.V., Pebay-Peyroula, E., Brandolin, G. (2006) Molecular, functional and pathological aspects of the mitochondrial ADP/ATP carrier. *Physiology* ;21:242-249
 - Debier, C., and Larondelle, Y. (2005) Vitamins A and E: Metabolism, role and transfer to offspring. *Br. J. Nutr.* 93, 153-174.
 - del Rincon, S.V., Rousseau, C., Samanta, R., and Miller, W.H.Jr. (2003). Retinoic acid-induced growth arrest of MCF-7 involves the selective regulation of the IRS-1/PI3-kinase/AKT pathway. *Oncogene* 22, 3353-3360.
 - Delia, D., Aiello, A., Lombardi, L., Pelicci, P.G., Grignani, F., Formelli, F., Menard, S., Costa, A., Veronesi, U., Pierotti, M.A. (1993) N-(4-hydroxyphenyl) retinamide induces apoptosis of malignant hemopoietic cell lines including those unresponsive to retinoic acid. *Cancer Res*; 53:6036-6041
 - Deltour L, Haselbeck RJ, Luan Ang H, Duester G (1997) *Biol Reprod* 56:102–109
 - Demetri GD, Fletcher CDM, Mueller E, Sarraf P, Naujoks R, Campbell N, Spiegelman BM, Singer S: Induction of solid tumor differentiation by the peroxisome proliferator activated receptor γ ligand troglitazone in patients with liposarcoma. *Proc Natl Acad Sci USA* 1999, 96:3951-3956
 - Di Renzo, J., Soderstrom, M., and Kurokawa, R. (1997) Peroxisome proliferator-activated receptor gamma transcriptionally up-regulates hormone-sensitive lipase via the involvement of specificity protein-1. *Endocrinology* 147: 875-884
 - Dianoux AC, Noël F, Fiore C, Trezeguet V, Kieffer S, Jaquinod M et al. Two distinct regions of the yeast mitochondrial ADP/ATP carrier are photolabeled by a new ADP analogue: 2-azido-3'-O-naphthoyl- $[\beta$ -32P]ADP. Identification of the binding segments by mass spectrometry. *Biochemistry* 2000;39:11477-11487
 - Doerner A, Pauschinger A, Badorff A, Noutsias M, Giessen S, Schulze K et al. Tissue-specific transcription pattern of the adenine nucleotide translocase isoforms in humans. *FEBS Lett* 1997;414:258–262
 - E. Cione, G. Genchi, Characterization of rat testes mitochondrial retinoylating system and its partial purification, *J. Bioenerg. Biomembr.* 36 (2004) 211–217
 - E. Cione, P. Tucci, A. Chimento, V. Pezzi, G. Genchi, Retinoylation reaction of proteins in Leydig (TM-3) cells, *J. Bioenerg. Biomembr.* 37 (2005) 43–48.
 - E. Rial, M. González-Barroso, C. Fleury, S. Iturrizaga, D. Sanchis, J. Jiménez-Jiménez, D. Ricquier, M. Gubern, F. Bouillaud, Retinoids activate proton transport by the uncoupling proteins UCP1 and UCP2, *EMBO J.* 18 (1999) 5827–5833.
 - Elstner E, Müller C, Koshizuka K, Williamson EA, Park D, Asou H, Shintaku P, Said JW, Heber D, Koeffler HP: Ligands for peroxisome proliferator-activated receptor γ and retinoic acid receptor inhibit growth and

- Elstner E, Williamson EA, Zang C, Fritz J, Heber D, Fenner M, Possinger K, Koeffler HP: Novel therapeutic approach: ligands for PPAR γ and retinoid receptors induce apoptosis in bcl-2-positive human breast cancer cells. *Breast Cancer Res Treat* 2002, 74:155–165
- F. Palmieri, The mitochondrial transporter family (SLC25): physiological and pathological implications, *Eur. J. Physiol.* 447 (2004) 689–709.
- Faergeman NJ, Knudsen J., Role of long-chain fatty acyl-CoA esters in the regulation of metabolism and cell signalling. *Biochem J* 1997;323:1-12
- Fiore C, Trezeguet V, Le Saux A, Roux P, Schwimmer C, Dianoux AC, et al. The mitochondrial ADP/ATP carrier: structural, physiological and pathological aspects. *Biochimie* 1998;80:137-150
- Genchi G, Wang W, Barua A, Bi dlack WR, Olson JA. Formation of beta-glucuronides and of beta-galacturonides of various retinoids catalyzed by induced and noninduced microsomal UDP-glucuronosyltransferases of rat liver. *Biochim Biophys Acta.* 1996 Mar 15;1289(2):284-90
- Genchi, G., and Olson, J. A. (2001). *Biochim. Biophys. Acta* 1530, 146–154
- Genschel U. Coenzyme A biosynthesis: reconstruction of the pathway in archaea and an evolutionary scenario based on comparative genomics. *Mol Biol Evol* 2004;21:1242–1251
- Ghyselinck, N. B., Bavik, C., Sapin, V., Mark, M., Bonnier, D., Hidelang, C., Derich, A., Nilsson, C.B., Hakansson, H., Sauvant, P., Azais-Braesco, V., Frasson, M., et al. (1999) Cellular retinol-binding protein I is essential for vitamin A homeostasis. *EMBO J.* 18, 4903-4914
- Gianni, M, Parrella, E., Raska, I., Jr., Gaillard, E., Nigro, e.A., Gaudon, C., Garattini, and Rochette-egly, C. (2006). P38MAPK-dependent phosphorylation and degradation of SRC-3/AIB1 and RAR-alpha mediated transcription. *EMBO J.* 25, 793-751
- Gianni, M., bauer, A., Garattini, e., Chambon, P., and Rochette-Egly, C. (2002). Phosphorylation by p38MAPK and recruitment of SUG-1 are required for RA-induced RAR gamma degradation and transactivation. *EMBO J.* 21, 3760-3769.
- Gianni,M., Ponzanelli, I., Mologni, L., Reichert, U., Rambaldi, A., Terao, M., and Garattini, E. (2000). Retinoid-dependent growth inhibition, differentiation and apoptosis in acute promyelocytic leukemia clls. Expression and activation of caspases. *Cell Death Differ.* 7, 447-460.
- Grommes C, Landreth GE, Heneka MT: Antineoplastic effects of peroxisome proliferator-activated receptor gamma agonists. *Lancet Oncol.* 2004, 5:419-429
- Harvey, P.W. and Everett, D.J. (2003) The adrenal cortex and steroidogenesis as cellular and molecular targets for toxicity: critical omissions from regulatory endocrine disrupter screening strategies for human health? *J Appl Toxicol.* 23, 81-87.
- Harvey, P.W., Everett, D.J. and Springall, C.J. (2007) Adrenal toxicology: a strategy for assessment of functional toxicity to the adrenal cortex and steroidogenesis *J. Appl. Toxicol.* 27, 103–115.
- Heldt HD, Klingenberg M. Differences between the reactivity of endogenous and exogenous adenine nucleotides in mitochondria as studied at low temperature. *Eur J Biochem* 1968;4:1-8.
- Hiscox S, Morgan L, Green TP, Barrow D, Gee J, Nicholson RI: Elevated Src activity promotes cellular invasion and motility in tamoxifen resistant breast cancer cells. *Breast Cancer Res Treat* 2005, 7:1-12
- Huang, M.E., Ye, Y.C., Chen, S.R., Chai, J.R., Lu, J.X., Zhoa, L., Gu, L.J., and Wang, Z.Y. (1988). Use of all-trans retinoic acid in the treatment of acute promyelocytic leukemia. *Blood* 72, 567-572

- Ikawa, H., Kameda, H., Kamitani, H., Baek, S.J., Nixon, J.B., His, L.C., Eling, T.E. (2001) Effect of PPAR activators on cytokine stimulated cyclooxygenase-2 expression in human colorectal carcinoma cells. *Exp Cell Res* 267:73–80
- J. C. Henquin Regulation of insulin secretion: a matter of phase control and amplitude modulation. *Diabetologia* (2009) 52:739–751
- J. C. Henquin Regulation of insulin secretion: a matter of phase control and amplitude modulation. *Diabetologia* (2009) 52:739–751
- J.L. Napoli 17 β -Hydroxysteroid dehydrogenase type 9 and other short-chain dehydrogenases:reductases that catalyze retinoid, 17 β - and 3 α -hydroxysteroid metabolism, *Molecular and Cellular Endocrinology* 171 (2001) 103–109
- Jones HE, Goddard L, Gee JMW, Hiscox S, Rubini M, Barrow D, Knowlden JM., Williams S, Wakeling AE, Nicholson RI: Insulin-like growth factor-I receptor signaling and acquired resistance to gefitinib (ZD1839, Iressa) in human breast and prostate cancer cells. *Endocr Relat Cancer* 2004, 11:793-814
- Kane MA, Chen N, Sparks S, Napoli JL (2005) *Biochem J* 388:363–369
- Kaschula,H.C., Jin, M., Desmond-Smith N.S., Travis G.H. (2006) Acyl CoA:retinol acyltransferase (ARAT) activity is present in bovine retinal pigment epithelium *Experimental Eye Research* 82 111–121
- Kawaguchi, R., Yu, J., Honda, J., Hu, J., Whitelegge, J., Ping, P., Wiita, P., Bok, D., and Sun, H. (2007) *Science* 315, 820–825
- Kitamura S, Miyazaki Y, Shinomura Y, Kondo S, Kanayama S, Matsuzawa Y: Peroxisome proliferator activated receptor γ induces growth arrest and differentiation markers of human colon cancer cells. *Jpn J Cancer Res* 1999, 90:75-80
- Kliewer SA, Umesono K, Mangelsdorf DJ, Evans RM: Retinoid X receptor interacts with nuclear receptors in retinoic acid, thyroid hormone, and vitamin D₃ signaling. *Nature* 1992, 355:446-449
- Klingenberg M, Appel M, Babel W, Aquila H. The binding of bongkrekate to mitochondria. *Eur J Biochem* 1983;131:647-654
- Klingenberg M. In “The Enzymes of Biological Membranes”. Ed.Martonosi AN Plenum Publishing Corp. New York vol. 4 pp 511-553. 1985
- Klingenberg M. Molecular aspects of the adenine nucleotide carrier from mitochondria. *Arch Biochem Biophys* 1989 270:1-14
- Knowlden JM, Hutcheson IR, Jones HE, Madden T, Gee JMW, Harper ME, Barrow D, Wakeling AE, Nicholson RI: Elevated levels of EGFR/c-erbB2 heterodimers mediate an autocrine growth regulatory pathway in Tamoxifen-resistant MCF-7 cells. *Endocrinology* 2003, 144:1032-1044
- Latham, J.A., and Dent, S.Y. (2007). Cross-regulation of histone modifications. *Nat. Struct. Mol. Biol.* 14, 1017–1024.
- Leblanc BP, Stunnenberg HG: 9-cis retinoic acid signaling: changing partners causes some excitement. *Genes Dev* 1995, 9:1811-1816
- Lefebvre, P., Chinetti, G., Fruchart, J.C. and Staels, B. (2006) Sorting out the roles of PPAR α in energy metabolism and vascular homeostasis. *Journal of Clinical Investigation.* 116:571-580.
- Lehrke, M., and Lazar, M.A. (2005) The many faces of PPAR γ . *Cell.* 123:993-999
- Lemberger, T., Desvergne, B., and Wahli, W. (1996) Peroxisome proliferator-activated receptors: a nuclear receptor signaling pathway in lipid physiology. *Annual Review of Cell and Developmental Biology.* 12:335-363
- Liden, M., and Eriksson, U. (2006). Understanding retinol metabolism-structure and function of retinol dehydrogenases. *J.Biol.Chem* 281 (19), 13001-13004.

- Lomo, J., Smeland, E. B., Ulven, S., Natarajan, V., Blomhoff, R., Ghandi, U., Dawson, M. I., and Blomhoff, H.K. (1998). RAR-, not RXR, ligands inhibit cell activation and prevent apoptosis in B-lymphocytes. *J. Cell. Physiol.* 175, 67-77.
- Lonard, D.M., and O'Malley, B.W. (2007). Nuclear receptor coregulators: judges, juries, and executioners of cellular regulation. *Mol. Cell* 27, 691–700.
- M.A. Kane, A.E. Folias, C. Wang, J.L. Napoli, Quantitative profiling of endogenous retinoic acid in vivo and in vitro by tandem mass spectrometry, *Anal. Chem.* 80 (2008) 1702–1708.
- Mangelsdorf, D.J., and Evans, R.M. (1995). The RXR heterodimers and orphan receptors. *Cell* 83, 841-850.
- Mangelsdorf, D.J., Kliewer, S.A., Kakizuka, A., Umesono, K., and Evans, R.M. (1993). Retinoid Receptors. *Recent Prog. Horm. Res.* 48, 99-121.
- Marill, J., Idres, N., Capron, C, Nguyen, E., and Chabot, G.G. (2003). Retinoic acid metabolism and mechanism of action: a review. *Curr. Drug. Metab.* 4, 1-10.
- Mc Ierney, E.M., Rose, D.W., and Flynn, S.E. (1998) Determinants of coactivator LXXLL motif specificity in nuclear receptor transcriptional activation. *Genes and Development* 12:3357-3368.
- Mellon S.H and Vaisse C.(1989) cAMP regulates P450scc gene expression by a cycloheximide insensitive mechanism in cultured mouse Leydig MA-10 cells. *Proc Natl Acad Sci U S A.* 86, 7775-7779.
- Mueller E, Sarraf P, Tontonoz P, Evans RM, Martin KJ, Zhang M, Fletcher C, Singer S, Spiegelman BM: Terminal differentiation of human breast cancer through PPAR γ . *Mol Cell* 1998, 1:465-470
- Myhre, A. M., Hagen, E., Blomhoff, R., and Norum, K. R. (1998). *J.Nutr. Biochem.* 9, 705–711.
- Myhre, A. M., Takahashi, N., Blomhoff, R., Breitman, T. R., and Norum, K. R. (1996). *J. Lipid Res.* 37, 1971–1977
- Napoli, J. L. (1999). Interactions of retinoid binding proteins and enzymes in retinoid metabolism. *Biochim. Biophys. Acta* 1440, 139-162.
- Neckelmann N, Li K, Wade RP, Shustewr R, Wallace DC. cDNA sequence of a human skeletal muscle ADP/ATP translocator: lack of a leader peptide, divergence from a fibroblast translocator cDNA and co-evolution with mitochondrial DNA genes. *Proc Natl Acad Sci USA* 1987;5:829–843
- Notario, B., Zamora, M., Vinas O., Mampel, T. All-trans-retinoic acid binds to and inhibits adenine nucleotide translocase and induces mitochondrial permeability transition, *Mol. Pharmacol.* 63 (2003) 224–231
- Ong. D. E. (1994). Cellular transport and metabolism of vitamin A: Roles of the cellular retinoid-binding proteins. *Nutr. Rev.* 52, 24-31.
- P. Tucci, E. Cione, G. Genchi, Retinoic acid-induced testosterone production and retinoylation reaction are concomitant and exhibit a positive correlation in Leydig (TM-3) cells, *J. Bioenerg. Biomembr* (in press), doi:10.1007/s10863-008-9156
- P.S. Bernstein, S-Y. Choi, Y-C. Ho, R.R. Rando, Photoaffinity labeling of retinoic acidbinding proteins, *Proc. Natl. Acad. Sci. U. S. A.* 92 (1995) 654–658.
- Paik, J., Blaner, W.S., Sommer, K. M., Moe, R., and Swisshlem, K. (2003). Retinoids, retinoic acid receptors, and breast cancer. *Cancer Invest.* 21, 304-312.
- Palmer, C.N.A., Hsu, M.H., Griffin, K.J., and Johnson, E.F. (1995) Novel sequence determinants in peroxisome proliferator signaling. *Journal of Biological Chemistry.* 270:16114-16121.
- Pebay-Peyroula E, Dahout-Gonzalez C, Khan R, Trezeguet V, Lauquin GJM, Brandolin G. Structure of mitochondrial ADP/ATP carrier in complex with carboxyatractyloside. *Nature* 2003;426:39-44
- Pfaff, E., Klingenberg, M., Heldt, H.W (1965) Unspecific permeation and specific exchange of adenine nucleotides in liver mitochondria. *Biochim Biophys Acta* 104:312-315

- Pinaire, J.A., Reifel-Miller, A. (2007) Therapeutic potential of retinoid x receptor modulators for the treatment of the metabolic syndrome. *PPAR Res.* 94153:94156.
- Pingitore, A., Cione, E., Senatore, V., Genchi, G. (2009) Adrenal glands and testes as steroidogenic tissues are affected by retinoylation reaction. *J Bioenerg Biomembr.* 41:215–221
- Radomska-Pandya, A., Chen, G., Czernik, P.J., Little, J.M., Samokyszyn, V.M., Carter, C.A., Nowak G., (2000) Direct interaction of all-trans-retinoic acid with protein kinase C (PKC). Implications for PKC signaling and cancer therapy, *J. Biol. Chem.* 275 22324–22330.
- Ralph, S.J., Low, P., Dong, L., Lawen, A., Neuzil, J (2006) Mitocans: mitochondrial targeted anti-cancer drugs as improved therapies and related patent documents. *Recent Patents Anticancer Drug Discov* 3:1327-1346
- Rangwala, S.M. and Lazar, M.A. (2004) Peroxisome proliferator-activated receptor gamma in diabetes and metabolism. *Trends Pharmacol Sci* 25:331–336
- Renstrom, B., and DeLuca, H. F. (1989). *Biochim. Biophys. Acta* 998, 69–74.
- Richards, J.S., and Hedin, L. (1988) Molecular aspects of hormone action in ovarian follicular development, ovulation, and luteinization. *Annu. Rev. Physiol.* 50, 441-463.
- Roberts-Thomson, S.J. (2000) Peroxisome proliferator activated receptors in tumorigenesis: targets of tumor promotion and treatment. *Immunol Cell Biol* 78:436-441
- Rousseau, C., Nichol, J.N., Petterson, F., Couture, M.C., and Miller, W.H., Jr (2004). ERbeta sensitize breast cancer cell to retinoic acid: Evidence of transcriptional cross talk. *Mol. Canc. Res.* 2, 523-531.
- Rubin, M., Fenig, E., Rosenauer, A., Menendez-Botet, C., Achkar, C., Bentel, J.M., Yahalom, J., Mendelsohn, J., Miller, W.H. (1994) 9-cis retinoic acid inhibits growth of breast cancer cells and downregulates estrogen receptor mRNA and protein. *Cancer Res* 54:6549-6556
- Ruff S.J., Ong D.E., Cellular retinoic acid binding protein is associated with mitochondria, *FEBS Lett.* 487 (2000) 282–286.
- Ruoho, A.E., Woldegiorgis, G., Kobayashi, C., Shrago, E.. (1989) Specific labeling of beef heart mitochondria ADP/ATP carrier with N-(3-iodo-4-azidophenylpropionamido)cysteiny-5-(2'-thiopyridyl)cysteine-coenzyme A (ACT-CoA), a newly synthesized 125I-coenzyme A derivative photolabel. *J Biol Chem* 264:4168-4172
- Saez, J.M. (1994) Leydig cells: Endocrine, paracrine, and autocrine regulation. *Endocr. Rev.* 15, 574-626.
- Schlezinger, J.J., Jensen, B.A., Mann, K.K., Ryu, H.Y., Sherr, D.H. (2002) Peroxisome proliferator-activated receptor γ -mediated NFkB activation and apoptosis in pre-B cells. *J Immunol* 169:6831–6841
- Sivaprasadarao, A., Sundaram, M., and Findlay, J.B. (1998). Interactions of retinol binding protein with transthyretin and its receptors. *Methods. Mol. Biol.* 89, 155-163
- Smiley, S.T., Reers, M., Mottola-Hartshorn, C., Lin, M., Chen, A., Smith, T.W., Steele, G.D., Chen, L.B. (1991) Intracellular heterogeneity in mitochondrial membrane potentials revealed by a J-aggregate forming lipophilic cation JC-1. *Proc Natl Acad Sci USA* 88:3671-3675
- Soprano, D.R., Soprano, K.J. (2003) Role of RARs and RXRs in mediating the molecular mechanism of action of Vitamin A. In “Molecular Nutrition” (J.Zempleni and H. Daniels, Eds), pp. 135-149. CABI, Cambridge, MA
- Staels, B., (2005) Fluid retention mediated by renal PPARgamma. *Cell Metab* 2:77–78
- Stepien, G., Torroni, A., Chung, A.B., Hodge, J.A., Wallace, D.C. (1992) Differential expression of adenine nucleotide translocator isoforms in mammalian tissues and during muscle cell differentiation. *J Biol Chem* 267:14592–14597
- Stocco, D.M. (2001) Tracking the role of a star in the sky of the new millennium, *Mol.Endocrinol.* 15 1245–1254.

- Suh, N., Wang, Y., Williams, C.R., Risingsong, R., Gilmer, T., Willson, T.M., Sporn, M.B. (1999) A new ligand for the peroxisome proliferator-activated receptor-gamma (PPAR-gamma), GW7845, inhibits rat mammary carcinogenesis. *Cancer Res* 59:5671-5673
- Sun S.Y., Yue P., Dawson M.I., Shroot B., Michel S., Lamph W.W., Heyman R.A., Teng M., Chandraratna R.A.S., Shudo K., Hong W.K., Lotan R. (1997) Differential effects of synthetic nuclear retinoid receptor selective retinoids on the growth of human non-small cell lung carcinoma cells. *Cancer Res*, 57:4931-4939
- Sun, Y.X., Wright, H.T., Janciasukiene, S. (2002) Alpha1-Antichymotrypsin/Alzheimer's peptide Abeta (1-42) complex perturbs lipid metabolism and activates transcription factors PPAR γ and NF κ B in human neuroblastoma (Kelly) cells. *J Neurosci Res*, 67:511-522
- Takahashi, N., and Breitman, T. R. (1990). Retinoic acid acylation: retinoylation. *Methods Enzymol.* 189, 233-239.
- Takahashi, N., and Breitman, T. R. (1994). Retinoylation of vimentin in the human myeloid leukemia cell line HL60. *J. Biol. Chem.* 264, 5159-5163.
- Takahashi, N., and Breitman, T. R. (1994). In *Vitamin A in Health and Disease* (Blomhoff, R., ed.), Marcel Dekker, New York, pp. 257-273.
- Thorens, B. Protein kinase A-dependent phosphorylation of GLUT2 in pancreatic β cells. *J. Biol. Chem.* 271, 8075-8081 (1996).
- Tontonoz, P., Hu E., Spiegelman B.M. (1994) Stimulation of adipogenesis in fibroblasts by PPAR gamma 2, a lipid-activated transcription factor. *Cell.* 79:1147-1156
- Tournier, S., Raynaud, F., Gerbaud, P., Lohmann, S. M., Anderson, W.B., and Evain-Brion, D. (1996). *J. Cell. Physiol.* 176, 196-203
- Towler, D. A., Gordon, J. L., Adams, S. P., and Glaser, L. (1988). *Annu. Rev. Biochem.* 57, 69-99.
- Tsubouchi, Y., Sano, H., Kawahito, Y., Mukai, S., Yamada, R., Kohno, M., Inoue, K., Hla, T., Kondo, M. (2000). Inhibition of human lung cancer cell growth by the peroxisome proliferator activated receptor γ agonists through induction of apoptosis. *Biochem Biophys Res Commun*, 270:400-405.
- Vázquez-Memije, M.E., Cárdenas-Méndez, M.J., Tolosa, A. and Hafidi, M.E. (2005) Respiratory chain complexes and membrane fatty acids composition in rat testis mitochondria throughout development and ageing. *Exp. Gerontol.* 40, 482-90.
- Veronesi, U., De Palo, G., Marubini, E., Costa, A., Formelli, F., Mariani, L., Decensi, A., Camerini, T., Del Turco, M.R., Di Mauro, M.R., Muraca, M.G., Del Vecchio, M. Et al.(1999) Randomized trial of fenretinide to prevent second breast malignancy in women with early breast cancer. *J. Natl. Cancer Inst.* 91, 1847-1856.
- Wada, M., Fukui, T., Kubo, Y., and Takahashi, N. (2001). Formation of retinoyl-CoA in rat tissues. *J. Biochem.*130, 457-463
- Waterman, M.R. (1994) Biochemical diversity of cAMP dependent transcription of steroid hydroxylase genes in the adrenal cortex. *J. Biol. Chem.* 269, 27783-27786.
- Waterman, M.R., and Bischof, L.J. (1997) Diversity of ACTH (cAMP)-dependent transcription of bovine steroid hydroxylase genes. *FASEB J.* 11, 419-427.
- Wei, L. N. (2004). Retinoids and receptor interacting protein 140 (RIP140) in gene regulation. *Curr. Med. Chem.* 11, 1527-1532.
- Westin, S., Rosenfeld, M.G., and Glass, C.K. (2000). Nuclear receptor coactivators. *Adv. Pharmacol.* 47, 89-112.
- Weston, A. D., Blumberg, B., and Underhill, T.M. (2003). Active repression by unliganded retinoid receptors in development: less is something more. *J. Cell. Biol.* 161, 223-228

- Wolbach S.B., Howe P.R., Nutrition classics: tissue changes following deprivation of fat soluble A vitamin, *J. Exp. Med.* 42 (1925) 753–777.
- Woldegiorgis, G., Shrago, E., Gipp, J., Yatvin, M. (1981) Fatty acyl coenzyme A-sensitive adenine nucleotide transport in a reconstituted liposome system. *J Biol Chem*;256:12297-12300
- Wu, Q., Dawson, M.I., Zheng, Y., Hobbs, P.D., Agadir, A., Jong, L., Li, Y., Liu, R., Lin, B.Z., Zhang, X.K. (1997) Inhibition of trans retinoic acid resistant human breast cancer cell growth by retinoid X receptor selective retinoids. *Mol Cell Biol* 17:6598-6608
- Xu, L., Glass, C.K., and Rosenfeld, M.G (1999). Coactivator and corepressor complexes in nuclear receptor function. *Curr. Opin. Genet. Dev.* 9, 140-147.
- Yang, Q., Sakurai, Y., and Kakudo, K. (2002). Retinoid, retinoic acid receptor beta and breast cancer. *Breast Cancer Res. Treat.* 76, 167-173
- Yee LD, Williams N, Wen P, Young DC, Lester J, Johnson MV, Farrar WB, Walker MJ, Povoski SP, Suster S, Eng C: Pilot study of rosiglitazone therapy in women with breast cancer: effects of short-term therapy on tumor tissue and serum markers. *Clin Cancer Res* 2007, 13:246-252
- Yuan, C.X., Ito, M., Fondell, J.D., Fu, Z.Y., and Roeder, R.G. (1998) The TRAP220 component of a thyroid hormone receptor associated protein (TRAP) coactivator complex interacts directly with nuclear receptors in a ligand-dependent fashion. *Proc. Natl. Acad. Sci. U. S. A* 95:7939-7944
- Zhang, X.K., Hoffmann, B., Tran, P.B.V., Graupner, G., Pfahl, M. (1992) Retinoid X receptor is an auxiliary protein for thyroid hormone and retinoic acid receptors. *Nature*, 355:441-445

Al Magnifico Rettore
Università della Calabria
SEDE

Presentazione del Collegio dei docenti del Dr. Pingitore Attilio per il conseguimento del titolo di “Dottore di Ricerca in Biochimica Cellulare ed attività dei Farmaci in Oncologia” (XXII ciclo).

L’attività scientifica del Dr. Attilio Pingitore, durante i tre anni del dottorato di Ricerca in “Biochimica Cellulare ed attività dei Farmaci in Oncologia” (XXII ciclo), è stata rivolta allo studio dei meccanismi attraverso cui i retinoidi esercitano i loro effetti in diversi tessuti e linee cellulari tumorali.

Durante il primo anno di dottorato il Dr. Attilio Pingitore ha appreso le tecniche di base (Cromatografia, Western Blotting, colture cellulari, handling di laboratorio) rafforzate da uno stage formativo presso il Centre of Excellence in Drug Discovery della *Glaxosmithkline sede di Verona*, nell’ambito del progetto “Tirocini Farindustria”. Lavorando presso dipartimento di Screening & Compound Profiling (direttore Dr. Wolfgang Jarolimek) ha pertanto appreso metodiche di colture cellulari con organismi geneticamente modificati di livello I e II, saggi Fluorometrici (Tecnologia FLIPR –Fluorometric Imaging Plate Reader) nonché applicazioni statistiche (piattaforme Spotfire® e ActivityBase®). Durante il secondo anno il Dr. Pingitore ha incentrato il suo lavoro sulla caratterizzazione dei meccanismi di retinoilazione in tessuti steroidogenici, apprendendo ed utilizzando metodiche di isolamento di strutture subcellulari (mitocondri, microsomi, membrane) e l’identificazione di proteine sia da tessuti che da linee cellulari immortalizzate. In particolare, il Dr. Pingitore ha rivolto la sua attenzione ai meccanismi di incorporazione di acido retinoico in tessuti steroidogenici e alla capacità dell’acido tutto trans retinoico e dei suoi isomeri di influenzare le attività delle proteine trasportatrici mitocondriali dimostrando come il carrier del 2-oxo glutarato (OGC) venga retinoilato e come la sua attività ne sia influenzata. I dati ottenuti hanno prodotto una pubblicazione internazionale sulla rivista *Biochimica et Biophysica Acta – Molecular and Cell Biology of Lipids (BBA)* e lo stesso lavoro è stato selezionato da parte di una commissione scientifica dei maggiori esperti del campo come Comunicazione Orale al “FASEB Summer Research Conference RETINOIDS 2008” tenutosi a New Haven (CT – USA). Inoltre, il dr. Pingitore ha successivamente studiato e caratterizzato la reazione di retinoilazione nelle ghiandole surrenali, secondo organo steroidogenico per eccellenza, dimostrando come mitocondri di ghiandole surrenali siano in grado di incorporare acido retinoico. I dati ottenuti hanno

prodotto una pubblicazione internazionale sulla rivista internazionale *Journal of Bioenergetics and Biomembranes (JBB)*. Nell'ambito dello studio delle modificazioni post traduzionali, il dr. Pingitore ha frequentato un corso avanzato di Chimica Biologica e dei Polipeptidi presso il *Dipartimento di Chimica* (direttore Prof. M.Przyblyski) del centro di eccellenza europeo presso l' *Università di Costanza (Germania)*, dove ha appreso tecniche di separazione proteica, isoelettrofocalizzazione, 2D SDS PAGE, analisi in proteomica, sintesi chimica (manuale ed automatica) di peptidi e polipeptidi lineari e ramificati, MALDI-TOF analisi, LC/MS/MS e tecniche di bioinformatica. Ha contestualmente svolto, presso lo stesso dipartimento, intensa attività di ricerca in qualità di visiting student, dove ha acquisito i dati necessari alla comprensione del meccanismo di modificazione dell'attività del carrier degli adenin nucleotidi (ANT) da parte del Coenzima A pubblicato sull' *International Journal of Biochemistry and Cell Biology (IJBCB)*. L'attenzione del Dr. Pingitore è stata anche rivolta al ruolo dei retinoidi nell'inibizione della crescita di cellule tumorali mammarie. E' infatti ben noto l'utilizzo sia dei derivati naturali che di sintesi del retinolo come agenti differenzianti e chemioterapici nelle terapie antitumorali, tra cui i tumori al seno, che sono fra le principali cause di morte nelle donne. I principali effetti dei retinoidi sono generalmente mediati da recettori nucleari quali RARs e RXRs. A tale proposito, il dr. Pingitore ha contribuito allo studio degli effetti pro-apoptotici di dosi nutriceutiche dell'acido 9 *cis*-retinoico (9-*cis* RA), ligando specifico di RXR in combinazione con il rosiglitazone (BRL), ligando selettivo di PPAR γ , su diverse linee cellulari di carcinoma mammario, quali MCF-7, MCF-7TR, T47-D, SKBR-3 e la controparte normale MCF-10. Considerato il diverso corredo recettoriale estrogenico che le linee cellulari tumorali studiate presentano, con una diversa responsività alla terapia antiestrogenica, i risultati aprono una nuova prospettiva per un approccio terapeutico basato su un meccanismo alternativo. I risultati hanno portato ad una pubblicazione sulla rivista internazionale *American Journal of Pathology (AJP)*. Il Dr. Pingitore, collaborando con il laboratorio del prof Picci dello stesso ateneo, ha condotto test in vitro sulla capacità delle stearyl-ferulate based solid nanoparticles (SF-SLNs), utilizzate come veicoli per proteggere dalla luce α -tocoferolo e β -carotene, di influenzare la vitalità di cellule di fibroblasti epidermici (RAT-1) risultando coautore di un articolo nella rivista internazionale *Colloids and Surfaces B Biointerfaces (CSBB)*. Nel terzo ed ultimo anno di ricerca il dr. Pingitore, in qualità di Visiting Scholar, presso il *Department of Nutritional Science and Toxicology* (chair J.L.Napoli) della *University of California – Berkeley – USA* - nei laboratori del prof.

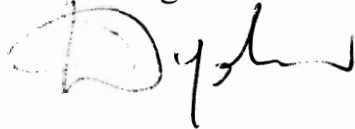
J.L.Napoli, ha rivolto la sua attenzione, utilizzando modelli in vivo (topi C56BL/6 Wild Type e Knock Out) e in vitro (colture cellulari primarie ed immortalizzate), sulla capacità dei derivati della vitamina A di influenzare il metabolismo del glucosio ed il rilascio di insulina. In particolare, gli studi di Glucose Sensing e Glucose Stimulated Insulin Secretion (GSIS) sono stati condotti, attraverso metodiche di ELISA, PCR, Real Time PCR, microscopia confocale. La determinazione dei diversi retinoidi è stata effettuata tramite l' applicazione della LC/MS/MS sistema tandem. I dati ottenuti sono attualmente sotto considerazione da parte della rivista internazionale e multidisciplinare *Science*.

Durante l'intero periodo del dottorato di ricerca il Dr. Attilio Pingitore ha mostrato notevole interesse nell'apprendimento di numerose tecniche laboratoristiche, evidenziando ottime capacità nell'esecuzione dei protocolli sperimentali e nella valutazione dei dati ottenuti. Il contributo scientifico del Dr. Pingitore è dimostrato dai lavori pubblicati su riviste internazionali di prestigio quali American Journal of Pathology, International Journal of Biochemistry and Cell Biology, Biochimica et Biophysica Acta – Molecular and Cell Biology of Lipids, Journal of Bioenergetics and Biomembranes, Colloids and Surfaces B Biointerfaces di cui è co-autore. Pertanto si esprime parere estremamente positivo sull'attività scientifica del Dr. Attilio Pingitore.

Rende, 24-11-2008


Il Coordinatore del Dottorato

Prof Diego Sisci



Il tutor

Dott.ssa Daniela Bonofiglio





Contents lists available at ScienceDirect

The International Journal of Biochemistry & Cell Biology

journal homepage: www.elsevier.com/locate/biocel



Coenzyme A enhances activity of the mitochondrial adenine nucleotide translocator

Erika Cione¹, Attilio Pingitore¹, Francesco Genchi, Giuseppe Genchi*

Department of Pharmaco-Biology, University of Calabria, Edificio Polifunzionale, 87036 Rende (CS), Italy

ARTICLE INFO

Article history:

Received 5 June 2009
Received in revised form 9 September 2009
Accepted 22 September 2009
Available online xxx

Keywords:

Mitochondria
Adenine nucleotide translocator
CoA

ABSTRACT

The adenine nucleotide translocator (ANT) accomplishes the exchange of ATP from the mitochondrial matrix with cytoplasmic ADP. While investigating the biochemical mechanism of retinoic acid (RA) on the ANT via retinoylation, we have found and subsequently demonstrated a positive influence of Coenzyme A (CoA) on the transport of ATP across the membranes of rat liver mitochondria. CoA enhances ANT activity in a dose-dependent manner modifying the V_{max} (673.3 ± 20.7 nmol ATP/mg protein/min versus 155.0 ± 1.9 nmol ATP/mg protein/min), the IC_{50} for the specific inhibitor carboxyatractyloside (CATR) (0.142 ± 0.012 μ M versus 0.198 ± 0.011 μ M) but not the K_m (22.50 ± 0.52 μ M versus 22.19 ± 0.98 μ M). Data suggest a likely enzymatic involvement in the interaction between ANT and CoA. The effect of CoA is observed in mitochondria from several different tissues.

© 2009 Elsevier Ltd. All rights reserved.

1. Introduction

Retinoylation, retinoic acid (RA) acylation, is a post-translational modification of proteins occurring in a variety of eukariotic cell lines and subcellular compartments both in vivo and in vitro (Takahashi and Breitman, 1989). The process occurs in the presence of Mg^{2+} , ATP, and CoA; the omission of these substrates in the in vitro assay incubation buffer markedly reduces the extent of retinoylation (Genchi and Olson, 2001; Cione and Genchi, 2004). The exchange of ADP for ATP generates vital energy: every day each human being synthesizes a quantity of ATP equivalent to his own mass. Adenine nucleotide translocator (ANT) exchanges ADP/ATP across the inner mitochondrial membrane. Discovered about four decades ago (Bruni et al., 1964; Pfaff et al., 1965), ANT is a well-studied protein (Klingenberg, 1989; Fiore et al., 1998) due to its abundance, its sensitivity to transport inhibitors and the robustness of the reconstitution method of transport activity in liposomes (Klingenberg, 1985). Consisting of two identical subunits of about 32 kDa, the ANT is present in two distinct conformational states, namely the cytosolic (c) and the matrix (m) states. The inhibitors carboxyatractyloside (CATR) and atractyloside (ATR) bind to c-state, while bongkreikic acid (BKA) binds to the m-state (Klingenberg et al., 1983). It is also assumed that the ANT is the rate-limiting step in energy metabolism (Heldt and Klingenberg, 1968). It has been demonstrated that Mg^{2+} inhibits the ADP/ATP exchange

and Mg^{2+} -nucleotides are not recognized by the ANT carrier in reconstituted proteoliposomes (Brandolin et al., 1980, 1981).

A previous study by Notario et al. (2003) demonstrated the negative regulation of *all trans* RA on ANT exchange activity. To provide insight to the biochemical mechanism of the *atRA* effect we studied the ANT exchange activity under retinoylating conditions (Genchi and Olson, 2001; Cione and Genchi, 2004). Instead of confirming the negative regulation of the ATP/ADP exchange (Notario et al., 2003) we found a positive modulation of the ANT activity due to the presence of CoA in the buffer rather than RA.

CoA is an enzyme cofactor in various reactions: it functions as an acyl group carrier and carbonyl activating group in numerous reactions central to cellular metabolism, and provides the 4-phosphopantetheine prosthetic group to proteins that play key roles in fatty acid, polyketide and non-ribosomal peptide biosynthesis. As acetyl-CoA, it is essential to the citric acid cycle, to the synthesis and oxidation of ketone bodies and to cholesterol synthesis. The importance of CoA is reflected in conserved biosynthetic pathway across animals, plants and micro-organisms (Genschel, 2004).

Palmitoyl-CoA and long chain acyl-CoA have been shown as potent inhibitors of the ATP/ADP exchange, when added to a suspension of liposomes reconstituted with ANT from rat or bovine heart or liver mitochondria, while CoA and palmitic acid have no effects (Brandolin et al., 1980; Woldegiorgis et al., 1981; Ruoho et al., 1989; Faergeman and Knudsen, 1997). The role of the ANT in energy-linked respiration is an important factor in assessing the potential significance of the acyl-CoA esters as inhibitors and implies that the ANT carrier, like other rate-limiting enzymes, must be carefully regulated. In order to better understand whether CoA

* Corresponding author. Tel.: +39 0984 493454; fax: +39 0984 493271.
E-mail address: genchi@unical.it (G. Genchi).

¹ Equally contributed.

is involved in ANT interaction, we used a novel experimental model that pre-incubates mitochondria in an isotonic buffer to mimic the cellular milieu rather than pre-loading vesicles with CoA or simultaneous addition of CoA with ADP or ATP. It seems reasonable to consider the possibility that the CoA might represent a natural ligand of the translocator; fatty acyl-esters share a common structural backbone with the ANT substrates. Therefore, we studied the activity of ANT after pre-incubation of isolated liver mitochondria into Tris-HCl buffer, pH 7.4, supplied with ATP-Mg²⁺ and CoA. Our results indicate that CoA is responsible for an enhanced transport activity of the ANT carrier protein suggesting a new role of CoA in energy-requiring processes.

2. Materials and methods

2.1. Chemicals

Hydroxyapatite (Bio-Gel HTP) was purchased from Bio-Rad (Milan, Italy); Amberlite XAD-2, ATP, BSA, cardiolipin, CATR, CoA, EDTA, L- α -phosphatidylcholine from egg yolk, PIPES, Tris, Triton X-100 and Triton X-114 from Sigma-Aldrich (Milan, Italy); Sephadex G-75 from Amersham Biosciences (Milan, Italy), [2,8-³H]ATP (32.7 Ci/mmol) and liquid scintillation cocktail Ultima-Flo™ from PerkinElmer (Boston, USA). All other chemicals used were of the highest purity commercially available.

2.2. Isolation of mitochondria

Male Wistar rats (250–300 g) were euthanized, according to practice procedures approved by the ethical committee, and livers were immediately removed. The tissue was first minced and then homogenized in 10 volumes of 250 mM sucrose, 10 mM Tris-HCl, 1 mM EDTA, pH 7.4, by use of a Potter-Elvehjem Teflon homogenizer and the mitochondria were isolated by differential centrifugation as described by Genchi et al. (1996). Mitochondria were then resuspended in sucrose-Tris-EDTA buffer to provide a protein concentration of 15–18 mg/mL. These suspensions were either immediately used or frozen at –70 °C. Protein concentration was measured by the Lowry procedure (Lowry et al., 1951) with bovine serum albumin (BSA) as reference standard. The purity of the mitochondrial preparation was checked by assaying marker enzymes for lysosomes, peroxisomes and plasma membranes.

2.3. Pre-incubation of mitochondria and purification of ANT

Mitochondria (20 mg protein) were pre-incubated in a buffer of 10 mM ATP, 150 μ M CoA, 27 mM MgCl₂, 50 mM sucrose, and 100 mM Tris, pH 7.4, in a final volume of 20 mL at 37 °C for 90 min. Then the suspension was centrifuged in a Sorvall centrifuge at 13,000 \times g for 10 min. The mitochondrial pellet was solubilized in 300 μ L 3% Triton X-100 (w/v), 20 mM Na₂SO₄, 1 mM EDTA, and 10 mM Pipes, pH 7.0. After 15 min at 4 °C, the mixture was centrifuged at 13,000 \times g for 10 min and then 225 μ L of Triton X-100 extract supplemented with 1 mg of cardiolipin were applied to 600 mg dry hydroxylapatite (HTP) column and eluted at 4 °C with the same buffer until the first milliliter was collected (partial purification). 2 mL of HTP eluates were pooled together and applied to a pasteur pipette filled with 1 mL of Matrex Gel Blue B pre-equilibrated with 4 mL 8 M Urea, 4 mL of water and 4 mL of Triton X-100 buffer (0.1% Triton X-100, 20 mM Na₂SO₄, 1 mM EDTA and 5 mM PIPES, pH 7.0) each in sequence. The resin was then eluted with 4 mL of 0.1% Triton X-100 buffer followed by two additions of 800 μ L of 6 mg/mL asolectin in 0.1% Triton X-100 buffer, the latter of which allows the recovery of the total purified ANT. The purity of the sample was verified via SDS PAGE and Coomassie staining (data not shown). Protein concentration was determined by the Lowry

method modified for the presence of Triton (Dulley and Grieve, 1975).

2.4. Reconstitution of the ADP/ATP carrier in liposomes and transport measurements

20 μ g of protein from the HTP eluate were added to 100 μ L of sonicated phospholipids (10%, w/v), 100 μ L of 10% Triton X-114 in 10 mM Pipes, 70 μ L of 200 mM ATP, 230 μ L of 10 mM Pipes, pH 7.0, in a final volume of 700 μ L. This mixture was applied to an Amberlite XAD-2 column for 15 times in agreement with Palmieri and Klingenberg (1979). All the operations were carried out at room temperature. External substrates were removed by a passage of the Amberlite XAD-2 eluate through a Sephadex G-75 column (0.75 cm \times 15 cm) pre-equilibrated with 50 mM NaCl and 10 mM Pipes, pH 7.0. The eluted proteoliposomes were split in 150 μ L aliquots and assayed at 25 °C for the transport measurements by the inhibitor stop method (Palmieri and Klingenberg, 1979), using 0.1 mM [³H]ATP to start the exchange and 20 mM pyridoxal 5'-phosphate to stop it after 10 min. At time zero, the inhibitor and [³H]ATP were added to the control sample. A further passage through a Sephadex G-75 column (0.5 cm \times 8 cm), eluting with 50 mM NaCl, allowed the removal of the external radioactivity. The proteoliposome fractions containing [³H]ATP were collected in 4 mL of scintillation cocktail. The experimental values were corrected by subtracting the respective control. A Tricarb 2100 TR scintillation counter was used and the counting efficiency was about 70–73%. To obtain K_m and V_{max} data, the exchange was performed as described above, stopping the process after 1 min. The kinetic values were calculated by GraphPad® Prism 4 software. When CATR was used, liposomes were preloaded with the inhibitor during the reconstitution passage.

2.5. Isoelectrofocusing and SDS PAGE

9 volumes of ice cold acetone were added to an equivalent volume of 20 μ g of Matrex Gel Blue B eluted protein followed with two washes in the same solvent to allow precipitation of the protein and further removal of interfering substances (like salts and detergent). The pellet was then solubilized in 150 μ L rehydration buffer [128 μ L 1.1 \times Zoom 2D protein solubilizer (Invitrogen), 0.7 μ L 2 M DTT, 0.5% ampholytes, trace of Bromophenol Blue, deionized water to 150 μ L]. A 3–10 IPG strip (Invitrogen) was then carefully covered with the buffer paying attention to provide a homogeneous distribution of the sample under the strip with no formation of air bubbles, according with the ZOOM IPG Runner System protocols provided by the manufacturer, and left overnight at room temperature. Isoelectrofocusing (IEF) was performed following 3 steps: 175 V, 15 min; 175–2000 V ramp, 45 min; 2000 V, 30 min.

Prior to perform the SDS PAGE separation the strip was removed from the IEF chamber, washed with milli-Q distilled water; equilibrated and alkylated with 223 mg iodoacetamide in 10 mL of equilibration buffer at room temperature.

The proteins were resolved into a 18% acrylamide gel with a ratio acrylamide:bisacrylamide of 30:0.2, and visualized with silver stain method.

2.6. Alignment and molecular docking

The 3D structure of the ANT carrier was calculated through homology modelling parameters by Swiss-PDB Viewer software (Guex and Peitch, 1997). The bovine heart ANT, whose crystalline structure has been resolved with a 2.2 Å resolution, was used as template structure (Pebay-Peyroula et al., 2003). In order to reduce steric or/and binding perturbations, the final structure was minimized through the GROMOS96 process (Van Gunsteren et al.,

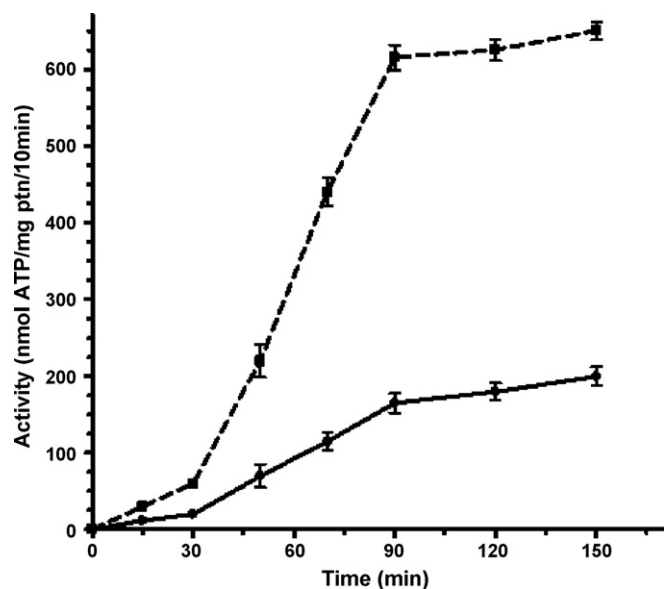


Fig. 1. Time course of ANT activity. Rat liver mitochondria were pre-incubated in 50 mM sucrose, 100 mM Tris-HCl, 10 mM ATP, 27 mM MgCl₂, pH 7.4 (control buffer ■) and in the same buffer supplemented with 150 μM CoA (▲) at 37 °C. At the indicated times the mitochondria were centrifuged, the ANT was extracted and partially purified. The exchange activity was assayed at 25 °C for 10 min as described in Section 2. Results are expressed as mean ± SEM of 3 independent experiments. Overall *P* value < 0.05 (*).

1996) implemented in the Swiss-PDB Viewer. Molecular-docking simulations were performed using the on-line server PatchDock (Sandak et al., 2002; Schneidman-Duhovny et al., 2003) available at <http://bioinfo3d.cs.tau.ac.il/PatchDock/index.html> and the structures were visualized and analyzed with PyMol software (DeLano, 2002).

3. Statistical analysis

Statistical analysis was performed by one-way ANOVA test followed by Dunnett's multiple comparison test. Values are shown as mean ± SEM of *n* independent experiments. Differences were considered significant at values of **P* < 0.05, ***P* < 0.01.

4. Results

The ANT represents the most abundant protein of the inner mitochondrial membrane, spans the inner mitochondrial membrane and allows the exchange of cytosolic ADP for mitochondrial ATP. In all the transport assays described below, the liposomal reconstituted system consisted of partially purified protein. In order to study whether CoA has any influence on the ANT, we used liver mitochondria in isotonic Tris-HCl buffer, pH 7.4, supplied with ATP-Mg²⁺ and CoA as experimental model. The [³H]ATP/ATP exchange was carried out at 25 °C and the transport activity of ANT versus mitochondria pre-incubation time with or without CoA was shown in Fig. 1. In the first section of the graph (0–30 min), there's a linear behaviour with slopes of 0.6 and 2.0, respectively for control and CoA incubation. In the second section (30–90 min), CoA pre-incubation shows a 3.8-fold greater increase in activity compared to control. Both CoA pre-incubated and control samples reach maximum activity at 90 min, that remains constant till 150 min. Therefore a pre-incubation time of 90 min was selected for all subsequent studies.

In order to study how different concentrations of CoA affect the ANT activity, mitochondria were pre-incubated with the coenzyme in a range of 0–150 μM. The treatment induced activation of

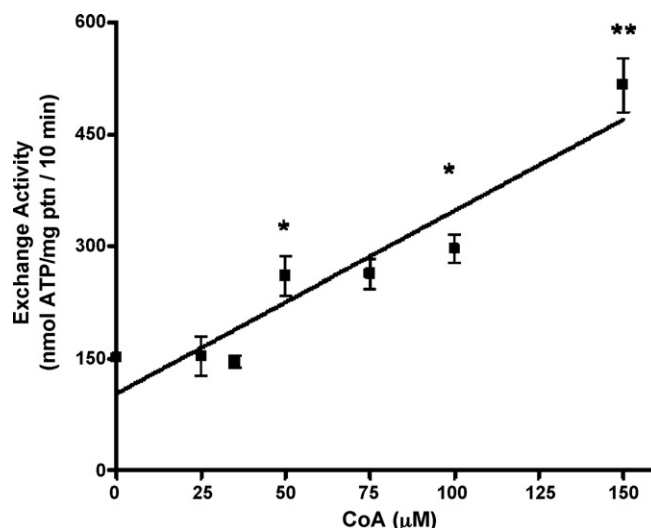


Fig. 2. Effect of CoA concentration on the ANT. After 90 min incubation at 37 °C in 50 mM sucrose, 100 mM Tris-HCl, 10 mM ATP, 27 mM MgCl₂, pH 7.4, in the presence of CoA from 0 to 150 μM, mitochondria were centrifuged and the ANT was extracted and partially purified. The exchange activity was assayed at 25 °C for 10 min as described in Section 2. Data were fit with a straight line and linear regression analysis resulted in a *R*² value of 0.8951. Results are expressed as mean ± SEM of 5 independent experiments. *P* < 0.05 (*) and *P* < 0.01 (**) versus control.

the ANT in a dose-dependent manner was shown in Fig. 2. Linear regression analysis resulted in a *R*² value of 0.8951.

To obtain *K_m* and *V_{max}* values with or without CoA, the dependence of the [³H]ATP/ATP exchange rate on ATP concentration at 25 °C was studied increasing the concentration of external [³H]ATP (in a range of 0–500 μM), while the internal concentration of ATP was constant at 20 mM. Michaelis-Menten equation was used to interpolate our data. In control experiments, *K_m* and *V_{max}* were 22.19 ± 0.98 μM and 155 ± 1.9 nmol ATP/mg protein/min; while with CoA, *K_m* and *V_{max}* were 22.85 ± 2.52 μM and 673.3 ± 20.74 nmol ATP/mg protein/min, respectively (Fig. 3).

3D imaging shows that the interaction between CoA and ANT is located within the cavity (Fig. 4) and molecular docking revealed

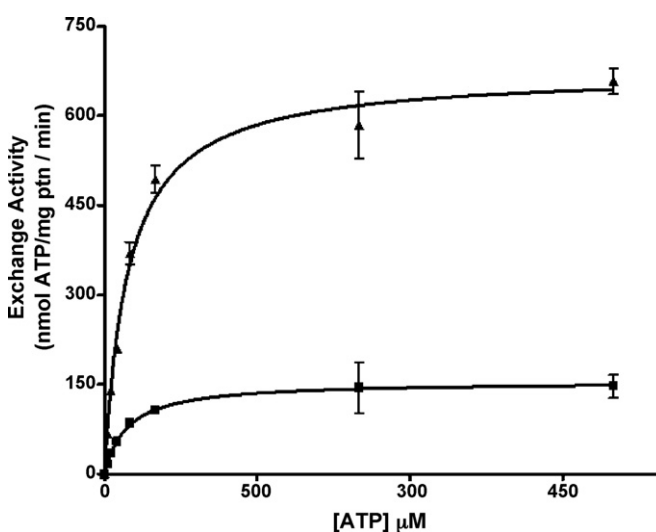


Fig. 3. Kinetic parameters of ATP transport in mitochondria. Mitochondria were pre-incubated in 50 mM sucrose, 100 mM Tris-HCl, 10 mM ATP, 27 mM MgCl₂, pH 7.4 (control buffer ■) and in the same buffer supplemented with 150 μM CoA (▲) at 37 °C. The exchange activity was assayed for 1 min with [³H]ATP, added at concentrations from 0 to 500 μM, at 25 °C. Other experimental procedures as in Fig. 2. Results are expressed as mean ± SEM of 3 independent experiments.

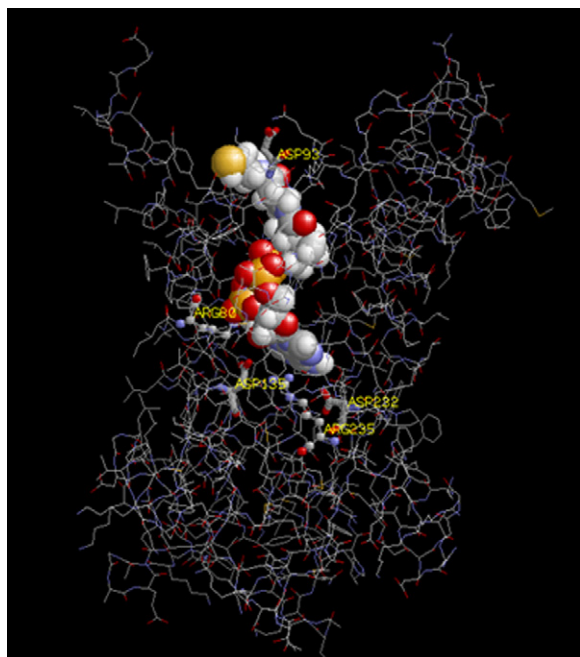


Fig. 4. 3D imaging: interaction between CoA and ANT. The 3D structure of the ANT carrier was calculated through homology modelling parameters by Swiss-PDB Viewer software. The template structure is the bovine heart ANT. The final structure was minimized through the GROMOS96 process implemented in the Swiss-PDB Viewer to reduce steric/binding perturbation. Molecular-docking simulations were performed on the on-line <http://bioinfo3d.cs.tau.ac.il/PatchDock/index.html> server PatchDock and the structures were visualized and analyzed with PyMol software.

that the R80, D135, D232 and R235 residues are all involved in the interaction between CoA and ATP on ANT protein (Table 1). All the above-mentioned amino acids are tightly conserved among species, including humans, and are key positions for CATR interaction resulting in inhibitory effects (Pebay-Peyroula et al., 2003).

To investigate the influence of CoA on the inhibitory effect of CATR on ANT activity, we used 150 μM CoA as described and a range of CATR concentrations from 0 to 10 μM preloaded into liposomes. The most prominent effect occurs at 0.1 μM CATR, where the transport activity of the control was less inhibited compared to the CoA treatment (Fig. 5). At 0.1 μM of inhibitor the ANT transport activity of the CoA-treated mitochondria was reduced of a further 20% compared to the control (60% and 80% of relative exchange activity, respectively). No significant differences were evident at 0.5 and 1 μM CATR, while a slight influence of CoA could be observed at 2 and 10 μM CATR. IC_{50} resulted changed with a value of $0.198 \pm 0.011 \mu\text{M}$ for control and $0.142 \pm 0.012 \mu\text{M}$ for CoA-treated samples.

Table 1
 Molecular docking of CoA and ATP interactions with ANT amino acid residues.

Amino acid residues	Molecular-docking simulation	
	CoA	ATP
R80	HF	HF
D95	LF	NA
D135	HF	NA
D232	VHF	HF
R235	VHF	VHF
R236	VHF	VHF

With the program *Patch-Doc*[®] twelve simulations have been carried out and the percentage of interactions of the binding region of the BTADT1–CATR complex respect to the binding region of the RnADT1–CoA and RnADT1–ATP complexes are expressed as very high frequency (VHF, 12/12), high frequency (HF, 10/12), low frequency (LF, 5/12) and not available (NA).

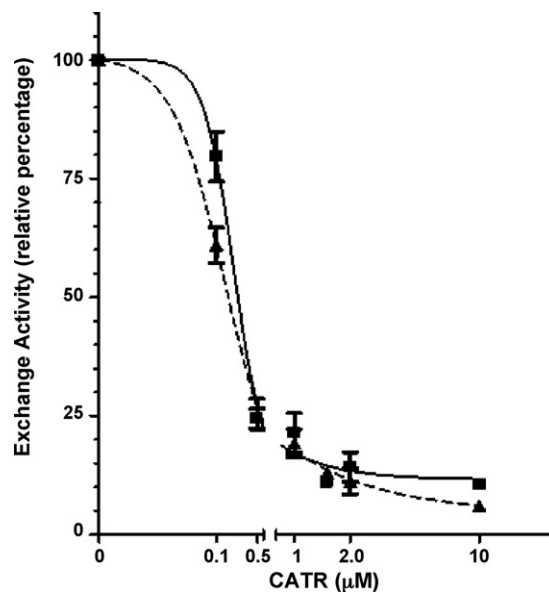


Fig. 5. Inhibition effect of CATR on ANT. Mitochondria were incubated for 90 min in 50 mM sucrose, 100 mM Tris–HCl, 10 mM ATP, 27 mM MgCl₂, pH 7.4 (control buffer ■) and in the same buffer plus 150 μM CoA (▲). Other experimental procedures as in Fig. 2 except that proteoliposomes were pre-loaded with CATR at the indicated concentrations. The exchange activity was assayed at 25 °C for 10 min as described in Section 2. Results are plotted as dose-response curve, $n = 3$. $P < 0.01$ (**) for 0.1 μM CATR versus control.

In order to evaluate the dependence of the observed CoA-induced activation on a specific ANT isoform, mitochondria prepared from different tissues were tested. ANT1 is mainly expressed in heart and skeletal muscle and ANT2 is expressed in tissues able to undergo proliferation, such as liver, while ANT3 is expressed ubiquitously. The highest transport activation was found in heart (6.7 activation fold), followed by liver (3.4 activation fold), and skeleton muscle (2.9 activation fold), while the lowest enhancement of transport activity was detected in brain (2.5 activation fold), as shown in Table 2.

To assess any modification on the protein between CoA-treated and -untreated samples, 2D electrophoresis of purified ANT were run on 18% AA/bisAA gel, resulting in a slightly shift towards the positive side of the IPG strip after CoA treatment (Fig. 6).

5. Discussion

The demonstration that ADP and ATP are the actual substrates for the ANT comes from experiments carried out either with

Table 2
 Exchange activity of ANT isolated from mitochondria of various tissues after pre-incubation, with or without CoA.

Tissue	Exchange activity (nmol ATP/mg ptn/10 min)		Activation fold
	– CoA	+ CoA	
Liver	151.3 \pm 2.6	512.2 \pm 40.8	3.4
Heart	77.7 \pm 4.6	519.0 \pm 7.7	6.7
Skeleton muscle	75.0 \pm 2.9	220.2 \pm 11.5	2.9
Brain	7.7 \pm 1.1	19.6 \pm 2.1	2.5

Mitochondria were pre-incubated for 90 min at 37 °C in 50 mM sucrose, 100 mM Tris–HCl, 10 mM ATP, 27 mM MgCl₂, pH 7.4 (control buffer) and in the same buffer supplemented with 150 μM CoA. ANT was isolated and partially purified. The exchange activities (nmol/mg protein/10 min) were determined as in Section 2. The activation fold was calculated as the ratio between the exchange activity of ANT from mitochondria pre-incubated in control buffer plus 150 μM CoA and control buffer. Results are expressed as mean \pm SEM of 5 independent experiments.

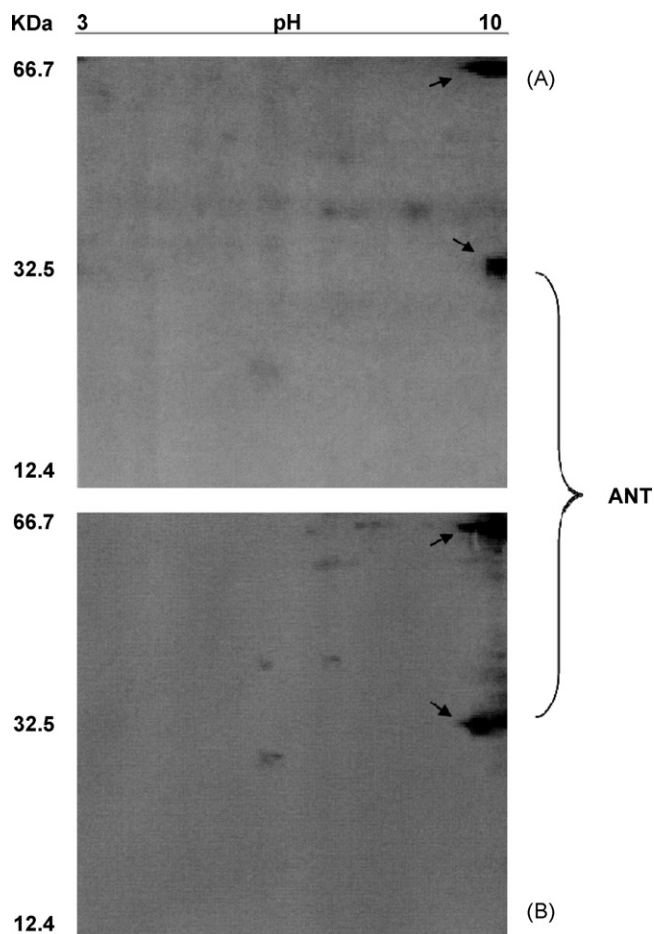


Fig. 6. 2D of ANT protein. Upon visualization with Silver Stain method, two main spots are highlighted at 64 and 32 kDa both in control (A), and in CoA-treated samples (B). Images were acquired in electronic format scanning the gels with a Canonscan Lite 100 scanner, in greyscale with a resolution of 600 DPI.

isolated mitochondria or after incorporation of the purified carrier into liposomes where the effectors were pre-loaded into the vesicles or added simultaneously with the substrates when starting the exchange. In our case, pre-incubation of mitochondria into an isotonic buffer supplemented with CoA led to completely unique results, which are opposite to the general behaviour provided by the literature (Brandolin et al., 1980; Woldegiorgis et al., 1981; Ruoho et al., 1989; Faergeman and Knudsen, 1997). When mitochondria are pre-incubated at 37 °C, the exchange activity of ANT during the first 30 min is almost equal to zero in control sample (20.0 ± 4.5 nmol/mg protein/10 min) and three times higher (60.0 ± 6.3 nmol/mg protein/10 min), when CoA is present (Fig. 1), suggesting that the relationship between ANT and CoA should be enzyme related. Activity rapidly increases between 30 and 90 min for CoA-treated (10.2-fold) and control mitochondria (8.25-fold) further supporting an enzymatic ANT/CoA relationship. The increase in control activity is probably due to endogenous mitochondrial CoA. Both CoA-treated and control reach maximum activity at 90 min (615.0 ± 16.1 nmol/mg protein/10 min and 165.0 ± 13.0 nmol/mg protein/10 min, respectively) leading to the maximum difference in CoA-mediated ANT exchange activity over control. In the 90 min period both curves are sigmoidal with the CoA-mediated activity curve 3–4-fold greater than the control curve additionally supporting a possible enzymatic mechanism. The incubation time of 90 min, the first point of maximum activity, was chosen for subsequent experiments. Once the system over-

comes the lag phase (0–30 min) ANT activity is directly proportional to CoA concentration in the range 0–150 μ M as shown in Fig. 2.

Kinetic properties of ANT were modified in the presence of CoA (Fig. 3). V_{max} , determined in the presence of CoA was more than four fold greater than control. No differences in K_m were observed in the presence of CoA. Enhanced V_{max} indicates a positive modulation of the carrier, suggesting that ANT could be poised to exchange when both anabolic and catabolic CoA-mediated biochemical events, requiring more energy to be transferred from the mitochondrial matrix to the cytoplasm, take place in the cell. Partial purification of ANT by chromatographic passage through an HTP column does not decrease the transport activity of the CoA-treated samples. CoA-mediated enhancement of ANT transport activity is observed in HTP eluates and in crude Triton X-100 extracts (with 4 and 9 nmol ATP/mg protein/10 min for mitochondria pre-incubated in control buffer, and control buffer plus 150 μ M CoA, respectively). Exchange activity of freshly prepared mitochondria, in the presence of CoA was almost tenfold higher than the control (1412.2 ± 52.8 nmol ATP/mg protein/10 min versus 153.7 ± 13.5 nmol ATP/mg protein/10 min). Moreover, because the K_m value is not affected by the CoA treatment, it is reasonable to affirm that the ATP binding site on ANT is not involved in the CoA interaction.

In order to identify the region involved in the CoA–ANT interaction, we performed a molecular-docking simulation. Results of the molecular-docking simulation indicate that R80, D135, D232 and R235 are all involved in the interaction with CoA as shown in Table 1 and Fig. 4. In addition the ATP binds to the same region and the same amino acids that are also responsible for CATR interaction (Pebay-Peyroula et al., 2003). As these simulated results are in contrast with the ones provided by the kinetic profile, we investigated the influence of CoA on CATR effect. The stronger inhibition given at 0.1 μ M (20% more than control) is reflected in a change in the IC_{50} value upon CoA pre-incubation. High concentration of CATR resulted in similar inhibition between control and CoA-treated due to the excess of inhibitor (Fig. 5). This result, together with the unchanged K_m , suggests that the binding site of CoA is different than that given for ATP/CATR. Stronger inhibition of ANT activity by CATR in the presence of CoA implies that the inhibitor interacts more easily with ANT when mitochondria are pre-incubated with CoA. According to Pebay-Peyroula et al. (2003) and our molecular-docking simulations, ATP and CATR share three residues of interaction on the ANT. Thus in absence of CATR, CoA effect would largely be on ATP. This supposition that CoA would facilitate interaction with ATP is consistent with the experimental data shown here: i.e. that ANT exchanges more ATP in presence of CoA. Therefore we can assert that the CoA binds to ANT independently from the ATP/CATR binding site and CoA interaction with the ANT protein leads to an increase in the transport activity as well as an increase in sensitivity to the CATR inhibitor and/or interaction with ATP. CoA shows a homology motif with the ADP both in the structure and in the net superficial charge. Therefore a contact between the protein and the CoA could be justified according to a proximity approach.

The segment spanning residues I311–K318, corresponding to the C-terminal end of the carrier, was also identified as an ADP binding site able to induce a conformational change of the dimeric structure (Dianoux et al., 2000). As CoA does not prevent ATP and CATR from binding ANT, we can hypothesize that the CoA interacts with the accessory site rather than the one localized in the cavity. Subsequently, an interaction between the –SH group of the β -mercaptoethylamine and the neighbour region could take place. More likely, a covalent bond between the –SH group and an acid residue on the portion of the ANT that spans the intermembrane space could be responsible of a “key mechanism” that leads to structure modification of the carrier.

Alternately, because CoA is strictly close to the ANT loops and helices, due to the charge pairing attractions, an enzyme, possibly bound to the outer side of the inner membrane, could provide the necessary enzymatic activity to conjugate the –SH of the CoA with the carrier protein. Based on current data, a CoA derivative or a CoA induced mechanisms cannot be excluded.

As shown in Fig. 6A and B, a shift in one of the bands attributed to the ANT is highlighted. Upon visualization with silver stain technique, two spots, at about 64 and 32 kDa, respectively, appear on both gels, while a 14 kDa protein is stained only in the purified ANT from CoA untreated samples (Fig. 6A). Although we were unable to understand the nature of the lower band, the other two stained proteins can be easily identified as a dimeric and monomeric form of the ANT, whose molecular weight is known to be 31.7 kDa. The purity of the protein sample is guaranteed by the isolation procedure and chromatographic passages on HTP first and Matrex Gel Blue B thereafter, verified with an increase in the specificity of the exchange activity (data not shown).

According to its chemical properties, the ANT is localized around pH 10 on the IPG strip (Fig. 6A): a shift towards the more positive side of the isoelectrofocusing strip upon incubation of rat liver mitochondria with CoA has been detected (Fig. 6B). This shift is most likely due to a modification of the charges on the carrier protein surface, as a result of treatment with CoA.

Although all the ANT isoforms share at least 90% nucleotide sequence identity, they have been implicated differently in several cellular functions (Battini et al., 1987; Neckelmann et al., 1987; Cozens et al., 1989; Stepien et al., 1992; Doerner et al., 1997). We now add the possibility that all the isoforms are similarly involved in the export functions (Table 2). ANT is a portion of ATP synthasome (Chen et al., 2004) and the ANT complex is involved in multiple diseases affecting both humans and animals in which ANT activity is disrupted. Among these, heart diseases, mitochondrial diseases, osteoporosis, macromolecular degeneration, immune deficiency, cystic fibrosis, type II diabetes, ulcers, nephro-toxicity, hearing loss, skin disorders, and cancer are found (Klingenberg, 1989; Dahout-Gonzalez et al., 2006). A new emerging class of drugs, named mitocans, are activators of either VADC or ANT and could be used as promising alternative cancer therapeutics (Ralph et al., 2006). Our findings could provide a novel therapeutic approach for treatment of all the above-mentioned diseases, or just lay the fundamentals for further discoveries in biochemistry.

Additionally, in the literature it is indicated the inhibition of key enzymes in metabolism by long chain acyl-CoA esters, besides the ADP/ATP translocator (Woldegiorgis et al., 1981). Our report that the exchange of ADP/ATP across the mitochondrial membranes is enhanced by CoA may provide insight into these enzymatic mechanisms influenced by CoA and suggest unique interactions and/or structural modifications may exist.

Acknowledgements

The authors thank Prof. Michael Przybiski (University of Konstanz, Germany) for his generous support on IEF and 2D and Dr. Maureen Kane (University of California, Berkeley) for critical reading of the manuscript. This research was supported by grants from Ministero dell'Istruzione, dell'Università e della Ricerca (MIUR, Italia) and IRCCS Associazione Oasi Maria SS.

References

Battini R, Ferrari S, Kaczmarek L, Calabretta B, Chen S, Baserga B. Molecular cloning of a cDNA for a human ADP/ATP carrier which is growth regulated. *J Biol Chem* 1987;262:4355–9.

- Brandolin G, Doussiere J, Gulik A, Gulik-Krzywicki T, Lauquin GJM, Vignais PV. Kinetic, binding and ultrastructural properties of the beef heart adenine nucleotide carrier protein after incorporation into phospholipid vesicles. *Biochim Biophys Acta* 1980;592:592–614.
- Brandolin G, Dupont Y, Vignais PV. Substrate-induced fluorescence change of the isolated ADP/ATP carrier protein in solution. *Biochem Biophys Res Commun* 1981;98:28–35.
- Bruni A, Luciani S, Contessa AR. Inhibition by atractyloside of the binding of adenine nucleotides of rat liver mitochondria. *Nature* 1964;201:1219–20.
- Chen C, Ko Y, Delannoy M, Ludtke SJ, Chiu W, Pedersen PL. Mitochondrial ATP synthasome three-dimensional structure by electron microscopy of the ATP synthase in complex formation with the carrier for Pi and ADP/ATP. *J Biol Chem* 2004;279:31761–8.
- Cione E, Genchi G. Characterization of rat testes mitochondrial retinoylating system and its partial purification. *J Bioenerg Biomembr* 2004;36:211–7.
- Cozens AL, Runswick MJ, Walker JE. DNA sequences of two expressed nuclear genes for human mitochondrial ADP/ATP translocase. *J Mol Biol* 1989;206:261–80.
- Dahout-Gonzalez C, Nury H, Trézéguet V, Lauquin GV, Pebay-Peyroula E, Brandolin G. Molecular, functional and pathological aspects of the mitochondrial ADP/ATP carrier. *Physiology* 2006;21:242–9.
- DeLano WL. The PyMOL Molecular Graphics System. Palo Alto: DeLano Scientific; 2002.
- Dianoux AC, Noël F, Fiore C, Trezeguet V, Kieffer S, Jaquinod M, et al. Two distinct regions of the yeast mitochondrial ADP/ATP carrier are photolabeled by a new ADP analogue: 2-azido-3'-O-naphthoyl-[β -³²P]ADP. Identification of the binding segments by mass spectrometry. *Biochemistry* 2000;39:11477–87.
- Doerner A, Pauschinger A, Badorff A, Noutsias M, Giessen S, Schulze K, et al. Tissue-specific transcription pattern of the adenine nucleotide translocase isoforms in humans. *FEBS Lett* 1997;414:258–62.
- Dulley JR, Grieve PA. A simple technique eliminating interference by detergents in the Lowry method of protein determination. *Anal Biochem* 1975;64:136–41.
- Faergeman NJ, Knudsen J. Role of long-chain fatty acyl-CoA esters in the regulation of metabolism and cell signalling. *Biochem J* 1997;323:1–12.
- Fiore C, Trezeguet V, Le Saux A, Roux P, Schwimmer C, Dianoux AC, et al. The mitochondrial ADP/ATP carrier: structural, physiological and pathological aspects. *Biochimie* 1998;80:137–50.
- Genchi G, Olson JA. retinoylation of protein in cell-free fractions of rat tissue in vitro. *Biochim Biophys Acta* 2001;1530:146–54.
- Genchi G, Wang W, Barua A, Bidlack WR, Olson JA. Formation of β -glucuronides and of β -galacturonides of various retinoids catalyzed by induced and noninduced microsomal UDP-glucuronosyl transferases of rat liver. *Biochim Biophys Acta* 1996;1289:284–90.
- Genschel U. Coenzyme A biosynthesis: reconstruction of the pathway in archaea and an evolutionary scenario based on comparative genomics. *Mol Biol Evol* 2004;21:1242–51.
- Guex N, Peitch MC. SWISS-MODEL and the Swiss-PDB Viewer: an environment for comparative protein modeling. *Electrophoresis* 1997;18:2714–23.
- Heldt HD, Klingenberg M. Differences between the reactivity of endogenous and exogenous adenine nucleotides in mitochondria as studied at low temperature. *Eur J Biochem* 1968;4:1–8.
- Klingenberg M. Martonosi AN, editor. The enzymes of biological membranes, 4. New York: Plenum Publishing Corp; 1985. p. 511–53.
- Klingenberg M. Molecular aspects of the adenine nucleotide carrier from mitochondria. *Arch Biochem Biophys* 1989;270:1–14.
- Klingenberg M, Appel M, Babel W, Aquila H. The binding of bongkrekate to mitochondria. *Eur J Biochem* 1983;131:647–54.
- Lowry OH, Rosebrough NJ, Randall RJ. Protein measurement with the Folin phenol reagent. *J Biol Chem* 1951;193:265–75.
- Neckelmann N, Li K, Wade RP, Shustewr R, Wallace DC. cDNA sequence of a human skeletal muscle ADP/ATP translocator: lack of a leader peptide, divergence from a fibroblast translocator cDNA and co-evolution with mitochondrial DNA genes. *Proc Natl Acad Sci USA* 1987;5:829–43.
- Notario B, Zamora M, Viñas O, Mampel T. All-trans-retinoic acid binds to and inhibits adenine nucleotide translocase and induces mitochondrial permeability transition. *Mol Pharmacol* 2003;63:224–31.
- Palmieri F, Klingenberg M. Direct methods for measuring metabolite transport and distribution in mitochondria. *Methods Enzymol* 1979;56:279–301.
- Pebay-Peyroula E, Dahout-Gonzalez C, Khan R, Trezeguet V, Lauquin GJM, Brandolin G. Structure of mitochondrial ADP/ATP carrier in complex with carboxyatractyloside. *Nature* 2003;426:39–44.
- Pfaff E, Klingenberg M, Heldt HW. Unspecific permeation and specific exchange of adenine nucleotides in liver mitochondria. *Biochim Biophys Acta* 1965;104:312–5.
- Ralph SJ, Low P, Dong L, Lawen A, Neuzil J. Mitocans: mitochondrial targeted anti-cancer drugs as improved therapies and related patent documents. *Recent Patents Anticancer Drug Discov* 2006;3:1327–46.
- Ruoho AE, Woldegiorgis G, Kobayashi C, Shrago E. Specific labelling of beef heart mitochondria ADP/ATP carrier with N-(3-iodo-4-azidophenylpropionamido)cysteiny-5-(2'-thiopyridyl)cysteine-coenzyme A (ACT-CoA), a newly synthesized 125I-coenzyme A derivative photolabel. *J Biol Chem* 1989;264:4168–72.

- Sandak B, Nussinov R, Wolfson HJ. Efficient unbound docking of rigid molecules. In: Proceedings of the 2nd workshop on algorithms in bioinformatics (WABI) lecture notes in computer science, 2452. Springer Verlag; 2002. p. 185–200.
- Schneidman-Duhovny D, Inbar Y, Polak V, Shatsky M, Halperin I, Benyamini H, et al. Taking geometry to its edge: fast unbound rigid (and hinge-bent) docking. *Proteins* 2003;52:107–12.
- Stepien G, Torroni A, Chung AB, Hodge JA, Wallace DC. Differential expression of adenine nucleotide translocator isoforms in mammalian tissues and during muscle cell differentiation. *J Biol Chem* 1992;267:14592–7.
- Takahashi N, Breitman TR. Retinoic acid (retinoylation) of a nuclear protein in the human acute myeloid leukemia cell line HL60. *J Biol Chem* 1989;264:5159–63.
- Van Gunsteren WF, Billeter SR, Eising AA, Hünenberger PH, Krüger P, Mark AE, et al. In: The GROMOS96 manual and user guide. Zurich: Hochschulverlag A.G.; 1996. p. 1–1042.
- Woldegiorgis G, Shrago E, Gipp J, Yatvin M. Fatty acyl coenzyme A-sensitive adenine nucleotide transport in a reconstituted liposome system. *J Biol Chem* 1981;256:12297–300.

Tumorigenesis and Neoplastic Progression

Combined Low Doses of PPAR γ and RXR Ligands Trigger an Intrinsic Apoptotic Pathway in Human Breast Cancer Cells

Daniela Bonofiglio,* Erika Cione,* Hongyan Qi,*
Attilio Pingitore,* Mariarita Perri,*
Stefania Catalano,* Donatella Vizza,*
Maria Luisa Panno,[†] Giuseppe Genchi,*
Suzanne A.W. Fuqua,[‡] and Sebastiano Andò^{1§¶}

From the Departments of Pharmacology¹ and Cellular Biology,² the Centro Sanitario,³ and the Faculty of Pharmacy, Nutritional and Health Sciences,⁴ University of Calabria, Arcavacata di Rende (Cosenza), Italy; and the Lester and Sue Smith Breast Center, Department of Medicine, Baylor College of Medicine, Houston, Texas

Ligand activation of peroxisome proliferator-activated receptor (PPAR) γ and retinoid X receptor (RXR) induces antitumor effects in cancer. We evaluated the ability of combined treatment with nanomolar levels of the PPAR γ ligand rosiglitazone (BRL) and the RXR ligand 9-*cis*-retinoic acid (9RA) to promote antiproliferative effects in breast cancer cells. BRL and 9RA in combination strongly inhibit of cell viability in MCF-7, MCF-7FR1, SKBR-3, and T-47D breast cancer cells, whereas MCF-10 normal breast epithelial cells are unaffected. In MCF-7 cells, combined treatment with BRL and 9RA up-regulated mRNA and protein levels of both the tumor suppressor p53 and its effector p21^{WAF1/CIP1}. Functional experiments indicate that the nuclear factor- κ B site in the p53 promoter is required for the transcriptional response to BRL plus 9RA. We observed that the intrinsic apoptotic pathway in MCF-7 cells displays an ordained sequence of events, including disruption of mitochondrial membrane potential, release of cytochrome *c*, strong caspase 9 activation, and, finally, DNA fragmentation. An expression vector for p53 antisense abrogated the biological effect of both ligands, which implicates involvement of p53 in PPAR γ /RXR-dependent activity in all of the human breast malignant cell lines tested. Taken together, our results suggest that multidrug regimens including a combination of PPAR γ and RXR ligands may provide a therapeutic advantage in breast

cancer treatment. (Am J Pathol 2009, 175:1270–1280; DOI: 10.2353/ajpath.2009.081078)

Breast cancer is the leading cause of death among women in the world. The principal effective endocrine therapy for advanced treatment on this type of cancer is anti-estrogens, but therapeutic choices are limited for estrogen receptor (ER) α -negative tumors, which are often aggressive. The development of cancer cells that are resistant to chemotherapeutic agents is a major clinical obstacle to the successful treatment of breast cancer, providing a strong stimulus for exploring new approaches *in vitro*. Using ligands of nuclear hormone receptors to inhibit tumor growth and progression is a novel strategy for cancer therapy. An example of this is the treatment of acute promyelocytic leukemia using all-*trans* retinoic acid, the specific ligand for retinoic acid receptors.^{1–3} A further paradigm for the use of retinoids in cancer therapy is for early lesions of head and neck cancer⁴ and squamous cell carcinoma of the cervix.⁵

The retinoic acid receptor, retinoid X receptor (RXR), and peroxisome proliferator receptor (PPAR) γ , ligand-activated transcription factors belonging to the nuclear hormone receptor superfamily, are able to modulate gene networks involved in controlling growth and cellular differentiation.⁶ Particularly, heterodimerization of PPAR γ with RXR by their own ligands greatly enhances DNA binding to the direct-repeated consensus sequence AGGTCA, which leads to transcriptional activation.⁷ Previous data show that PPAR γ , poorly expressed in normal breast epithelial cells,⁸ is present at higher levels in

Supported by AIRC, MURST, and Ex 60%.

Portions of this work were presented as an Abstract at Società Italiana di Patologia XXIX National Congress in Rende, Italy, on September 10–13, 2008.

Accepted for publication June 5, 2009.

Supplemental material for this article can be found on <http://ajp.ajmpathol.org>.

Address reprint requests to Prof. Sebastiano Andò, Faculty of Pharmacy Nutritional and Health Sciences, University of Calabria, 87036 Arcavacata - Rende (Cosenza), Italy. E-mail: sebastiano.ando@unical.it.

breast cancer cells,⁹ and its synthetic ligands, such as thiazolidinediones, induce growth arrest and differentiation in breast carcinoma cells *in vitro* and in animal models.^{10–11} Recently, studies in human cultured breast cancer cells show the thiazolidinedione rosiglitazone (BRL), promotes antiproliferative effects and activates different molecular pathways leading to distinct apoptotic processes.^{12–14}

Apoptosis, genetically controlled and programmed death leading to cellular self-elimination, can be initiated by two major routes: the intrinsic and extrinsic pathways. The intrinsic pathway is triggered in response to a variety of apoptotic stimuli that produce damage within the cell, including anticancer agents, oxidative damage, and UV irradiation, and is mediated through the mitochondria. The extrinsic pathway is activated by extracellular ligands able to induce oligomerization of death receptors, such as Fas, followed by the formation of the death-inducing signaling complex, after which the caspases cascade can be activated.

Previous data show that the combination of PPAR γ ligand with either *all-trans* retinoic acid or 9-*cis*-retinoic acid (9RA) can induce apoptosis in some breast cancer cells.¹⁵ Furthermore, Elstner et al demonstrated that the combination of these drugs at micromolar concentrations reduced tumor mass without any toxic effects in mice.⁶ However, in humans PPAR γ agonists at high doses exert many side effects including weight gain due to increased adiposity, edema, hemodilution, and plasma-volume expansion, which preclude their clinical application in patients with heart failure.^{16–18} The undesirable effects of RXR-specific ligands on hypertriglyceridemia and suppression of the thyroid hormone axis have been also reported.¹⁹ Thus, in the present study we have elucidated the molecular mechanism by which combined treatment with BRL and 9RA at nanomolar doses triggers apoptotic events in breast cancer cells, suggesting potential therapeutic uses for these compounds.

Materials and Methods

Reagents

BRL49653 (BRL) was from Alexis (San Diego, CA), the irreversible PPAR γ -antagonist GW9662 (GW), and 9RA were purchased from Sigma (Milan, Italy).

Plasmids

The p53 promoter-luciferase plasmids, kindly provided by Dr. Stephen H. Safe (Texas A&M University, College Station, TX), were generated from the human p53 gene promoter as follows: p53-1 (containing the -1800 to +12 region), p53-6 (containing the -106 to +12 region), p53-13 (containing the -106 to -40 region), and p53-14 (containing the -106 to -49 region).²⁰ As an internal transfection control, we cotransfected the plasmid pRL-CMV (Promega Corp., Milan, Italy) that expresses Renilla luciferase enzymatically distinguishable from firefly luciferase by the strong cytomegalovirus enhancer promoter. The pGL3 vector containing three copies of a peroxisome

proliferator response element sequence upstream of the minimal thymidine kinase promoter ligated to a luciferase reporter gene (3XPPRE-TK-pGL3) was a gift from Dr. R. Evans (The Salk Institute, San Diego, CA). The p53 anti-sense plasmid (AS/p53) was kindly provided from Dr. Moshe Oren (Weizmann Institute of Science, Rehovot, Israel).

Cell Cultures

Wild-type human breast cancer MCF-7 cells were grown in Dulbecco's modified Eagle's medium-F12 plus glutamax containing 5% newborn calf serum (Invitrogen, Milan, Italy) and 1 mg/ml penicillin-streptomycin. MCF-7 tamoxifen resistant (MCF-7TR1) breast cancer cells were generated in Dr. Fuqua's laboratory similar to that described by Herman²¹ maintaining cells in modified Eagle's medium with 10% fetal bovine serum (Invitrogen), 6 ng/ml insulin, penicillin (100 units/ml), streptomycin (100 μ g/ml), and adding 4-hydroxytamoxifen in tentfold increasing concentrations every weeks (from 10^{-9} to 10^{-6} final). Cells were thereafter routinely maintained with 1 μ mol/L 4-hydroxytamoxifen. SKBR-3 breast cancer cells were grown in Dulbecco's modified Eagle's medium without red phenol, plus glutamax containing 10% fetal bovine serum and 1 mg/ml penicillin-streptomycin. T-47D breast cancer cells were grown in RPMI 1640 medium with glutamax containing 10% fetal bovine serum, 1 mmol/L sodium pyruvate, 10 mmol/L HEPES, 2.5g/L glucose, 0.2 U/ml insulin, and 1 mg/ml penicillin-streptomycin. MCF-10 normal breast epithelial cells were grown in Dulbecco's modified Eagle's medium-F12 plus glutamax containing 5% horse serum (Sigma), 1 mg/ml penicillin-streptomycin, 0.5 μ g/ml hydrocortisone, and 10 μ g/ml insulin.

Cell Viability Assay

Cell viability was determined with the 3-(4,5-dimethylthiazol-2-yl)-2,5-diphenyltetrazolium (MTT) assay.²² Cells (2×10^5 cells/ml) were grown in 6 well plates and exposed to 100 nmol/L BRL, 50 nmol/L 9RA alone or in combination in serum free medium (SFM) and in 5% charcoal treated (C1)-fetal bovine serum; 100 μ l of MTT (5 mg/ml) were added to each well, and the plates were incubated for 4 hours at 37°C. Then, 1 ml 0.04 N HCl in isopropanol was added to solubilize the cells. The absorbance was measured with the Ultrospec 2100 Pro-spectrophotometer (Amersham-Biosciences, Milan, Italy) at a test wavelength of 570 nm.

Immunoblotting

Cells were grown in 10-cm dishes to 70% to 80% confluence and exposed to treatments in SFM as indicated. Cells were then harvested in cold PBS and resuspended in lysis buffer containing 20 mmol/L HEPES (pH 8), 0.1 mmol/L EGTA, 5 mmol/L MgCl₂, 0.5 M/L NaCl, 20% glycerol, 1% Triton, and inhibitors (0.1 mmol/L sodium orthovanadate, 1% phenylmethylsulfonyl fluoride, and 20

mg/ml aprotinin). Protein concentration was determined by Bio-Rad Protein Assay (Bio-Rad Laboratories, Hercules, CA). A 40 μ g portion of protein lysates was used for Western blotting, resolved on a 10% SDS-polyacrylamide gel, transferred to a nitrocellulose membrane, and probed with an antibody directed against the p53, p21^{WAF1/CIP1} (Santa Cruz Biotechnology, CA). As internal control, all membranes were subsequently stripped (0.2 M/L glycine, pH 2.6, for 30 minutes at room temperature) of the first antibody and reprobed with anti-glyceraldehyde-3-phosphate dehydrogenase antibody (Santa Cruz Biotechnology). The antigen-antibody complex was detected by incubation of the membranes for 1 hour at room temperature with peroxidase-coupled goat anti-mouse or anti-rabbit IgG and revealed using the enhanced chemiluminescence system (Amersham Pharmacia, Buckinghamshire UK). Blots were then exposed to film (Kodak film, Sigma). The intensity of bands representing relevant proteins was measured by Scion Image laser densitometry scanning program.

Reverse Transcription-PCR Assay

MCF-7 cells were grown in 10 cm dishes to 70% to 80% confluence and exposed to treatments in SFM as indicated. Total cellular RNA was extracted using TRIZOL reagent (Invitrogen) as suggested by the manufacturer. The purity and integrity were checked spectroscopically and by gel electrophoresis before carrying out the analytical procedures. Two micrograms of total RNA were reverse transcribed in a final volume of 20 μ l using a RETROscript kit as suggested by the manufacturer (Promega). The cDNAs obtained were amplified by PCR using the following primers: 5'-G1GGAAGGAAATTTGCG1GT-3' (p53 forward) and 5'-CCAGTGTGATGATGGTGAGG-3' (p53 reverse), 5'-CC1TCATGCCAGCTACTTCC-3' (p21 forward) and 5'-CTGTGCTCACTTCAGGGTCA-3' (p21 reverse), 5'-CTCAA-CATCTCCCCCTTCTC-3' (36B4 forward) and 5'-CAAA-TCCCATATCCTCGTCC-3' (36B4 reverse) to yield, respectively, products of 190 bp with 18 cycles, 270 bp with 18 cycles, and 408 bp with 12 cycles. To check for the presence of DNA contamination, reverse transcription (RT)-PCR was performed on 2 μ g of total RNA without Monoley murine leukemia virus reverse transcriptase (the negative control). The results obtained as optical density arbitrary values were transformed to percentage of the control taking the samples from untreated cells as 100%.

Transfection Assay

MCF-7 cells were transferred into 24-well plates with 500 μ l of regular growth medium/well the day before transfection. The medium was replaced with SFM on the day of transfection, which was performed using Fugene 6 reagent as recommended by the manufacturer (Roche Diagnostics, Mannheim, Germany) with a mixture containing 0.5 μ g of promoter-luc or reporter-luc plasmid and 5 ng of pRL-CMV. After transfection for 24 hours, treatments were added in SFM as indicated, and cells were incubated for an additional 24 hours. Firefly and Renilla

luciferase activities were measured using the Dual Luciferase Kit (Promega). The firefly luciferase values of each sample were normalized by Renilla luciferase activity, and data were reported as relative light units.

MCF-7 cells plated into 10 cm dishes were transfected with 5 μ g of AS/p53 using Fugene 6 reagent as recommended by the manufacturer (Roche Diagnostics). The activity of AS/p53 was verified using Western blot to detect changes in p53 protein levels. Empty vector was used to ensure that DNA concentrations were constant in each transfection.

Electrophoretic Mobility Shift Assay

Nuclear extracts from MCF-7 cells were prepared as previously described.²³ Briefly, MCF-7 cells plated into 10-cm dishes were grown to 70% to 80% confluence, shifted to SFM for 24 hours, and then treated with 100 nmol/L BRL, 50 nmol/L 9RA alone and in combination for 6 hours. Thereafter, cells were scraped into 1.5 ml of cold PBS, pelleted for 10 seconds, and resuspended in 400 μ l cold buffer A (10 mmol/L HEPES-KOH [pH 7.9] at 4°C, 1.5 mmol/L MgCl₂, 10 mmol/L KCl, 0.5 mmol/L dithiothreitol, 0.2 mmol/L phenylmethylsulfonyl fluoride, and 1 mmol/L leupeptin) by flicking the tube. Cells were allowed to swell on ice for 10 minutes and were then vortexed for 10 seconds. Samples were then centrifuged for 10 seconds and the supernatant fraction was discarded. The pellet was resuspended in 50 μ l of cold Buffer B (20 mmol/L HEPES-KOH [pH 7.9], 25% glycerol, 1.5 mmol/L MgCl₂, 420 mmol/L NaCl, 0.2 mmol/L EDTA, 0.5 mmol/L dithiothreitol, 0.2 mmol/L phenylmethylsulfonyl fluoride, and 1 mmol/L leupeptin) and incubated in ice for 20 minutes for high-salt extraction. Cellular debris was removed by centrifugation for 2 minutes at 4°C, and the supernatant fraction (containing DNA-binding proteins) was stored at -70°C. The probe was generated by annealing single-stranded oligonucleotides and labeled with [³²P]ATP (Amersham Pharmacia) and T4 polynucleotide kinase (Promega) and then purified using Sephadex G50 spin columns (Amersham Pharmacia). The DNA sequence of the nuclear factor (NF) κ B located within p53 promoter as probe is 5'-AGTTGAGGGGACTT-TCCCAGGC-3' (Sigma Genosys, Cambridge, UK). The protein-binding reactions were performed in 20 μ l of buffer [20 mmol/L HEPES (pH 8), 1 mmol/L EDTA, 50 mmol/L KCl, 10 mmol/L dithiothreitol, 10% glycerol, 1 mg/ml bovine serum albumin, 50 μ g/ml polydeoxyinosinic deoxycytidylic acid] with 50,000 cpm of labeled probe, 20 μ g of MCF7 nuclear protein, and 5 μ g of polydeoxyinosinic deoxycytidylic acid. The mixtures were incubated at room temperature for 20 minutes in the presence or absence of unlabeled competitor oligonucleotides. For the experiments involving anti-PPAR γ and anti-RXR α antibodies (Santa Cruz Biotechnology), the reaction mixture was incubated with these antibodies at 4°C for 30 minutes before addition of labeled probe. The entire reaction mixture was electrophoresed through a 6% polyacrylamide gel in 0.25 \times Tris borate-EDTA for 3 hours at 150 V. Gel was dried and subjected to autoradiography at -70°C.

Chromatin Immunoprecipitation Assay

MCF-7 cells were grown in 10 cm dishes to 50% to 60% confluence, shifted to SFM for 24 hours, and then treated for 1 hour as indicated. Thereafter, cells were washed twice with PBS and cross-linked with 1% formaldehyde at 37°C for 10 minutes. Next, cells were washed twice with PBS at 4°C, collected and resuspended in 200 μ l of lysis buffer (1% SDS, 10 mmol/L EDTA, 50 mmol/L Tris-HCl, pH 8.1), and left on ice for 10 minutes. Then, cells were sonicated four times for 10 seconds at 30% of maximal power (Vibra Cell 500 W; Sonics and Materials, Inc., Newtown, CT) and collected by centrifugation at 4°C for 10 minutes at 14,000 rpm. The supernatants were diluted in 1.3 ml of immunoprecipitation buffer (0.01% SDS, 1.1% Triton X-100, 1.2 mmol/L EDTA, 16.7 mmol/L Tris-HCl [pH 8.1], 16.7 mmol/L NaCl) followed by immunoclearing with 60 μ l of sonicated salmon sperm DNA/protein A agarose (DBA Srl, Milan, Italy) for 1 hour at 4°C. The precleared chromatin was immunoprecipitated with anti-PPAR γ , anti-RXR α , or anti-RNA Pol II antibodies (Santa Cruz Biotechnology). At this point, 60 μ l salmon sperm DNA/protein A agarose was added, and precipitation was further continued for 2 hours at 4°C. After pelleting, precipitates were washed sequentially for 5 minutes with the following buffers: Wash A [0.1% SDS, 1% Triton X-100, 2 mmol/L EDTA, 20 mmol/L Tris-HCl (pH 8.1), 150 mmol/L NaCl]; Wash B [0.1% SDS, 1% Triton X-100, 2 mmol/L EDTA, 20 mmol/L Tris-HCl (pH 8.1), 500 mmol/L NaCl]; and Wash C [0.25 M LiCl, 1% NP-40, 1% sodium deoxycholate, 1 mmol/L EDTA, 10 mmol/L Tris-HCl (pH 8.1)], and then twice with 10 mmol/L Tris, 1 mmol/L EDTA. The immunocomplexes were eluted with elution buffer (1% SDS, 0.1 M/L NaHCO₃). The eluates were reverse cross-linked by heating at 65°C and digested with proteinase K (0.5 mg/ml) at 45°C for 1 hour. DNA was obtained by phenol-chloroform-isoamyl alcohol extraction. Two microliters of 10 mg/ml yeast tRNA (Sigma) were added to each sample, and DNA was precipitated with 95% ethanol for 24 hours at -20°C and then washed with 70% ethanol and resuspended in 20 μ l of 10 mmol/L Tris, 1 mmol/L EDTA buffer. A 5 μ l volume of each sample was used for PCR with primers flanking a sequence present in the p53 promoter: 5'-CTGAGAGCAAACGCAAAAG-3' (forward) and 5'-CAGCCCGAACGCAAAGTGTC-3' (reverse) containing the κ B site from -254 to -42 region. The PCR conditions for the p53 promoter fragments were 45 seconds at 94°C, 40 seconds at 57°C, and 90 seconds at 72°C. The amplification products obtained in 30 cycles were analyzed in a 2% agarose gel and visualized by ethidium bromide staining. The negative control was provided by PCR amplification without a DNA sample. The specificity of reactions was ensured using normal mouse and rabbit IgG (Santa Cruz Biotechnology).

JC-1 Mitochondrial Membrane Potential Detection Assay

The loss of mitochondrial membrane potential was monitored with the dye 5,5',6,6'-tetra-chloro-1,1',3,3'-tetraeth-

ylbenzimidazolyl-carbocyanine iodide (JC-1) (Biotium, Hayward). In healthy cells, the dye stains the mitochondria bright red. The negative charge established by the intact mitochondrial membrane potential allows the lipophilic dye, bearing a delocalized positive charge, to enter the mitochondrial matrix where it aggregates and gives red fluorescence. In apoptotic cells, the mitochondrial membrane potential collapses, and the JC-1 cannot accumulate within the mitochondria, it remains in the cytoplasm in a green fluorescent monomeric form.²¹ MCF-7 cells were grown in 10 cm dishes and treated with 100 nmol/L BRL and/or 50 nmol/L 9RA for 48 hours, then cells were washed in ice-cold PBS, and incubated with 10 mmol/L JC-1 at 37°C in a 5% CO₂ incubator for 20 minutes in darkness. Subsequently, cells were washed twice with PBS and analyzed by fluorescence microscopy. The red form has absorption/emission maxima of 585/590 nm. The green monomeric form has absorption/emission maxima of 510/527 nm. Both healthy and apoptotic cells can be visualized by fluorescence microscopy using a wide band-pass filter suitable for detection of fluorescein and rhodamine emission spectra.

Cytochrome C Detection

Cytochrome C was detected by western blotting in mitochondrial and cytoplasmic fractions. Cells were harvested by centrifugation at 2500 rpm for 10 minutes at 4°C. The pellets were suspended in 36 μ l RIPA buffer plus 10 μ g/ml aprotinin, 50 mmol/L PMSF and 50 mmol/L sodium orthovanadate and then 4 μ l of 0.1% digitonine were added. Cells were incubated for 15 minutes at 4°C and centrifuged at 12,000 rpm for 30 minutes at 4°C. The resulting mitochondrial pellet was resuspended in 3% Triton X-100, 20 mmol/L Na₂SO₄, 10 mmol/L PIPES, and 1 mmol/L EDTA (pH 7.2) and centrifuged at 12,000 rpm for 10 minutes at 4°C. Proteins of the mitochondrial and cytosolic fractions were determined by Bio-Rad Protein Assay (Bio-Rad Laboratories). Equal amounts of protein (40 μ g) were resolved by 15% SDS-polyacrylamide gel electrophoresis, electrotransferred to nitrocellulose membranes, and probed with an antibody directed against the cytochrome C (Santa Cruz Biotechnology). Then, membranes were subjected to the same procedures described for immunoblotting.

Flow Cytometry Assay

MCF-7 cells (1×10^6 cells/well) were grown in 6 well plates and shifted to SFM for 24 hours before adding treatments for 48 hours. Thereafter, cells were trypsinized, centrifuged at 3000 rpm for 3 minutes, washed with PBS. Addition of 0.5 μ l of fluorescein isothiocyanate-conjugated antibodies, anti-caspase 9 and anti-caspase 8 (Calbiochem, Milan, Italy), in all samples was performed and then incubated for 45 minutes in at 37°C. Cells were centrifuged at 3000 rpm for 5 minutes, the pellets were washed with 300 μ l of wash buffer and centrifuged. The last passage was repeated twice, the supernatant removed, and cells dissolved in 300 μ l of wash buffer.

Finally, cells were analyzed with the FACScan (Becton Dickinson and Co., Franklin Lakes, NJ).

DNA Fragmentation

DNA fragmentation was determined by gel electrophoresis. MCF-7 cells were grown in 10 cm dishes to 70% confluence and exposed to treatments. After 56 hours cells were collected and washed with PBS and pelleted at 1800 rpm for 5 minutes. The samples were resuspended in 0.5 ml of extraction buffer (50 mmol/L Tris-HCl, pH 8; 10 mmol/L EDTA, 0.5% SDS) for 20 minutes in rotation at 4°C. DNA was extracted three times with phenol-chloroform and one time with chloroform. The aqueous phase was used to precipitate nucleic acids with 0.1 volumes of 3M sodium acetate and 2.5 volumes cold ethanol overnight at -20°C. The DNA pellet was resuspended in 15 µl of H₂O treated with RNase A for 30 minutes at 37°C. The absorbance of the DNA solution at 260 and 280 nm was determined by spectrophotometry. The extracted DNA (40 µg/lane) was subjected to electrophoresis on 1.5% agarose gels. The gels were stained with ethidium bromide and then photographed.

Statistical Analysis

Statistical analysis was performed using analysis of variance followed by Newman-Keuls testing to determine differences in means. *P* < 0.05 was considered as statistically significant.

Results

Nanomolar Concentrations of the Combined BRL and 9RA Treatment Affect Cell Viability in Breast Cancer Cells

Previous studies demonstrated that micromolar doses of PPAR_γ ligand BRL and RXR ligand 9RA exert antiproliferative effects on breast cancer cells.^{13,15,25-26} First, we tested the effects of increasing concentrations of both ligands on breast cancer cell proliferation at different times in the presence or absence of serum media (see Supplemental Figure 1 at <http://ajp.amjpathol.org>). Thus, to investigate whether low doses of combined agents are able to inhibit cell growth, we assessed the capability of 100 nmol/L BRL and 50 nmol/L 9RA to affect normal and malignant breast cell lines. We observed that treatment with BRL alone does not elicit any significant effect on cell viability in all breast cell lines tested, while 9RA alone reduces cell vitality only in T47-D cells (Figure 1A). In the presence of both ligands, cell viability is strongly reduced in all breast cancer cells: MCF-7, its variant MCF-7TR1, SKBR-3, and T-47D; while MCF-10 normal breast epithelial cells are completely unaffected (Figure 1A). In MCF-7 cells the effectiveness of both ligands in reducing tumor cell viability still persists in SFM, as well as in 5% CT-FBS (Figure 1B).

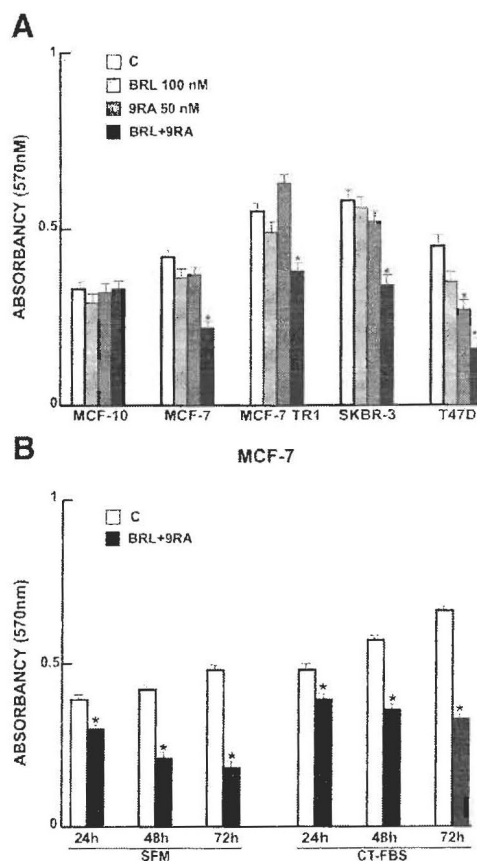


Figure 1. Cell vitality in breast cell lines. **A:** Breast cells were treated for 48 hours in SFM in the presence of 100 nmol/L BRL or/and 50 nmol/L 9RA. Cell vitality was measured by MTT assay. Data are presented as mean ± SD of three independent experiments done in triplicate. **B:** MCF-7 cells were treated for 24, 48, and 72 hours with 100 nmol/L BRL and 50 nmol/L 9RA in the presence of SFM and 5% CT-FBS. **P* < 0.05 and ***P* < 0.01 treated versus untreated cells.

BRL and 9RA Up-Regulate p53 and p21^{WAF1/Cip1} Expression in MCF-7 Cells

Our recent work demonstrated that micromolar doses of BRL activate PPAR_γ, which in turn triggers apoptotic events through an up-regulation of p53 expression.¹⁷ On the basis of these results, we evaluated the ability of nanomolar doses of BRL and 9RA alone or in combination to modulate p53 expression along with its natural target gene p21^{WAF1/Cip1} in MCF-7 cells. A significant increase in p53 and p21^{WAF1/Cip1} content was observed by Western blot only on combined treatment after 24 and 36 hours (Figure 2A). Furthermore, we showed an up-regulation of p53 and p21^{WAF1/Cip1} mRNA levels induced by BRL plus 9RA after 12 and 24 hours (Figure 2B).

Low Doses of PPAR_γ and RXR Ligands Transactivate p53 Gene Promoter

To investigate whether low doses of BRL and 9RA are able to transactivate the p53 promoter gene, we transiently transfected MCF-7 cells with a luciferase reporter construct (named p53-1) containing the upstream region of the p53 gene spanning from -1800 to +12 (Figure

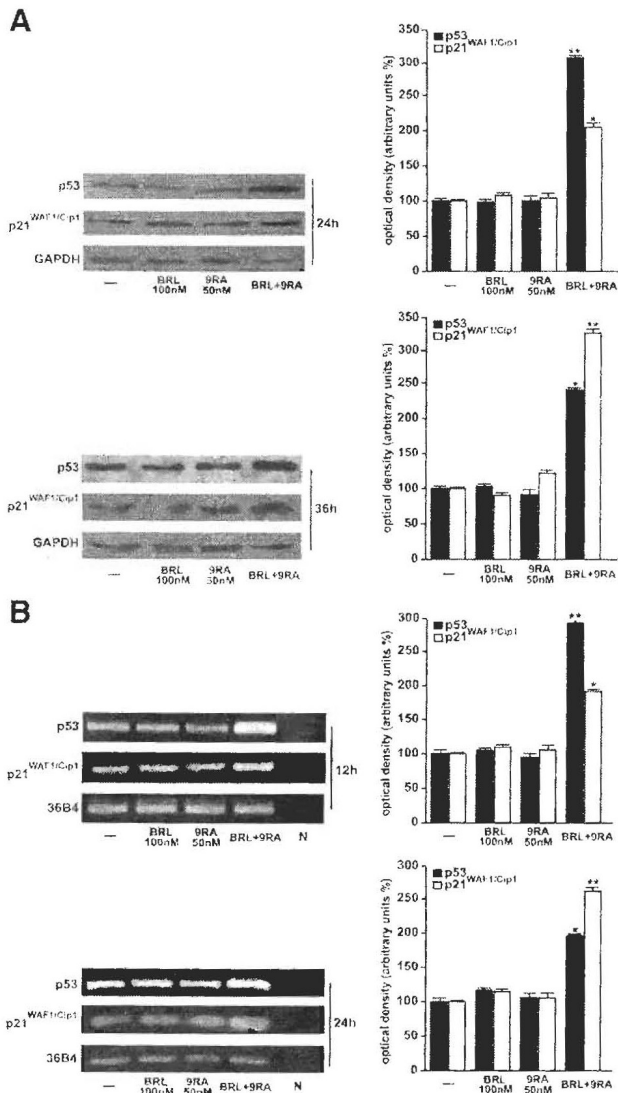


Figure 2. Upregulation of p53 and p21^{WAF1/Cip1} expression induced by BRL plus 9RA in MCF-7 cells. **A:** Immunoblots of p53 and p21^{WAF1/Cip1} from extracts of MCF-7 cell treated with 100 nmol/L BRL and 50 nmol/L 9RA alone or in combination for 24 and 36 hours. GAPDH was used as loading control. The side panels show the quantitative representation of data (mean \pm SD) of three independent experiments after densitometry. **B:** p53 and p21^{WAF1/Cip1} mRNA expression in MCF-7 cells treated as in A for 12 and 24 hours. The side panels show the quantitative representation of data (mean \pm SD) of three independent experiments after densitometry and correction for 36B4 expression. * $P < 0.05$ and ** $P < 0.01$ combined treated versus untreated cells. N: RNA sample without the addition of reverse transcriptase (negative control).

3A). Treatment for 24 hours with 100 nmol/L BRL or 50 nmol/L 9RA did not induce luciferase expression, whereas the presence of both ligands increased in the transactivation of p53-1 promoter (Figure 3B). To identify the region within the p53 promoter responsible for its transactivation, we used constructs with deletions to different binding sites such as CTF-1, nuclear factor-Y, NF κ B, and GC sites (Figure 3A). In transfection experiments performed using the mutants p53-6 and p53-13 encoding the regions from -106 to +12 and from -106 to -40, respectively, the responsiveness to BRL plus 9RA was still observed (Figure 3B). In contrast, a construct with a deletion in the NF κ B domain (p53-14) encoding the sequence from -106 to -49, the transactiva-

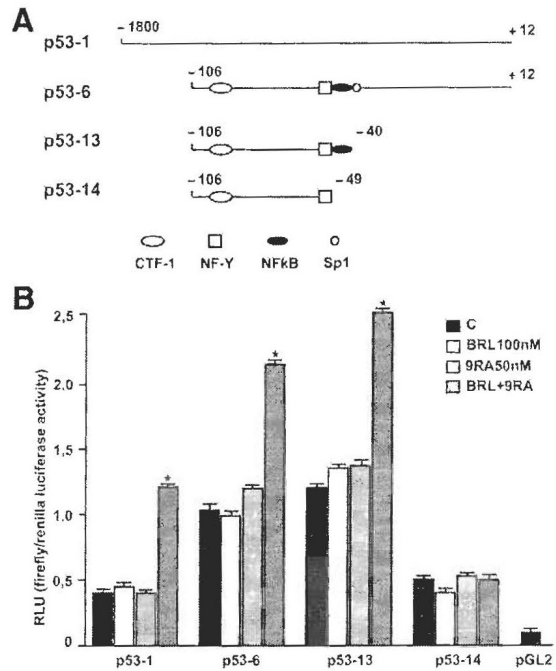


Figure 3. BRL and 9RA transactivate p53 promoter gene in MCF-7 cells. **A:** Schematic map of the p53 promoter fragments used in this study. **B:** MCF-7 cells were transiently transfected with p53 gene promoter luciferase constructs (p53-1, p53-6, p53-13, p53-14) and treated for 24 hours with 100 nmol/L BRL and 50 nmol/L 9RA alone or in combination. The luciferase activities were normalized to the Renilla luciferase as internal transfection control and data were reported as RLU values. Columns are mean \pm SD of three independent experiments performed in triplicate. * $P < 0.05$ combined treated versus untreated cells. pGL2: basal activity measured in cells transfected with pGL2 basal vector; RLU, relative light units; CTF-1, CCAAT-binding transcription factor-1; NF-Y, nuclear factor-Y; NF κ B, nuclear factor- κ B.

tion of p53 by both ligands was absent (Figure 3B), suggesting that NF κ B site is required for p53 transcriptional activity.

Heterodimer PPAR γ /RXR α binds to NF κ B Sequence in Electrophoretic Mobility Shift Assay and in Chromatin Immunoprecipitation Assay

To gain further insight into the involvement of NF κ B site in the p53 transcriptional response to BRL plus 9RA, we performed electrophoretic mobility shift assay experiments using synthetic oligodeoxyribonucleotides corresponding to the NF κ B sequence within p53 promoter. We observed the formation of a specific DNA binding complex in nuclear extracts from MCF-7 cells (Figure 4A, lane 1), where specificity is supported by the abrogation of the complex by 100-fold molar excess of unlabeled probe (Figure 4A, lane 2). BRL treatment induced a slight increase in the specific band (Figure 4A, lane 3), while no changes were observed on 9RA exposure (Figure 4A, lane 4). The combined treatment increased the DNA binding complex (Figure 4A, lane 5), which was immunodepleted and supershifted using anti-PPAR γ (Figure 4A, lane 6) or anti-RXR α (Figure 4A, lane 7) antibodies. These data indicate that heterodimer PPAR γ /RXR α binds to NF κ B site located in the promoter of p53 *in vitro*.

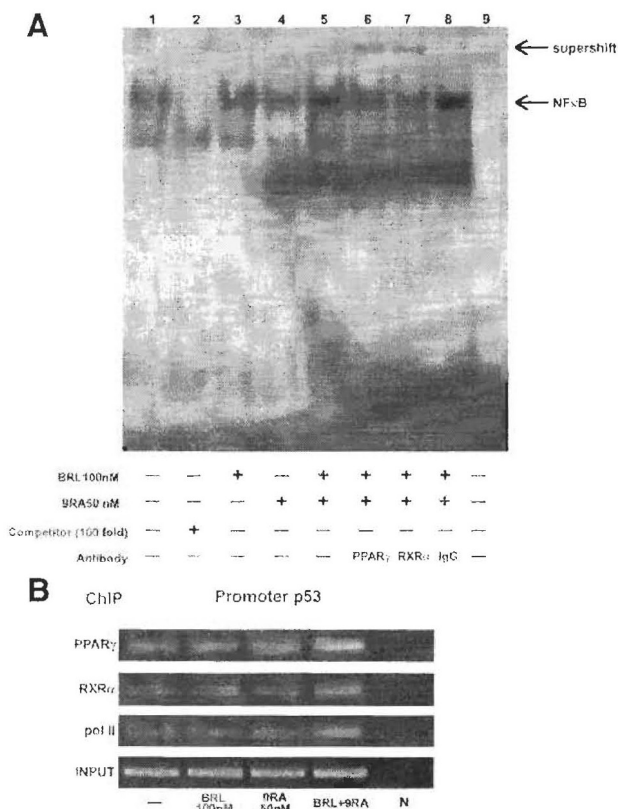


Figure 4. PPAR_γ/RXR_α binds to NF κ B sequence in electrophoretic mobility shift assay and in chromatin immunoprecipitation assay. **A:** Nuclear extracts from MCF-7 cells (lane 1) were incubated with a double-stranded NF κ B consensus sequence probe labeled with [³²P] and subjected to electrophoresis in a 6% polyacrylamide gel. Competition experiments were done, adding as competitor a 100-fold molar excess of unlabeled probe (lane 2). Nuclear extracts from MCF-7 were treated with 100 nmol/L BRL (lane 3), 50 nmol/L 9RA (lane 4), and in combination (lane 5). Anti-PPAR_γ (lane 6), anti-RXR_α (lane 7), and IgG (lane 8) antibodies were incubated. Lane 9 contains probe alone. **B:** MCF-7 cells were treated for 1 hour with 100 nmol/L BRL and/or 50 nmol/L 9RA as indicated, and then cross-linked with formaldehyde and lysed. The soluble chromatin was immunoprecipitated with anti-PPAR_γ, anti-RXR_α, and anti-RNA Pol II antibodies. The immunocomplexes were reverse cross-linked, and DNA was recovered by phenol/chloroform extraction and ethanol precipitation. The p53 promoter sequence containing NF κ B was detected by PCR with specific primers. To control input DNA, p53 promoter was amplified from 30 μ l of initial preparations of soluble chromatin (before immunoprecipitation). N: negative control provided by PCR amplification without DNA sample.

The interaction of both nuclear receptors with the p53 promoter was further elucidated by chromatin immunoprecipitation assays. Using anti-PPAR_γ and anti-RXR_α antibodies, protein-chromatin complexes were immunoprecipitated from MCF-7 cells treated with 100 nmol/L BRL and 50 nmol/L 9RA. PCR was used to determine the recruitment of PPAR_γ and RXR_α to the p53 region containing the NF κ B site. The results indicated that either PPAR_γ or RXR_α was constitutively bound to the p53 promoter in untreated cells and this recruitment was increased on BRL plus 9RA exposure (Figure 4B). Similarly, an augmented RNA-Pol II recruitment was obtained by immunoprecipitating cells with an anti-RNA-Pol II antibody, indicating that a positive regulation of p53 transcription activity was induced by combined treatment (Figure 4B).

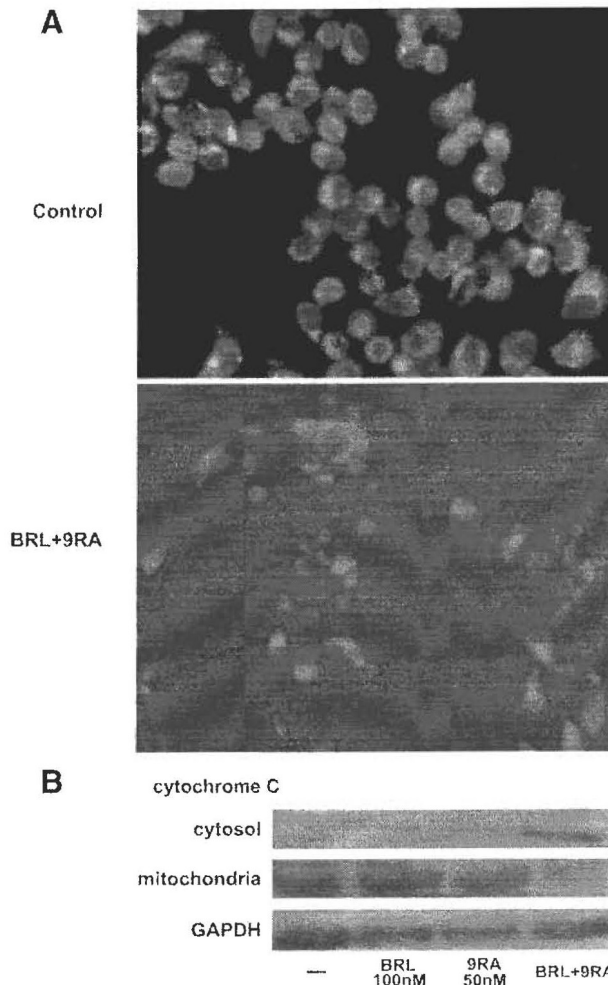


Figure 5. Mitochondrial membrane potential disruption and release of cytochrome C induced by BRL and 9RA in MCF-7 cells. **A:** MCF-7 cells were treated with 100 nmol/L BRL plus 50 nmol/L 9RA for 48 hours and then used fluorescence microscopy to analyze the results of JC-1 (5,5',6,6'-tetrachloro-1,1',3,3'-tetraethylbenzimidazolylcarbocyanine iodide) kit. In control non-apoptotic cells, the dye stains the mitochondria red. In treated apoptotic cells JC-1 remains in the cytoplasm in a green fluorescent form. **B:** MCF-7 cells were treated for 48 hours with 100 nmol/L BRL and/or 50 nmol/L 9RA. GAPDH was used as loading control.

BRL and 9RA Induce Mitochondrial Membrane Potential Disruption and Release of Cytochrome C from Mitochondria into the Cytosol in MCF-7 Cells

The role of p53 signaling in the intrinsic apoptotic cascades involves a mitochondria-dependent process, which results in cytochrome C release and activation of caspase-9. Because disruption of mitochondrial integrity is one of the early events leading to apoptosis, we assessed whether BRL plus 9RA could affect the function of mitochondria by analyzing membrane potential with a mitochondria fluorescent dye JC-1.^{24,27} In non-apoptotic cells (control) the intact mitochondrial membrane potential allows the accumulation of lipophilic dye in aggregated form in mitochondria, which display red fluorescence (Figure 5A). MCF-7 cells treated with 100 nmol/L BRL or 50 nmol/L 9RA exhibit red fluorescence indicating

Table 1. Activation of caspases in MCF-7 cells

	% of Activation	SD
Caspase 9		
Control	14.16	\pm 2.565
BRL 100 nmol/L	17.23	\pm 1.678
9RA 50 nmol/L	18.14	\pm 0.986
BRL + 9RA	33.88*	\pm 5.216
Caspase 8		
Control	9.20	\pm 1.430
BRL 100 nmol/L	8.12	\pm 1.583
9RA 50 nmol/L	7.90	\pm 0.886
BRL + 9RA	10.56	\pm 2.160

Cells were stimulated for 48 hours in presence of 100 nmol/L BRL and 50 nmol/L 9RA, alone or in combination. The activation of caspase 9 and caspase 8 was analyzed by flow cytometry. Data are presented as mean \pm SD of triplicate experiments. **P* < 0.05 combined-treated versus untreated cells

intact mitochondrial membrane potential (data not shown). Cells treated with both ligands exhibit green fluorescence, indicating disrupted mitochondrial membrane potential, where JC-1 cannot accumulate within the mitochondria, but instead remains as a monomer in the cytoplasm (Figure 5A). Concomitantly, cytochrome C release from mitochondria into the cytosol, a critical step in the apoptotic cascade, was demonstrated after combined treatment (Figure 5B).

Caspase-9 Cleavage and DNA Fragmentation Induced by BRL Plus 9RA in MCF-7 Cells

BRL and 9RA at nanomolar concentration did not induce any effects on caspase-9 separately, but activation was observed in the presence of both compounds (Table 1). No effects were elicited by either the combined or the

separate treatment on caspase-8 activation, a marker of extrinsic apoptotic pathway (Table 1). Since internucleosomal DNA degradation is considered a diagnostic hallmark of cells undergoing apoptosis, we studied DNA fragmentation under BRL plus 9RA treatment in MCF-7 cells, observing that the induced apoptosis was prevented by either the PPAR γ -specific antagonist GW or by AS/p53, which is able to abolish p53 expression (Figure 6A).

To test the ability of low doses of both BRL and 9RA to induce transcriptional activity of PPAR γ , we transiently transfected a peroxisome proliferator response element reporter gene in MCF-7 cells and observed an enhanced luciferase activity, which was reversed by GW treatment (see Supplemental Figure 2 at <http://ajp.amjpathol.org>). These data are in agreement with previous observations demonstrating that PPAR γ /RXR heterodimerization enhances DNA binding and transcriptional activation.^{16, 20}

Finally, we examined in three additional human breast malignant cell lines: MCF-7 TR1, SKBR-3, and T-47D the capability of low doses of a PPAR γ and an RXR ligand to trigger apoptosis. DNA fragmentation assay showed that only in the presence of combined treatment did cells undergo apoptosis in a p53-mediated manner (Figure 6B), implicating a general mechanism in breast carcinoma.

Discussion

The key finding of this study is that the combined treatment with low doses of a PPAR γ and an RXR ligand can selectively affect breast cancer cells through cell growth inhibition and apoptosis.

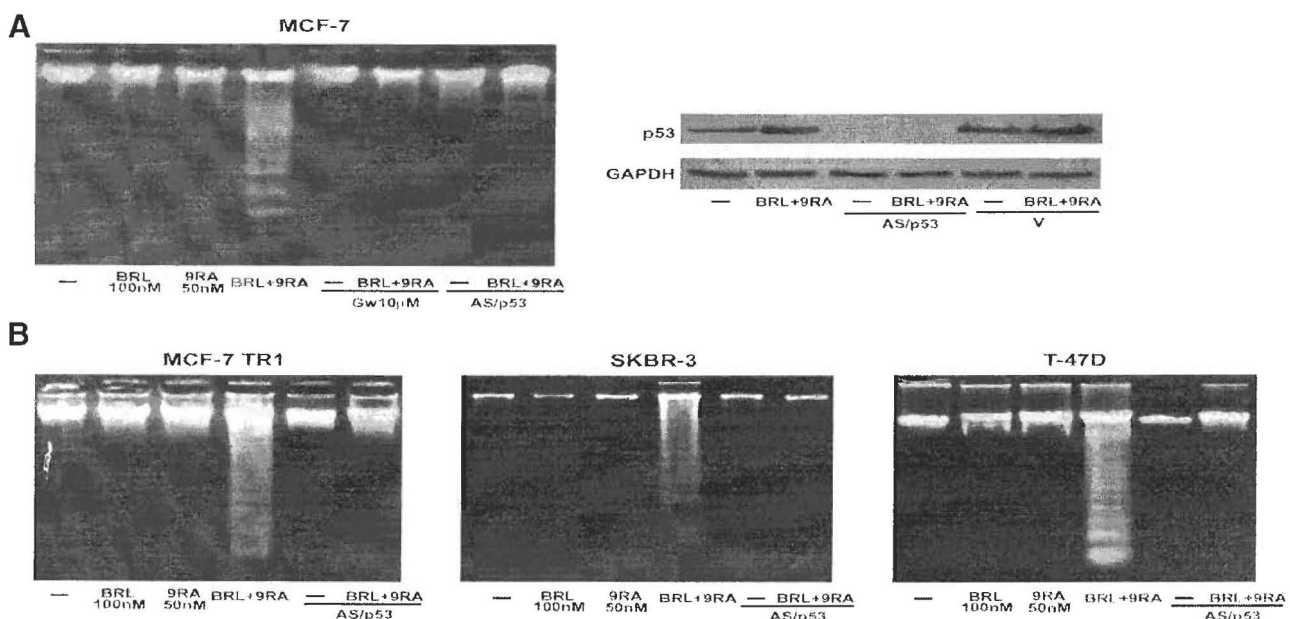


Figure 6. Combined treatment of BRL and 9RA trigger apoptosis in breast cancer cells. **A:** DNA laddering was performed in MCF-7 cells transfected and treated as indicated for 50 hours. One of three similar experiments is presented. The side panel shows the immunoblot of p53 from MCF-7 cells transfected with an expression plasmid encoding for p53 antisense (AS-p53) or empty vector (V) and treated with 100 nmol/L BRL plus 50 nmol/L 9RA for 50 hours. GAPDH was used as loading control. **B:** DNA laddering was performed in MCF-7 TR1, SKBR-3, and T-47D cells transfected with AS-p53 or empty vector (V) and treated as indicated. One of three similar experiments is presented.

The ability of PPAR γ ligands to induce differentiation and apoptosis in a variety of cancer cell types, such as human lung,³⁰ colon,³¹ and breast,¹⁹ has been exploited in experimental cancer therapies.³² PPAR γ agonist administration in liposarcoma patients resulted in histological and biochemical differentiation markers *in vivo*.³³ However, a pilot study of short-term therapy with the PPAR γ ligand rosiglitazone in early-stage breast cancer patients did not elicit significant effects on tumor cell proliferation, although the changes observed in PPAR γ expression may be relevant to breast cancer progression.³⁴ On the other hand, the natural ligand for RXR, 9RA,³⁵ has been effective *in vitro* against many types of cancer, including breast tumor.^{36–40} Recently, RXR-selective ligands were discovered to inhibit proliferation of all-*trans* retinoic acid-resistant breast cancer cells *in vitro* and caused regression of the disease in animal models.⁴¹ The additive antitumoral effects of PPAR γ and RXR agonists, both at elevated doses, have been shown in human breast cancer cells (^{15,42} and references therein). However, high doses of both ligands have remarkable side effects in humans, such as weight gain and plasma volume expansion for PPAR γ ligands,^{16–19} and hypertriglyceridemia and suppression of the thyroid hormone axis for RXR ligands.¹⁹

In the present study, we demonstrated that nanomolar concentrations of BRL and 9RA in combination exert significant antiproliferative effects on breast cancer cells, whereas they do not induce noticeable influences on normal breast epithelial MCF10 cells. However, the induced overexpression of PPAR γ in MCF10 cells makes these cells responsive to the low combined concentration of BRL and 9RA (data not shown). Although PPAR γ is known to mediate differentiation in most tissues, its role in either tumor progression or suppression is not yet clearly elucidated. It has been demonstrated in animals studies that an overexpression of PPAR γ increases the risk of breast cancer already in mice susceptible to the disease.⁴³ However, it remains still questionable if the enhanced PPAR γ expression does correspond to an enhanced content of functional protein, which according to previous suggestion should be carefully controlled in a dose-response study.⁴⁴ For instance, the expression of PPAR γ is under complex regulatory mechanisms, sustained by cell-specific distinct promoters mediating the changes in expression of PPAR γ .⁴⁵

Here we demonstrated for the first time the molecular mechanism underlying antitumoral effects induced by combined low doses of both ligands in MCF-7 cells, where an up-regulation of tumor suppressor gene p53 was concomitantly observed. Functional assays with deletion constructs of the p53 promoter showed that the NF κ B site is required for the transcriptional response to BRL plus 9RA treatment. NF κ B was shown to physically interact with PPAR γ ,⁴⁶ which in some circumstances binds to DNA cooperatively with NF κ B.^{47–49} It has been previously reported that micromolar doses of both PPAR γ and RXR agonists synergize to generate an increased level of NF κ B-DNA binding able to trigger apoptosis in Pre-B cells.⁵⁰ Our electrophoretic mobility shift assay and chromatin immunoprecipitation assay demonstrated that

PPAR γ /RXR α complex is present on p53 promoter in the absence of exogenous ligand. Only BRL and 9RA in combination increased the binding and the recruitment of either PPAR γ or RXR α on the NF κ B site located in the p53 promoter sequence. BRL plus 9RA at the doses tested also increased the recruitment of RNA-Pol II to p53 promoter gene illustrating a positive transcriptional regulation able to produce a consecutive series of events in the apoptotic pathway.

Changes in mitochondrial membrane permeability, an important step in the induction of cellular apoptosis, is concomitant with collapse of the electrochemical gradient across the mitochondrial membrane, through the formation of pores in the mitochondria leading to the release of cytochrome C into the cytoplasm, and subsequently with cleavage of procaspase-9. This cascade of events, featuring the mitochondria-mediated death pathway, was detected in BRL plus 9RA-treated MCF-7 cells. The activation of caspase 9, in the presence of no changes in the biological activity of caspase 8, support that in our experimental model only the intrinsic apoptotic pathway is the effector of the combined treatment with the two ligands.

The crucial role of p53 gene in mediating apoptosis is raised by the evidence that the effects on the apoptotic cascade were abrogated in the presence of AS/p53 in all breast cancer cell lines tested, including tamoxifen resistant breast cancer cells. In tamoxifen-resistant breast cancer cells, other authors have observed that epidermal growth factor receptor, insulin-like growth factor-1R, and c-Src signaling are constitutively activated and responsible for a more aggressive phenotype consistent with an increased motility and invasiveness.^{51–53} Although more relevance of our findings should derive from *in vivo* studies, these results give emphasis to the potential use of the combined therapy with low doses of both BRL and 9RA as novel therapeutic tool particularly for breast cancer patients who develop resistance to anti-estrogen therapy.

References

1. Byrington A, Staples C, Paulson K, Lassalle P, Gjertsen BT, Bruserud O: *In vivo* biological effects of ATRA in the treatment of AML. *Expert Opin Investig Drugs* 2008, 17:1623–1633.
2. Ravand F, Estey E, Jones D, Federi S, O'Brien S, Fiorentino J, Pierce S, Bramble D, Estrov Z, Wierda W, Ferrajoli A, Verstovsek S, Garcia-Manero G, Cortes J, Kantarjian H: Effective treatment of acute promyelocytic leukemia with all-*trans*-retinoic acid, arsenic trioxide, and gemtuzumab ozogamicin. *J Clin Oncol* 2009, 27:504–510.
3. Montesinos P, Bergua JM, Vellenga E, Rayon C, Parody R, de la Serna J, León A, Esteve J, Milone G, Debén G, Rivas C, González M, Tormo M, Diaz-Mediavilla J, González JD, Negri S, Arnulfo E, Brunet S, Lowenberg B, Sanz MA: Differentiation syndrome in patients with acute promyelocytic leukemia treated with all-*trans* retinoic acid and anthracycline chemotherapy: characteristics, outcome, and prognostic factors. *Blood* 2009, 113:775–783.
4. Sun SY, Yue P, Mao L, Dawson MI, Shroot B, Lamph WW, Heyman RA, Chandraratna RA, Shudo K, Hong WK, Lotan R: Identification of receptor-selective retinoids that are potent inhibitors of the growth of human head and neck squamous cell carcinoma cells. *Clin Cancer Res* 2000, 6:1563–1573.
5. Abu J, Batuwangala M, Herbert K, Symonds P: Retinoic acid and retinoid receptors: potential chemopreventive and therapeutic role in cervical cancer. *Lancet Oncol* 2005, 6:712–720.

6. Mangelsdorf DJ, Thummel C, Beato M, Herrlich P, Schütz G, Umesono K, Blumberg B, Kastner P, Mark M, Chambon P, Evans RM: The nuclear receptor superfamily: the second decade. *Cell* 1995, 83:835-839.
7. Heyman RA, Mangelsdorf DJ, Dyck JA, Stein RB, Eichele G, Evans RM, Thaler C: 9-cis retinoic acid is a high affinity ligand for the retinoid X receptor. *Cell* 1992, 68:397-406.
8. Elstner E, Müller C, Koshizuka K, Williamson EA, Park D, Asou H, Shintzka P, Said JW, Heber D, Koefler HP: Ligands for peroxisome proliferator-activated receptor γ and retinoic acid receptor inhibit growth and induce apoptosis of human breast cancer cells *in vitro* and in BXH mice. *Proc Natl Acad Sci USA* 1998, 95:8806-8811.
9. Tontonoz P, Hu E, Spiegelman BM: Stimulation of adipogenesis in fibroblasts by PPAR γ 2, a lipid-activated transcription factor. *Cell* 1994, 79:1147-1156.
10. Mueller E, Sarraf P, Tontonoz P, Evans RM, Martin KJ, Zhang M, Fletcher C, Singer S, Spiegelman BM: Terminal differentiation of human breast cancer through PPAR γ . *Mol Cell* 1998, 1:465-470.
11. Suh N, Wang Y, Williams CR, Risingsong R, Gilmer T, Wilson TM, Sporn MB: A new ligand for the peroxisome proliferator-activated receptor- γ (PPAR- γ). GW7845, inhibits rat mammary carcinogenesis. *Cancer Res* 1999, 59:5671-5673.
12. Bonfiglio D, Aquila S, Catalano S, Gabriele S, Belmonte M, Middea E, Qi H, Morelli C, Gentile M, Maggiolini M, Andò S: Peroxisome proliferator-activated receptor- γ activates p53 gene promoter binding to the nuclear factor- κ B sequence in human MCF7 breast cancer cells. *Mol Endocrinol* 2006, 20:3083-3092.
13. Bonfiglio D, Gabriele S, Aquila S, Catalano S, Gentile M, Middea E, Giordano F, Andò S: Estrogen receptor α binds to peroxisome γ proliferator activated receptor (PPAR) response element and negatively interferes with PPAR γ signaling in breast cancer cells. *Clin Cancer Res* 2005, 11:6139-6147.
14. Bonfiglio D, Gabriele S, Aquila S, Qi H, Belmonte M, Catalano S, Andò S: Peroxisome proliferator-activated receptor γ activates fas ligand gene promoter inducing apoptosis in human breast cancer cells. *Breast Cancer Res Treat* 2009, 113:423-434.
15. Elstner E, Williamson EA, Zang C, Fritz J, Heber D, Fenner M, Possinger K, Koefler HP: Novel therapeutic approach: ligands for PPAR γ and retinoid receptors induce apoptosis in bcl-2-positive human breast cancer cells. *Breast Cancer Res Treat* 2002, 74:155-165.
16. Arakawa K, Ishihara T, Aoto M, Inamasu M, Kitamura K, and Saito A: An anti-diabetic thiazolidinedione induces eccentric cardiac hypertrophy by cardiac volume overload in rats. *Clin Exp Pharmacol Physiol* 2004, 31:8-13.
17. Rangwala SM and Lazar MA: Peroxisome proliferator-activated receptor γ in diabetes and metabolism. *Trends Pharmacol Sc* 2004, 25:331-336.
18. Staels B: Fluid retention mediated by renal PPAR γ . *Cell Metab* 2005, 2:77-78.
19. Pina re JA, Reifel-Miller A: Therapeutic potential of retinoid x receptor modulators for the treatment of the metabolic syndrome. *PPAR Res* 2007, 2007:94156.
20. Qin C, Nguyen T, Stewart J, Samudio I, Burghardt R, Safe S: Estrogen up-regulation of p53 gene expression in MCF-7 breast cancer cells is mediated by calcineurin kinase IV-dependent activation of a nuclear factor κ B/CCAAT-binding transcription factor-1 complex. *Mol Endocrinol* 2002, 16:1793-1809.
21. Hermin MF, Katzenellenbogen BS: Response-specific antiestrogen resistance in a newly characterized MCF-7 human breast cancer cell line resulting from long-term exposure to trans-hydroxytamoxifen. *J Steroid Biochem Mol Biol* 1996, 59:121-134.
22. Mosmann T: Rapid colorimetric assay for cellular growth and survival: application to proliferation and cytotoxicity assays. *J Immunol Methods* 1983, 65:55-63.
23. Andrews NC, Fallier DV: A rapid micropreparation technique for extraction of DNA-binding proteins from limiting numbers of mammalian cells. *Nucleic Acids Res* 1991, 19:2499.
24. Cossarizza A, Baccarini-Contini M, Kalashnikova G, Franceschi C: A new method for the cytofluorimetric analysis of mitochondrial membrane potential using the J-aggregate forming lipophilic cation 5,5',6,6'-tetrachloro-1,1',3,3'-tetraethylbenzimidazolylcarbo cyanine iodide (JC-1). *Biochem Biophys Res Commun* 1993, 197:40-45.
25. Mehta RG, Williamson E, Patel MK, Koefler HP: A ligand of peroxisome proliferator-activated receptor γ , retinoids, and prevention of preneoplastic mammary lesions. *J Natl Cancer Inst* 2000, 92:418-423.
26. Crowe DL, Chandraratna RA: A retinoid X receptor (RXR) selective retinoid reveals that RXR- α is potentially a therapeutic target in breast cancer cell lines, and that it potentiates antiproliferative and apoptotic responses to peroxisome proliferator-activated receptor ligands. *Breast Cancer Res* 2004, 6:R546-R555.
27. Smiley ST, Reers M, Mottola-Hartshorn C, Lin M, Chen A, Smith TW, Steele GD, Chen LB: Intracellular heterogeneity in mitochondrial membrane potentials revealed by a J-aggregate forming lipophilic cation JC-1. *Proc Natl Acad Sci USA* 1991, 88:3671-3675.
28. Kliewer SA, Umesono K, Mangelsdorf DJ, Evans RM: Retinoid X receptor interacts with nuclear receptors in retinoic acid, thyroid hormone, and vitamin D3 signaling. *Nature* 1992, 355:446-449.
29. Zhang XK, Hoffmann B, Tran PBV, Graupner G, Pfahl M: Retinoid X receptor is an auxiliary protein for thyroid hormone and retinoic acid receptors. *Nature* 1992, 355:441-445.
30. Tsubouchi Y, Sano H, Kawahito Y, Mukai S, Yamada R, Kohno M, Inoue K, Hla T, Kondo M: Inhibition of human lung cancer cell growth by the peroxisome proliferator activated receptor γ agonists through induction of apoptosis. *Biochem Biophys Res Commun* 2000, 270:400-405.
31. Kitamura S, Miyazaki Y, Shinomura Y, Kondo S, Kanayama S, Matsuzawa Y: Peroxisome proliferator activated receptor γ induces growth arrest and differentiation markers of human colon cancer cells. *Jpn J Cancer Res* 1999, 90:75-80.
32. Roberts-Thomson SJ: Peroxisome proliferator activated receptors in tumorigenesis: targets of tumor promotion and treatment. *Immunol Cell Biol* 2000, 78:436-441.
33. Demetri GD, Fletcher CDM, Mueller E, Sarraf P, Naujoks R, Campbell N, Spiegelman BM, Singer S: Induction of solid tumor differentiation by the peroxisome proliferator activated receptor γ ligand troglitazone in patients with liposarcoma. *Proc Natl Acad Sci USA* 1999, 96:3951-3956.
34. Yee LD, Williams N, Wen P, Young DC, Lester J, Johnson MV, Farrar WB, Walker MJ, Povoski SP, Suster S, Eng C: Pilot study of rosiglitazone therapy in women with breast cancer: effects of short-term therapy on tumor tissue and serum markers. *Clin Cancer Res* 2007, 13:246-252.
35. Leblanc BP, Stunnenberg HG: 9-cis retinoic acid signaling: changing partners causes some excitement. *Genes Dev* 1995, 9:1811-1816.
36. Goo MF, Tsuchida R, Eichler-Jonsson C, Das B, Baruchel S, Malkin D: Vascular endothelial growth factor acts in an autocrine manner in rhabdomyosarcoma cell lines and can be inhibited with all-trans-retinoic acid. *Oncogene* 2005, 24:8025-8037.
37. Mizuguchi Y, Wada A, Nakagawa K, Ito M, Okano T: Antitumoral activity of 13-demethyl or 13-substituted analogues of all-trans retinoic acid and 9-cis retinoic acid in the human myeloid leukemia cell line HL-60. *Biol Pharm Bull* 2006, 29:1803-1809.
38. Wan H, Hong WK, Lotan R: Increased retinoic acid responsiveness in lung carcinoma cells that are nonresponsive despite the presence of endogenous retinoic acid receptor (RAR) β by expression of exogenous retinoid receptors retinoid X receptor α , RAR α , and RAR γ . *Cancer Res* 2001, 61:556-564.
39. Wu K, DuPré E, Kim H, Tin-U CK, Brissonnette RP, Lamph WW, Brown PH: Receptor-selective retinoids inhibit the growth of normal and malignant breast cells by inducing G1 cell cycle blockade. *Breast Cancer Res Treat* 2006, 96:147-157.
40. Simeone AM, Tan AM: How retinoids regulate breast cancer cell proliferation and apoptosis. *Cell Mol Life Sci* 2004, 61:1475-1484.
41. Bischoff ED, Gottardis MM, Moon TE, Heyman RA, Lamph WW: Beyond tamoxifen: the retinoid X receptor selective ligand LGD1069 (TARGRETIN) causes complete regression of mammary carcinoma. *Cancer Res* 1998, 58:479-484.
42. Grommes C, Landreth GE, Heneka MT: Antineoplastic effects of peroxisome proliferator-activated receptor γ agonists. *Lancet Oncol* 2004, 5:419-429.
43. Saez E, Rosenfeld J, Livo'si A, Olson P, Lombardo E, Nelson M, Banayo E, Cardiff RD, Izpisua-Belmonte JC, Evans RM: PPAR γ signaling exacerbates mammary gland tumor development. *Genes Dev* 2004, 18:528-40.
44. Sporn MB, Suh N, Mangelsdorf DJ: Prospects for prevention and treatment of cancer with selective PPAR γ modulators (SPARMs). *Trends Mol Med* 2001, 7:395-400.
45. Wang X, Southard RC, Kilgore MW: The increased expression of

Adrenal glands and testes as steroidogenic tissue are affected by retinoylation reaction

Attilio Pingitore · Erika Cione · Valentina Senatore · Giuseppe Genchi

Received: 18 January 2009 / Accepted: 24 May 2009 / Published online: 12 June 2009
© Springer Science + Business Media, LLC 2009

Abstract This study was undertaken to better understand the physiological role of the retinoylation process in steroidogenic tissues. In adrenal gland mitochondria, the retinoylation extent was found equal to that of testes mitochondria but without ATP in the incubation buffer. We pointed out that the endogenous mitochondrial ATP in adrenal glands is much higher than in testes, about 1.3×10^{-2} M and 5.2×10^{-8} M, respectively. In addition, less CoASH is required for the maximal acylation activity of the retinoyl moiety to protein(s) compared to testes. The fatty acid analysis revealed a different composition of mitochondrial membranes of these two tissues. Among the different values of fatty acids, it is important to note that adrenal glands contain a much higher amount of C18:0 and a much lower amount of C22:5 ω 6 and C22:6 ω 3 than testes in the mitochondrial membranes. In addition, there were also differences in arachidonic acid (ARA, C20:4 ω 6) content between adrenal glands and testes mitochondria. These different values in the fatty acids composition should explain the different extent of the retinoylation process between the two organs.

Keywords Rat · Adrenal glands · Testes · Mitochondria · Retinoylation reaction

Abbreviations

RA all-*trans*-retinoic acid
ACTH corticotrophin
LH luteotropin
CoASH coenzyme A

AMG 3-(4-aminophenyl)-3-ethyl-piperidine-2,6-dione
DMSO dimethyl sulfoxide
EDTA ethylenediaminetetraacetic acid

Introduction

Adrenal glands and gonads synthesize and secrete steroid hormones in response to pituitary hormones such as corticotropin (ACTH) or luteotropin (LH) (Saez 1994; Waterman 1994). The binding of these peptide hormones to their cognate receptors is coupled to the formation of cAMP and activation of the protein kinase A signalling pathway (Waterman and Bischof 1997; Richards and Hedin 1988). In particular, adrenal glands are *vital* to health and have an important role in development and reproduction (Harvey and Everett 2003).

Retinoic acid (RA) acylation, also known as retinoylation, is a post-translational modification of proteins occurring in a variety of eukaryotic cell lines and subcellular compartments both in vivo and in vitro. Retinoylated proteins that have been identified so far include cAMP-binding proteins, vimentin, the cytokeratins, and some nuclear proteins (Takahashi and Breitman 1989; Takahashi and Breitman 1990; Takahashi and Breitman 1994; Tournier et al. 1996; Myhre et al. 1996; Renstrom and DeLuca 1996; Myhre et al. 1998). This process occurs in the presence of Mg^{2+} , ATP and CoASH. The omission of these substrates in the incubation buffer markedly reduced the extent of retinoylation (Genchi and Olson 2001; Cione and Genchi 2004) as the transfer mechanism involves the formation of a retinoyl-CoA intermediate (Kubo et al. 2005). Moreover, the incorporation of all-*trans*-retinoic acid and retinoyl-CoA into proteins is enzymatic judging from the inhibition of the process in the

A. Pingitore · E. Cione · V. Senatore · G. Genchi (✉)
Department of Pharmaco-Biology, University of Calabria,
87036 Rende, CS, Italia
e-mail: genchi@unical.it

presence of N-ethylmaleimide (NEM) and the inactivation by heating and SDS denaturation of subcellular fractions containing enzyme or/and protein substrates (Genchi and Olson 2001; Kubo et al. 2005). We have previously shown (Cione et al. 2005) that the retinoylation reaction occurred on protein(s) of TM-3 Leydig cell line by RA. The reaction involves the formation of a thioester bond and occurs on pre-existing protein. It is important to note that both db-cAMP and forskolin increase the retinoylation level on the protein of TM-3 cells of about 75% and 80% respectively (Cione et al. 2005). These results suggested that the retinoylation reaction could be regulated by cAMP-activated enzymes.

Previously, we have seen that RA-induced steroidogenesis and retinoylation are parallel events and exhibit a positive correlation (Tucci et al. 2008). Therefore in this context, we examined the retinoylation process on adrenal glands mitochondria to better understand whether the physiological role of the retinoylation process is steroidogenic tissues dependent.

Materials and methods

Chemicals

[11-12 ^3H] All-*trans*-retinoic acid (^3H]RA) (50 Ci/mmol) was purchased from PerkinElmer (Boston USA). All-*trans*-retinoic acid (RA) and 3-(4-aminophenyl)-3-ethylpiperidine-2,6-dione (AMG) were obtained from Sigma-Aldrich (Milano, Italia). All other chemicals used were of analytical reagent grade.

Isolation of mitochondria

Rats were killed by decapitation, according to practice procedures approved by the ethical committee, and adrenal glands and testes were immediately removed. Mitochondria were isolated by differential centrifugation as described by Genchi and Olson (2001) and suspended in a medium containing 250 mM sucrose, 10 mM Tris/HCl, pH 7.4, 1 mM EDTA at a concentration of 5–8 mg protein/ml. Protein concentration was determined by the Lowry procedure (Lowry et al. 1951) with bovine serum albumin (BSA) as the reference standard. These mitochondrial suspensions were either used immediately or frozen at -80°C . The purity of the mitochondrial preparation was checked by assaying marker enzymes for lysosomes, peroxisomes and plasma membranes.

Incorporation of radioactive RA

^3H]RA or RA was dissolved in ethanol under yellow safe-light. The concentration of RA was spectrophotometrically

determined, the ethanol was evaporated under nitrogen, and the dry residue resuspended in DMSO. The RA solution was diluted into the retinoylation buffer such that the final concentration of DMSO was no higher than 0.5%. The buffers were 5 mM ATP, 50 μM CoASH, 27 mM MgCl_2 , 50 mM sucrose, 100 mM Tris, pH 7.4 for adrenal glands mitochondrial preparation, and 10 mM ATP, 150 μM CoA, 27 mM MgCl_2 , 50 mM sucrose, 100 mM Tris, pH 7.4 for testes mitochondria; the retinoylation reaction was carried out at 37°C for 90 min in a final ratio of 1 mg protein /1 ml. The reaction was stopped by adding TCA at a final concentration of 5%. The mixture was centrifuged in an Eppendorf centrifuge at 13,000 rpm for 10 min, and the precipitate was extracted seven times with 0.5 ml CHCl_3 : CH_3OH (2:1) containing 0.005% BHT. The pellet was solubilized in 0.2 ml 1% SDS, 40 mM Tris, 2 mM EDTA, pH 7.5, at 50°C and counted in a TriCarb 2100TR liquid scintillation counter (Packard). The counting efficiency was about 75%.

Mitochondrial ATP concentration

The amount of endogenous ATP in isolated mitochondria from testes and adrenal glands was determined using the bioluminescence method described by Drew and Leeuwenburgh (2003) with a commercial ATP kit (Molecular Probes) according to manufacturer instructions.

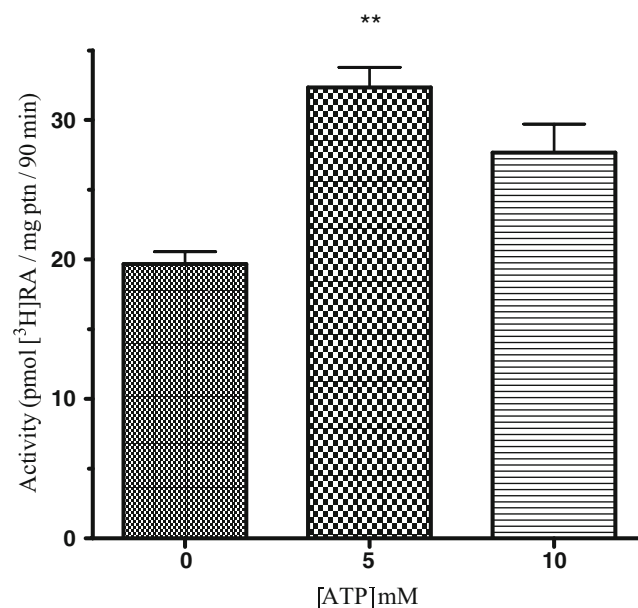


Fig. 1 Adrenal Glands Mitochondria are affected by RA. Retinoylation reaction (^3H]RA, 100 nM) on rat adrenal glands mitochondria at 37°C for 90 min in the absence and in the presence of 5 and 10 mM ATP. For other conditions see “Material and methods”. The data represent the mean \pm SD of three independent experiments. ** P value < 0.01 compared to the control (no ATP)

Fatty acid analysis of rat testes and adrenal gland mitochondrial membranes

Fatty acid composition of testes and adrenal gland mitochondrial membranes was determined. Briefly, mitochondria from both tissues were saponified with ethanolic KOH solution for 2 h at 90°C. Fatty acids were extracted as described by Muci et al. (1992), and their corresponding methyl esters were prepared by *trans*-esterification with methanolic boron trifluoride (17% BF₃) at 65°C for 30 min.

Fatty acid methyl esters (FAMES) were then analyzed by gas-liquid chromatography.

Statistical analysis

Statistical analysis was performed by ANOVA followed by Dunnett's Multiple Comparison test. Values are shown as the mean ± SD of *n* independent experiments. Differences were considered significant at values of *P* < 0.05.

Results

Retinoylation reaction on adrenal glands mitochondria

As shown in Fig. 1, the retinoylation extent (about 20 pmol/mg protein/90 min) for adrenal glands mitochondria without ATP in the incubation buffer reaches the maximum activity found for testes mitochondria (Genchi and Olson 2001; Cione and Genchi 2004) after the same incubation time. In addition, the concentration of CoASH, required to have the maximum activity in adrenal glands mitochondria without ATP in the incubation buffer, was lower than that used for testes mitochondria, as shown in Fig. 2 A–B.

Proteins retinoylated in cell fractions of adrenal glands homogenates and ATP quantification

In the standard conditions, without ATP in the incubation buffer, the mitochondrial fraction of the adrenal glands clearly was the most active to incorporate [³H]RA (Table 1). All fractions other than the mitochondria showed relative activities lower than that of the homogenate. In addition endogenous ATP quantification in both mitochondrial preparations showed a very significant difference between testes and adrenal glands (Table 2).

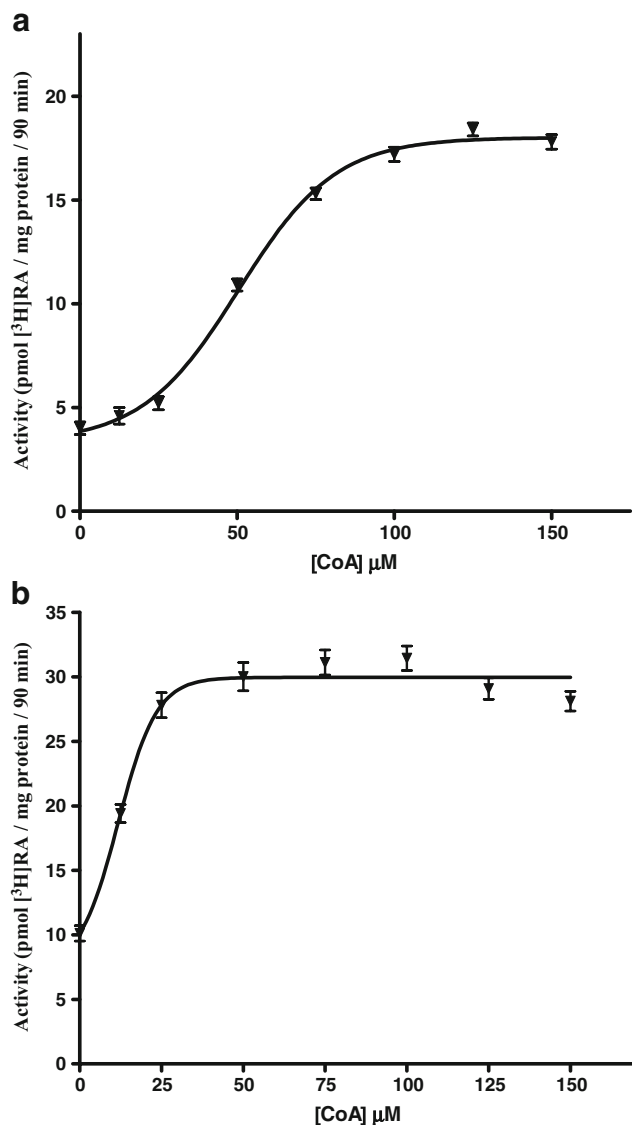


Fig. 2 Relationship between the retinoylation activity of testes and adrenal glands. The retinoylation activity of mitochondria from rat testes (A) and adrenal glands (B) is plotted as a function of indicated CoA concentrations under the standard conditions for 90 min at 37°C, with 10 mM (A) and 5 mM ATP (B) respectively. The data represent the mean ± SD of three independent experiments. Overall *P* value < 0.01 (**)

Table 1 Retinoylation reaction on adrenal glands cellular sub-fractions

Cell fraction	Incorporated radioactivity (pmol [³ H]RA/mg protein/90min)
Homogenate	8.32–8.09
Nuclei	6.89–6.53
Mitochondria	21.05–20.45
Microsomes	3.49–3.80
Cytosol	1.55–2.16

Incorporation of [³H]RA (100 nM) into proteins by cellular fractions of adrenal glands in duplicate, incubated in a buffer without ATP for 90 min at 37°C, as described in “Materials and Methods”

Table 2 Mitochondrial ATP quantification

Adrenal Glands	1.3×10^{-2} M
Testes	5.2×10^{-8} M

Content of ATP in adrenal glands and testes mitochondria determined as in “Material and methods”

Time dependence of incorporation of [3 H]RA into protein(s) and activation energy determination

[3 H]RA incorporated into protein(s) increased with the time of incubation at 37°C. The incorporation rate was essentially linear for 20 min but then reached a plateau between 30 and 90 min, remaining constant until 150 min. Because the experimental intent was to compare the incorporation of radioactivity into protein(s) between testes and adrenal glands, a 90 min incubation time was selected for all subsequent studies (Fig. 3). The Arrhenius plot for adrenal glands mitochondria showed a straight line in the range of 5–40°C, and the value of activation energy for retinoylation reaction was 19.36 kJ/mol (not shown).

Effect of aminoglutethimide on retinoylation process

3-(4-aminophenyl)-3-ethyl-piperidine-2,6-dione, also known as aminoglutethimide, is a specific inhibitor of cytochrome P450_{scc} (side chain cleavage) that had no effect on the retinoylation process in both testes and adrenal glands mitochondria, as shown in Fig. 4.

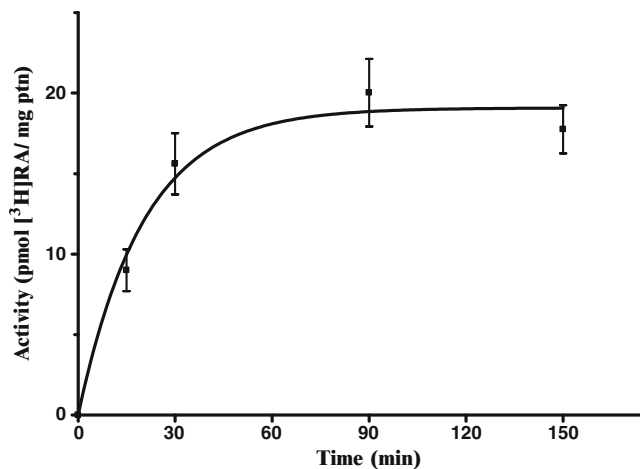


Fig. 3 Time-course of [3 H]RA Incorporation. Time-dependent incorporation of [3 H]RA (100 nM) into delipidated protein from rat adrenal glands mitochondria, incubated under standard assay conditions but without ATP at 37°C for the times indicated. The data represent the mean \pm SD of five independent experiments. Overall P value <0.01 (**)

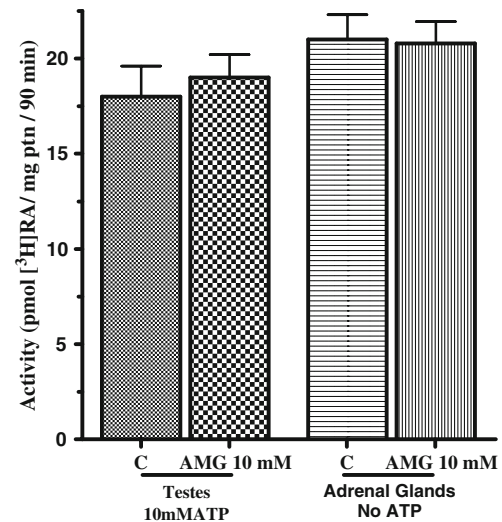


Fig. 4 Effect of aminoglutethimide on retinoylation reaction. Testes and adrenal glands mitochondria were incubated with 10 mM AMG but in the presence of 10 mM ATP (testes) and in the absence of ATP (adrenal glands). Other conditions are as described in “Material and methods”. The data represent the mean \pm SD of three independent experiments

Fatty acid composition of adrenal glands and testes mitochondria

Significant differences in fatty acid composition of rat mitochondrial adrenal glands and testes were detected. A low percentage of docosahexaenoic acid (DHA, C22:6 ω 3) and an even lower percentage of docosapentaenoic acid

Table 3 Fatty Acid composition (mol %) of rat mitochondrial membrane phospholipids from adrenal glands and testes

Fatty Acid	Adrenal Glands	Testes
14:0	0.48 \pm 0.01	0
16:0	11.52 \pm 0.35	28 \pm 0.41
18:0	31.96 \pm 0.85	4.7 \pm 0.14
18:1 ω 9	9.94 \pm 0.02	6.2 \pm 0.19
18:2 ω 6	9.25 \pm 0.11	3.4 \pm 0.10
20:4 ω 6	34.30 \pm 1.12	23.4 \pm 0.96
20:5 ω 3	n. d.	0.9 \pm 0.01
22:5 ω 6	0.38 \pm 0.04	24.8 \pm 0.94
22:6 ω 3	0.80 \pm 0.06	8.4 \pm 0.13
Σ saturated	44.11 \pm 1.19	32.7 \pm 1.02
Σ unsaturated	55.82 \pm 1.17	67.1 \pm 1.29
Σ sat./ Σ unsat.	0.79 \pm 0.03	0.49 \pm 0.01

The fatty acid composition of adrenal glands and testes mitochondrial membranes was determined by gas-liquid chromatography as Muci et al. (1992). The data are the mean \pm SD of three independent determinations. Σ saturated = sum of saturated fatty acids; Σ unsaturated = sum of unsaturated fatty acids

(DPA, C22:5 ω6) were found in the membranes of mitochondria from adrenal glands compared to testes, together with a 85% increment of the stearic acid (C18:0) and a 30% increment of the arachidonic acid (ARA, C20:4 ω6) in adrenal glands. Therefore, significant changes were measured in the ratio of total saturated/unsaturated fatty acids between the two tissues as shown in Table 3. Figs. 5 A–C and 6 A–C highlighted the differences in saturated and unsaturated fatty acid composition, respectively, between adrenal glands and testes.

Discussion

Adrenal glands as steroidogenic tissue synthesize and secrete steroid hormones in response to pituitary hormones corticotrophin (ACTH) and/or luteotropin (LH) (Saez 1994; Waterman 1994). The binding of these peptide hormones to

their receptors is coupled to the formation of cAMP that activate protein kinase A signalling pathway (Waterman and Bischof 1997; Richards and Hedin 1988). The adrenal glands are known for their help in regulating glucose levels through cortisol, for their natural anti-inflammatory activity, and for sex hormones supplementation to the organisms. Among these, the dehydroepiandrosterone (DHEA) can be converted into sex hormones, including estrone and testosterone. In this latter concern, it is known that retinoids are important in maintaining testes function. In fact, vitamin A-deficient diet causes the cessation of spermatogenesis, loss of mature germ cells and a reduction in testosterone level in mice and rat testes (Wolbach and Howe 1925; Ganguly et al. 1980; Appling and Chytil 1981). Previously we have shown that the retinoylation process occurs on pre-existing protein(s) growing of TM-3 cells and it is probably regulated by cAMP-activated enzymes; moreover under forskolin stimulus the retinoylation reaction was increased

Fig. 5 Saturated fatty acid composition (mol %) of rat mitochondrial membrane phospholipids from adrenal glands and testes. The fatty acid composition of adrenal glands and testes mitochondrial membranes was determined by gas-liquid chromatography as Muci et al. (1992). Other conditions are as described in Table 3. The data represent the mean±SD of four independent experiments. ** P value <0.01

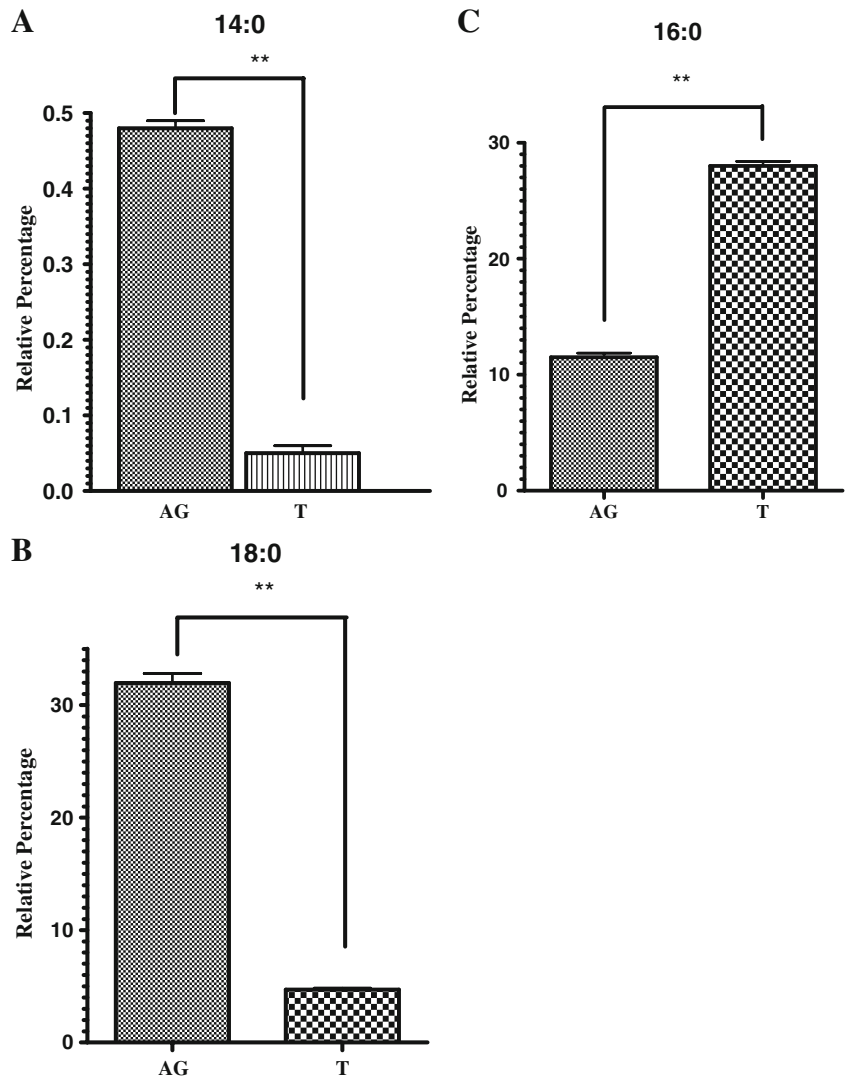
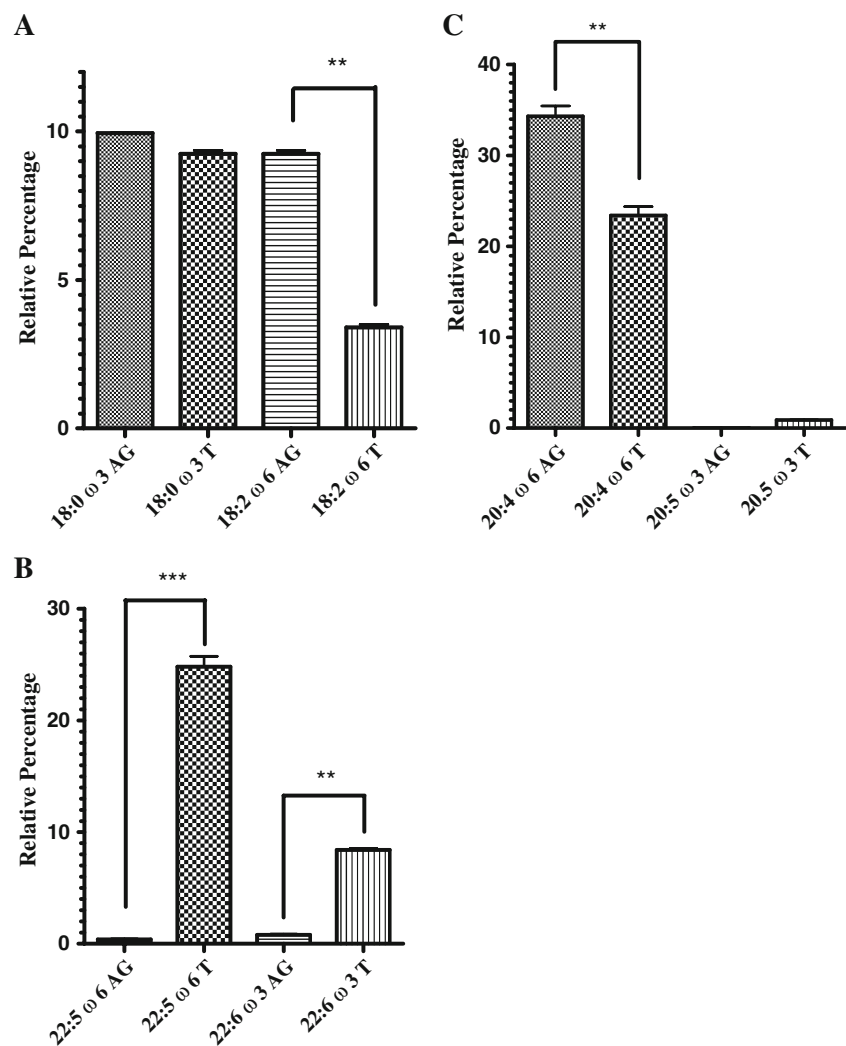


Fig. 6 Unsaturated fatty acid composition (mol %) of rat mitochondrial membrane phospholipids from adrenal glands and testes. Experimental conditions are as described in Table 3. The data represent the mean \pm SD of three independent experiments. ** P value <0.01; *** P value <0.001



by 80% respect to the control value (Cione et al. 2005). In addition, we found that testosterone production and retinoylation reaction are concomitant and exhibit a positive correlation in Leydig cells (Tucci et al. 2008). Therefore, the aim of this paper is to evaluate the post translational modification triggered by RA in adrenal glands, since they are the second main steroidogenic organ in the male. In the mitochondrial compartment of adrenal glands after 90 min at 37°C, the value of [3 H]RA incorporated reached that of testes (Cione and Genchi 2004) with no need of ATP supplementation in the incubation buffer (Fig. 1). However among the cellular sub-fractions, adrenal glands mitochondria were 2.5-fold more active in binding retinoic acid than the homogenate (Table 1), providing a further evidence of a mitochondrial localization of the retinoylation system in steroidogenic tissues. The great difference in the endogenous ATP levels between the two organs, 1.3×10^{-2} M for adrenal glands and 5.2×10^{-8} M for testes, is the reason for which no extra ATP is required in the incubation buffer of

the retinoylation reaction (Table 2). In our case, the Arrhenius plot of the retinoylation reaction showed that changes exist in the process of the transferring of the retinoyl moiety to the protein(s) between adrenal glands and testes: the adrenal glands activation energy was found equal to 19.36 kJ/mol in contrast with the 43.5 kJ/mol value determined for testes (Cione and Genchi 2004). Most likely our retinoylated protein(s), such as the enzymatic complex that allows the transfer of the retinoyl moiety, are embedded within the inner mitochondrial membrane and/or are localized on both sides of the membrane because the retinoylation does not require external ATP supplementation to occur. A further evidence of it comes from Genchi and Olson (2001) as mitoplasts from testes are still labelled with 3 HRA. In addition, the concentration of CoASH, required for the retinoylation process was lower in adrenal glands mitochondria than in testes as shown in Fig. 2 A–B. Several proteins in Leydig cells are regulated by a cAMP-dependent pathway and are involved in steroidogenesis;

first of all, the cytochrome P450_{scc} (side chain cleavage) (Mellon and Vaisse 1989) that catalyzes the conversion of cholesterol to pregnenolone. In our experimental procedures the aminoglutethimide a specific inhibitor of cytochrome P450_{scc} had no effect on the retinoylation process in both testes and adrenal glands mitochondria giving us the proof that this enzyme is not involved in the retinoylation process as shown in Fig. 4.

Moreover, differences in fatty acid composition in mitochondrial rat preparation of adrenal glands and testes were highlighted. Fig. 5 (A–C) shows the differences in saturated fatty acid composition. In particular a lower percentages of myristic acid (14:0), as well as stearic acid (18:0), were found in the testes mitochondrial membranes than in adrenal gland, about 10-fold and 7-fold less, respectively as shown in Fig. 5A–B. In addition, a 3-fold higher amount of palmitic acid (16:0) was found only in testes mitochondria (Fig. 5C). The differences in unsaturated fatty acid composition are shown in Fig. 6 (A–C). A much lower percentage of docosapentaenoic acid (DPA, C22:5 ω6) about 65-fold less and a lower percentage of docosahexaenoic acid (DHA, C22:6 ω3) about 10-fold less were found in the adrenal glands membranes of mitochondria compared to testes (Fig. 6B). In the meanwhile, about a 30% higher amount of arachidonic acid (ARA, C20:4 ω6) was found in adrenal gland mitochondria (Fig. 6C). ARA has the important physiological function of maintaining membrane content and permitting the activity of enzymes of the respiratory chain (Vazquez-Memije et al. 2005): in the case of the retinoylation reaction the difference in the ARA content could contribute to the different behaviour of the two tissues in incorporating RA. Therefore, the about 2-fold change in the ratio of total saturated/unsaturated fatty acids between adrenal glands and testes leads us to postulate a relationship between fatty acids and the retinoylation process (Table 3). The different fluidity of the membranes, deriving from the fatty acids composition, should justify the different values of the retinoylation and the activation energy between the adrenal glands and the testes. It should be stressed that the membrane lipid composition, the degree of unsaturation and the length of the fatty acid chains play important roles in determining the influence of membranes lipids with respect to the specific enzyme activities in the mitochondria (Brenner 1984; Daum 1985; Crider and Xie 2003).

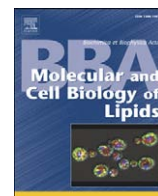
In conclusion, in the present study we demonstrated that RA action by the retinoylation process on protein(s) of rat adrenal glands and testes mitochondria is steroidogenic tissue

dependent, that cytochrome P450_{scc} is not affected by the process and that probably docosapentaenoic acid (DPA, C22:5 ω6) should play a fundamental role to allow the transfer of the retinoyl moiety. However, since adrenal glands are arguably the neglected organ in endocrine toxicology (Harvey et al. 2007), it cannot be excluded that perhaps the retinoylation process is toxic/protective for that organ.

Acknowledgements We thank Dr G.V. Gnoni (University of Lecce) for performing fatty acids analysis. This research was supported by grants from Ministero dell'Istruzione, dell'Università e della Ricerca (MIUR, Italia) and IRCCS Associazione Oasi Maria SS.

References

- Appling DR, Chytil F (1981) *Endocrinology* 108:2120–2124
- Brenner RR (1984) *Prog Lipid Res* 23:69–96
- Cione E, Genchi G (2004) *J Bioenerg Biomembr* 36:211–217
- Cione E, Tucci P, Chimento A, Pezzi V, Genchi G (2005) *J Bioenerg Biomembr* 37:43–48
- Crider BP, Xie X (2003) *J Mol Chem* 278:44281–44288
- Daum G (1985) *Biochim Biophys Acta* 822:1–42
- Drew B, Leeuwenburgh C (2003) *Am J Physiol Regul Integr Comp Physiol* 285:R1259–R1267
- Ganguly J, Rao MR, Murthy SK, Sarada K (1980) *Vitam Horm* 38:1–54
- Genchi G, Olson JA (2001) *Biochim Biophys Acta* 1530:146–154
- Harvey PW, Everett DJ (2003) *J. Appl Toxicol* 23:81–87
- Harvey PW, Everett DJ, Springall CJ (2007) *J Appl Toxicol* 27:103–115
- Kubo Y, Wada M, Obba T, Takahashi N (2005) *J Biochem* 138:493–500
- Lowry OH, Rosebrough NJ, Randall RJ (1951) *J Biol Chem* 193:265–275
- Mellon SH, Vaisse C (1989) *Proc Natl Acad Sc USA* 86:7775–7779
- Muci MR, Cappello AR, Vonghia G, Bellitti E, Zezza L, Gnoni GV (1992) *Int J Vitam Nutr Res* 62:330–333
- Myhre AM, Takahashi N, Blomhoff R, Breitman TR, Norum KR (1996) *J Lipid Res* 37:1971–1977
- Myhre AM, Hagen E, Blomhoff R, Norum KR (1998) *J Nutr Biochem* 9:705–711
- Renstrom B, DeLuca HF (1996) *Biochim Biophys Acta* 998:69–74
- Richards JS, Hedin L (1988) *Annu Rev Physiol* 50:441–463
- Saez JM (1994) *Endocr Rev* 15:574–626
- Takahashi N, Breitman TR (1989) *J Biol Chem* 264:5159–5163
- Takahashi N, Breitman TR (1990) *Methods Enzymol* 189:233–239
- Takahashi N, Breitman TR (1994) In: Blomhoff R (ed) *Vitamin A in health and disease*. Marcel Dekker, New York, pp 257–273
- Tournier S, Raynaud F, Gerbaud P, Lohmann SM, Anderson WB, Evain-Brion D (1996) *J Cell Physiol* 167:196–203
- Tucci P, Cione E, Genchi G (2008) *J Bioenerg Biomembr* 40:111–115
- Vázquez-Memije ME, Cárdenas-Méndez MJ, Tolosa A, Hafidi ME (2005) *Exp Gerontol* 40:482–490
- Waterman MR (1994) *J Biol Chem* 269:27783–27786
- Waterman MR, Bischof LJ (1997) *FASEB J* 11:419–427
- Wolbach SB, Howe PR (1925) *J Exp Med* 42:753–777



Influence of all-*trans*-retinoic acid on oxoglutarate carrier via retinoylation reaction

E. Cione, A. Pingitore, M. Perri, G. Genchi*

Department of Pharmaco-Biology, University of Calabria, Edificio Polifunzionale, 87036 Rende (CS), Italy

ARTICLE INFO

Article history:

Received 1 May 2008

Received in revised form 17 September 2008

Accepted 24 September 2008

Available online 14 October 2008

Keywords:

Retinoic acid

2-Oxoglutarate carrier

Retinoylation reaction

ABSTRACT

All-*trans*-retinoic acid (atRA), an activated metabolite of vitamin A, is incorporated covalently into proteins both *in vivo* and *in vitro*. AtRA reduced the transport activity of the oxoglutarate carrier (OGC) isolated from testes mitochondria to 58% of control via retinoylation reaction. Labeling of testes mitochondrial proteins with ³HatRA demonstrated the binding of atRA to a 31.5 kDa protein. This protein was identified as OGC due to the competition for the labeling reaction with 2-oxoglutarate, the specific OGC substrate. The role of retinoylated proteins is currently being explored and here we have the first evidence that retinoic acids bind directly to OGC and inhibit its activity in rat testes mitochondria via retinoylation reaction. This study indicates the evidence of a specific interaction between atRA and OGC and establishes a novel mechanism for atRA action, which could influence the physiological biosynthesis of testosterone in situations such as retinoic acid treatment.

© 2008 Elsevier B.V. All rights reserved.

1. Introduction

Oxoglutarate carrier (OGC), also known as the oxoglutarate/malate carrier, catalyzes the transport of 2-oxoglutarate in electroneutral exchange for some other dicarboxylates to which malate is bound with the highest affinity. In proteoliposomes OGC has been shown to exist as a homodimer and to function according to a sequential antiport mechanism. These results have been interpreted by assuming two separate and coordinated substrate translocation pathways, one in each monomer. OGC plays an important role in the malate–aspartate shuttle and is also involved in the oxoglutarate–isocitrate shuttle, nitrogen metabolism and gluconeogenesis from lactate when the carbon skeleton for gluconeogenesis is provided by 2-oxoglutarate exported from the mitochondria by the OGC [1].

Vitamin A and its metabolites play important roles in vision, reproduction, cell proliferation and differentiation, embryogenesis, immune response, and growth. The all-*trans*- and 9-*cis*-isomers of retinoic acid interact with the nuclear retinoid receptors, RAR and RXR, inducing differentiation and apoptosis of many types of cells [2–4]. Some biological effects of vitamin A, however, are not dependent on retinoic acid receptors; 11-*cis*-retinal in vision [5], all-*trans*-retinol in embryologic development [6], and 14-hydroxy-4,14-retroretinol in the growth of B lymphoblastoid cells and in the maintenance of T-cell activation [7] in particular. Moreover, in enucleated 3T3 fibroblasts, atRA inhibits phorbol ester-induced fibronectin release [8] and binds to and inhibits the adenine nucleotide translocator in bovine heart and mouse liver mitochondria [9]. AtRA is incorporated into proteins of cells in culture [10–13] and of rat tissues both *in vivo* [14] and *in vitro* [15–18].

The covalent linkage between RA and proteins is probably a thioester or labile O-ester bond in most cases [10]. Retinoylated proteins that have been identified so far include cAMP-binding proteins, vimentin, the cytokeratins, and some nuclear proteins [10–16]. In our current investigation, we have studied OGC carrier activity both from mitochondria extracted from whole rat testes and TM-3 cells. Previously we have demonstrated that mitochondria from rat testes [17,18] and TM-3 cells [19] were extremely active in incorporating retinoic acid. Moreover, it was highlighted how the retinoylation reaction and testosterone biosynthesis are positively correlated when Leydig cell cultures are incubated with atRA at 100 nM [20].

It is well known that many biosynthetic pathways of testosterone are NADPH or NADH dependent; therefore OGC was chosen as the experimental target for its involvement in the malate–aspartate shuttle and oxoglutarate–isocitrate shuttle to provide the necessary reducing equivalents between cytosol and mitochondria and vice versa. In this study we demonstrate how the activity of OGC is influenced by retinoic acid. The efforts were focused on the OGC from rat testes as the retinoylation process is more efficient in this tissue.

2. Materials and methods

2.1. Chemicals

[11-12 ³H] all-*trans*-retinoic acid (³HatRA) (50 Ci/mmol), [1-¹⁴C] 2-oxoglutarate and ECL were purchased from PerkinElmer (Boston USA). All-*trans*-retinoic acid (atRA) was obtained from Sigma-Aldrich (Milano, Italia); egg yolk phospholipids from Fluka; DMEM/F12, fetal calf serum (FCS), penicillin and streptomycin from Gibco (Invitrogen Life Technologies, Italia). All other chemicals used were of analytical reagent grade.

* Corresponding author. Dipartimento Farmaco-Biologico, Università della Calabria, 87036 Rende (CS), Italy. Tel.: +39 0984 493454; fax: +39 0984 493271.

E-mail address: genchi@unical.it (G. Genchi).

Table 1
Effect of mitochondrial carrier inhibitors on retinoylation reaction

Carrier inhibitors on retinoylation reaction	pmol/mg ptn×90 min	SEM	n	% Inhibition
Control	21,47	2,44	23	
Mersalyl 1 mM	1,84	0,09	5	91,43
NEM 5 mM	2,47	0,28	5	88,49
2-Cyano-4-hydroxycinnamate 5 mM	11,90	1,23	3	44,58
1,2,3-Benzenetricarboxylate 5 mM	18,93	1,99	3	11,83

Mitochondria from testes were incubated 90 min in a buffer as described in materials and methods with ³HatRA, 100 nM final concentration, at 37 °C. Then the reaction was stopped with TCA and the radioactivity detected in a liquid scintillation counter. Results are presented as Mean±SEM of three independent experiments. **P<0.01 compared to the control. 1,2,3-Benzenetricarboxylate P>0.05.

2.2. Isolation of mitochondria

Rats were killed by decapitation, according to practice procedures approved by the ethical committee, and testes were immediately removed. Mitochondria were isolated by differential centrifugation as described by Cione and Genchi [18] and suspended in a medium containing 250 mM sucrose, 10 mM Tris/HCl, pH 7.4, 1 mM EDTA at a concentration of 15–18 mg protein/ml. Protein concentration was determined by the Lowry procedure [21] with BSA as the reference standard. This mitochondrial suspension was either used immediately or frozen at -80 °C. The purity of the mitochondrial preparation for both whole testes and TM-3 cells was checked by assaying marker enzymes for lysosomes, peroxisomes and plasma membranes.

2.3. Incubation and extraction

AtRA or ³HatRA were dissolved in ethanol and 3 µL of the solution was added to the tissue preparation (0.5 mg protein), and incubated in the presence of 10 mM ATP, 150 µM CoA, 27 mM MgCl₂, 50 mM sucrose, and 100 mM Tris, pH 7.4, in a total volume of 0.5 ml at 37 °C for 90 min. The inhibitors were added together with ³HatRA. The mitochondrial suspensions were centrifuged and protein extracted in 3% Triton X-114, 20 mM Na₂SO₄, 1 mM EDTA, 10 mM Pipes, pH 7.0, and after 10 min on ice, the mixture was centrifuged at 13000 rpm for 5 min.

2.4. Reconstitution and determination of OGC activity

20 µg of protein from the Triton X-114 extract of mitochondria were added to 100 µL of sonicated phospholipids (10% w/v), 100 µL of 10% Triton X-114 in Pipes 10 mM, 40 µL of malate 200 mM, 230 µL Pipes 10 mM pH 7.0 in a final volume of 700 µL and were applied to an Amberlite XAD-2 column in agreement with Palmieri and Klingenberg [22]. All the operations were carried out at room temperature.

In order to determine the OGC transport activity, the external malate was removed by passing 650 µL of the proteoliposomal suspension through a Sephadex G-75 column pre-equilibrated with 50 mM NaCl and 10 mM Pipes, pH 7.0. The first 600 µL of the slightly turbid eluate, containing the proteoliposomes, were collected, transferred to 1.5 mL microcentrifuge tubes (150 µL each), and used for transport measurements by the inhibitor stop method [22]. Transport was carried out at 25 °C by adding 0.1 mM [¹⁴C] 2-oxoglutarate and stopped after 10 min by the addition of 20 mM pyridoxal 5'-phosphate. In control samples, the pyridoxal 5'-phosphate was added together with the labeled substrate at time zero. To remove the external radioactivity, each sample was passed through a Sephadex G-75 column (0.5×8 cm). The liposomes, eluted with 50 mM NaCl, were collected in 4 mL of scintillation cocktail and counted using a Tricarb 2100 TR scintillation counter with a counting efficiency of about 70–73%. The exchange activity was evaluated as the difference between the experimental and the control values as previously published by Bisaccia et al. [23].

2.5. Labeling with ³HatRA and western blot analysis

Direct labeling with ³HatRA was performed according to a method described previously [24]. Under yellow safe-light, 5 µCi/5 µL of ³HatRA (40–60 Ci/mmol) in ethanol (1 µCi/µL) were added to 1.5 mL glass microcentrifuge tubes for each sample tested. After the ethanol was removed under nitrogen, 20 µg of Triton extract of testes mitochondrial protein were added to each tube, and the final volume was adjusted to 10 µL with incubation buffer, pH 7.4, for a final concentration of 10 µM ³HatRA, while 2-oxo-glutarate was added at a final concentration of 10 mM. The samples were incubated at 37 °C [11] and shaken for 90 min under yellow light, after which 10 µL of SDS-polyacrylamide gel electrophoresis sample buffer was added, the samples were boiled and then loaded to run with standard SDS-polyacrylamide gel electrophoresis techniques. The gel was stained with Coomassie Brilliant Blue, soaked in Amplify (Amersham Biosciences) and then used for fluorography at -80 °C for 30 days.

In order to verify the presence of the OGC protein, western blot analysis was performed using overnight rabbit monoclonal antibody to OGC at 4 °C (1:500 dilution in TBST). On the next day the membrane was incubated for 1 h at room temperature with horseradish peroxidase-conjugate antibodies to rabbit immunoglobulin G (1:2000 dilution) and the immune complex was detected with chemiluminescence reagents (ECL).

2.6. Cell cultures

Leydig (TM-3) cell line, derived from testes of immature BALB/c mice, was generously donated by Dr. S. Andò (University of Calabria), and cultured in DMEM/F12 medium supplemented with 10% FCS, 2 mM glutamine, 1% of a stock solution containing 10,000 IU/mL penicillin and 10,000 µg/mL streptomycin and was grown on 90 mm plastic tissue culture dishes in a humidified atmosphere of 5% CO₂ in air at 37 °C. Cells from exponentially growing stock cultures were removed from the plate with trypsin (0.05% w/v) and EDTA (0.02% w/v). Cell number was estimated with a Burkert camera and cell viability by trypan blue dye exclusion. The medium was changed twice weekly. TM-3 cells were subcultured when confluent.

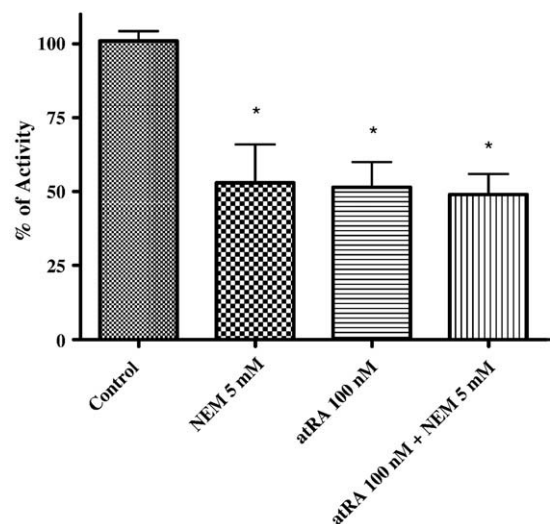


Fig. 1. Effects of N-ethylmaleimide on OGC activity after retinoylation reaction. Mitochondria from testes were incubated for 90 min in buffer with atRA, 100 nM final concentration, at 37 °C. OGC was extracted as described in materials and methods. After extraction and reconstitution into liposomes the exchange activity was assayed by adding ¹⁴C 2-oxo-glutarate 0.1 mM. Results are presented as Mean±SEM of three independent experiments. *P<0.05 compared to the control.

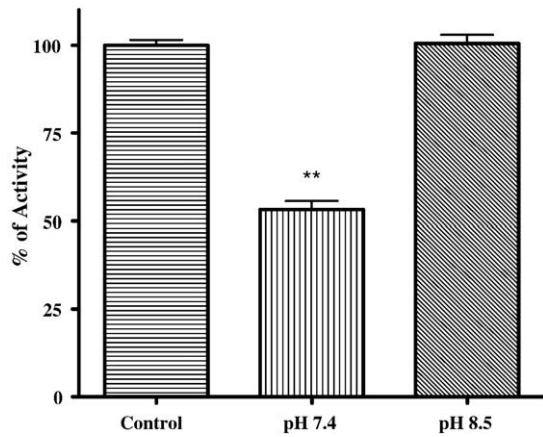


Fig. 2. Effects of pH on OGC activity after retinoylation reaction. Mitochondria from testes were incubated for 90 min at different pH with atRA, 100 nM final concentration, at 37 °C. OGC was extracted as described in materials and methods. After extraction and reconstitution in liposomes the exchange activity was assayed. The optimum pH for OGC activity was found at 7.5 while no effects were highlighted at a pH higher than 7.5. Results are presented as Mean±SEM of five independent experiments. ** $P < 0.01$ compared to the control.

2.7. TM-3 cells treated with atRA and mitochondrial isolation

TM-3 cells growing exponentially were removed by trypsin/EDTA, harvested by centrifugation and resuspended at 1×10^6 cells/mL in DMEM/F12 medium supplemented with serum. The next day the medium was removed and replaced with serum-free DMEM/F12. The cells were incubated at 37 °C in a humidified atmosphere of 5% CO₂ in air for 24 h in the presence of 10 or 100 nM atRA dissolved in DMSO and diluted into the growth medium such that the final DMSO concentration was no higher than 0.01%. After the above mentioned treatments, TM-3 cells were collected by trypsinization and isolated by centrifugation at 1200 $\times g$ for 5 min at 4 °C. The pellet was solubilized in 180 μ L RIPA buffer. After the addition of 20 μ L of 0.1% digitonin, the cells were incubated for 15 min at 4 °C and mitochondria were isolated by differential centrifugation at 4 °C.

2.8. Statistical analysis

Statistical analysis was performed by ANOVA followed by Dunnett's multiple comparison test. Values are shown as mean±SEM of (n) independent experiments. Differences were considered significant at values of $P < 0.05$.

3. Results

3.1. Carrier inhibitors on retinoylation reaction

As shown in Table 1, both mercurial and maleimide compounds strongly inhibit the retinoylation processes by about 90%. In addition, 2-cyano-4-hydroxycinnamate, an inhibitor of OGC [25], shows 45% inhibition when used at a concentration of 5 mM; conversely at the same concentration 1,2,3-benzotricarboxylate, an inhibitor of citrate carrier, has a very weak effect (12% inhibition).

3.2. Effects of *N*-ethylmaleimide, atRA and pH on OGC activity

The sulphhydryl group reagent, NEM, at 5 mM, markedly reduced the OGC activity by 47%. A similar inhibition of 51% was highlighted for 100 nM atRA, and when the two compounds are co-incubated the activity was reduced to 49%, equal to RA alone as shown in Fig. 1. Fig. 2 shows the pH effect on OGC activity. The optimum pH for atRA inhibition was found at 7.4 while no effects were highlighted at pH 8.5.

3.3. AtRA binds to OGC

To study a direct interaction between atRA and OGC, we labeled testes mitochondrial proteins with ³HatRA in the incubation buffer. As shown in Fig. 3, few mitochondrial proteins bind to ³HatRA and specifically a 31.5-kDa protein was detected. We observed that the labeling of the 31.5-kDa protein was prevented when 2-oxo-glutarate, the specific OGC substrate, was added. This demonstrates that OGC was labeled by ³HatRA. It is presumed that the binding is covalent on the basis of the work of Takahashi and Breitman [10]. In Fig. 4 (A–B) the effects of different concentrations of atRA on isolated mitochondria from the TM-3 cell line are shown. OGC activity decreased to 54% of control values with 10 nM atRA and 38% of control values when

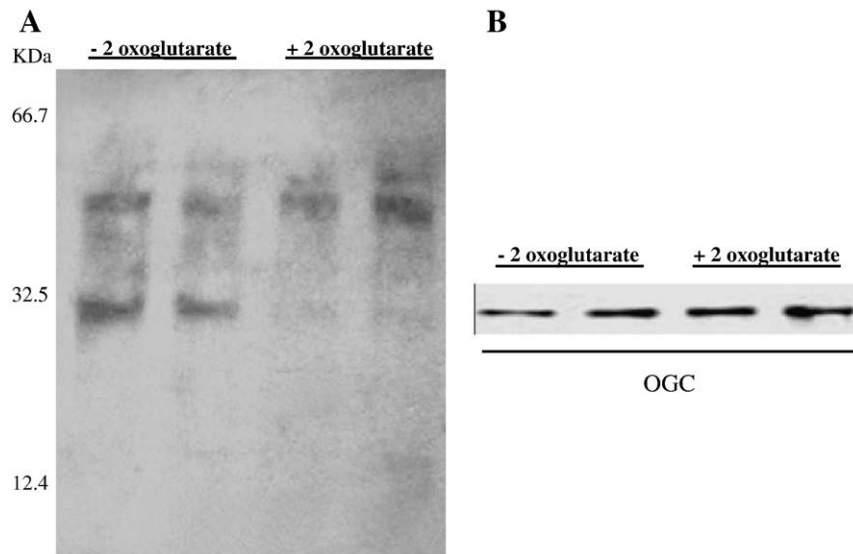


Fig. 3. Labeling of OGC by ³HatRA. (A) Testes mitochondrial protein was labeled with ³HatRA by retinoylation process as described in materials and methods. In fluorography, lanes 1 and 2 correspond to 20 μ g of mitochondrial testes protein labeled with ³HatRA. In lanes 3 and 4 10 mM of α -ketoglutarate was added to 20 μ g of mitochondrial testes protein together with ³HatRA. (B) OGC presence was verified by immunoblotting.

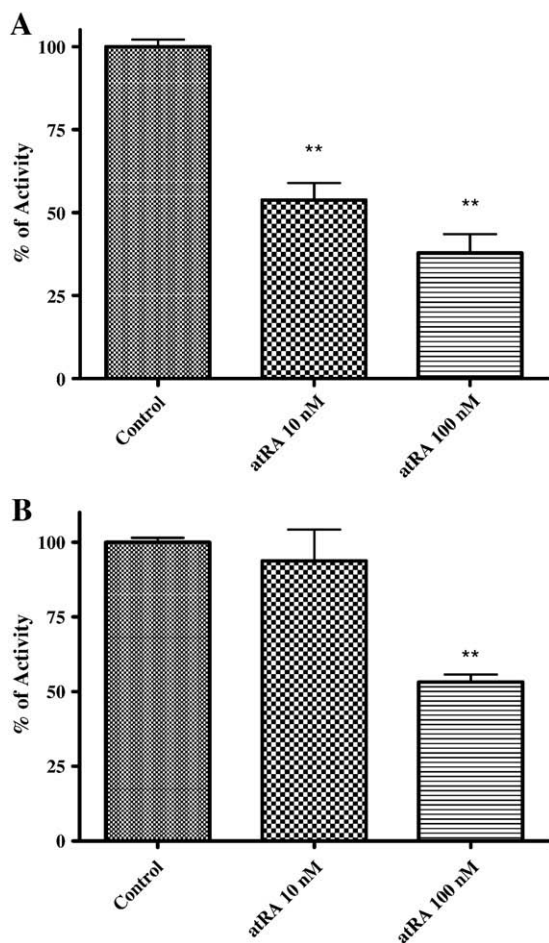


Fig. 4. Effect of atRA on OGC from TM-3 cells. (A) 1×10^6 /mL cells were treated with various concentrations of atRA for 24 h; then the mitochondria were isolated, the OGC extracted and the activity assayed as described in materials and methods. (B) Mitochondria from testes were incubated for 90 min as described in materials and methods with different concentrations of atRA at 37 °C. The proteins were then extracted and the OGC exchange activity assayed as described in materials and methods. Results are presented as Mean \pm SEM of three individual experiments. ** $P < 0.01$ compared to the control.

atRA was used at a concentration of 100 nM as shown in Fig. 4A. Conversely no effect was highlighted at 10 nM of atRA on OGC extracted from whole tissue, as shown in Fig. 4B. Similar effects were highlighted when 13-*cis*-RA was used at the same concentrations of atRA in TM-3 with the exception that 10 nM 13-*cis*-RA was more active in inhibiting OGC activity (Fig. 5A–B).

4. Discussion

Retinoylation is one of several covalent modifications of proteins. Biochemical similarities exist among retinoylation, palmitoylation and myristoylation: in all of these processes the substrate binds covalently to pre-existing protein via a thioester bond after the formation of a CoA-protein intermediate [26,27]. As the biosynthetic steps that lead to testosterone production are mainly NADH/NADPH dependent, the oxoglutarate carrier (OGC) was chosen as the experimental target for its involvement in the oxoglutarate–isocitrate shuttle that provides for the necessary exchange of reducing equivalents between the mitochondria and the cytosol. In addition, the strong inhibitory effect of 2-cyano-4-hydroxycinnamate (an inhibitor of OGC) but not 1,2,3-benzotricarboxylate (an inhibitor of citrate carrier) on the retinoylation processes (as highlighted in Table 1) was the start point for our further investigation in this paper. Our results showed that transport activity of OGC from rat testes mitochondria was strongly influenced

by NEM and atRA (Fig. 1). In humans, cows and rats there is only one gene encoding OGC: according to the amino acid sequence the bovine OGC protein contains three cysteines: Cys184 located in TMS IV and Cys221 and Cys224 in TMS V. Mercurials and maleimides interact only with Cys184 of the purified and reconstituted OGC, as Cys221 and Cys224 are linked by a disulphide bridge [1]. Therefore we propose that atRA, via retinoylation reaction, could bind the OGC on the same residue (Cys184), as the inhibitory effect of atRA is still the same when NEM is present concomitantly as shown in Fig. 1, leading us to hypothesize the existence of a putative amino acid sequence related to the atRA binding site in OGC. For what concerns OGC and its involvement in testosterone biosynthesis, the first enzymatic step is to convert cholesterol in pregnenolone: the reaction occurs in the mitochondrial matrix and requires reducing equivalents mainly as NADPH; conversely the role of the OGC is to carry out reducing equivalents from the mitochondria to the cytoplasm.

Previously we have demonstrated that there is a positive correlation between retinoylation reaction and testosterone biosynthesis [20]: the action of RA to slow down the OGC transport activity is in agreement with the testosterone synthetic process as reducing equivalents are more necessary to convert cholesterol in the matrix rather than in the cytoplasm [28]. At the same time the retinoylation

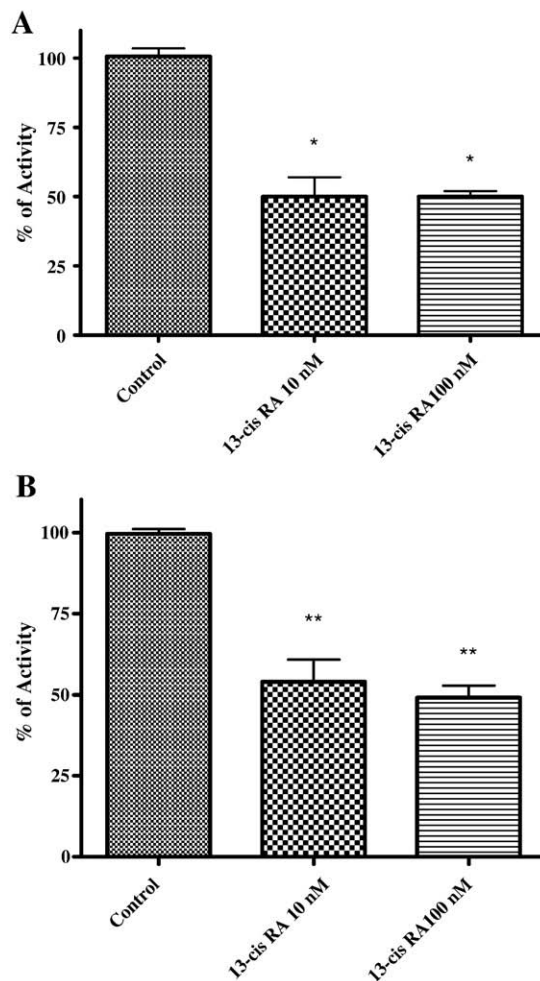


Fig. 5. Effect of 13-*cis*-RA on OGC. (A) 1×10^6 /mL TM-3 cells were treated with various concentrations of 13-*cis*-RA for 24 h and then the mitochondria were isolated, proteins extracted and the activity assayed as described in materials and methods. (B) Mitochondria from testes were incubated for 90 min with different concentrations of 13-*cis*-RA at 37 °C. Then the OGC was extracted and the activity tested as described in materials and methods. Results are presented as Mean \pm SEM of three individual experiments. ** $P < 0.01$ compared to the control.

reaction is tightly dependent on the pH: in fact the inhibitory effect of atRA on OGC is lost when the pH is higher than 7.5 (Fig. 2). To gain insight into the interaction of atRA and OGC two separate assays could be performed: the first through photolabeled testes mitochondrial protein with ³HatRA, because atRA binds covalently to proteins under UV light exposure [35], and the second via retinoylation reaction with ³HatRA [24]. Performing the latter we observed how the atRA binding to a 31.5 kDa protein was prevented by 2-oxoglutarate, the specific OGC substrate (Fig. 3). Fluorography of the electrophoresed proteins revealed the labeling of very few mitochondrial proteins. Under normal conditions, atRA is present in the testes at nanomolar concentrations [29]. Our results show that, only in mitochondria derived from the Leydig TM-3 cell line, does atRA have effects on OGC at concentration of 10 nM and in a stronger manner inhibit the OGC activity at a concentration of 100 nM (Fig. 4A). Interestingly, the concentrations of atRA required for producing this effect in steroidogenic cells are lower than those required with mitochondria isolated from the whole organ, supporting the above-mentioned view that steroidogenic cells can be more sensitive to atRA than isolated mitochondria (Fig. 4B). In addition 13-*cis*-RA has been shown as a competitive inhibitor of atRA in the retinoylation process [18]. In this case 13-*cis*-RA exerts its effects of reducing OGC transport activity on mitochondria from whole tissue at a lower concentration than atRA (Fig. 5A), most likely thanks to the altered conformation of this isomer that may allow it to better interact with OGC both in mitochondria from cultured cells or whole tissue (Fig. 5B). Our study, along with others [9,30,31], suggests that specific interactions occur among retinoids and non-nuclear receptor proteins, such as PKC, ANT and OGC, which are different from nuclear receptors, take place. Thus, the extra-nuclear action of retinoids seems to be a more general and important phenomena leading to both physiological and also pharmacological relevance.

It is known that retinoids play an essential role in spermatogenesis in rodents. In fact, a vitamin A-deficient diet causes the cessation of spermatogenesis, loss of mature germ cells and a reduction in testosterone level in mice and rat testes [32,33].

There is argument in favour of biological action of atRA through OGC binding and inhibition. AtRA does not exist in the cell in free form but is bound to proteins such as cellular retinoic acid binding protein (CRABP). The existence of a CRABP associated with mitochondria that binds and keeps retinoic acid in the organelle has been described by Ruff and Ong [34]. This mitochondrial CRABP could explain how retinoic acids could concentrate and regulate OGC in the mitochondrial compartment *in vivo*. In conclusion, in the present study we demonstrate that atRA via retinoylation reaction is able to influence OGC and that this effect is another level of control in steroidogenesis.

Acknowledgements

We thank Dr. James Chithalen for the helpful comments and English revision. This research was supported by grants from Ministero dell'Istruzione, dell'Università e della Ricerca (MIUR, Italia) and IRCCS Associazione Oasi Maria SS. We also thank Dr. F. Palmieri (University of Bari) for the generous gift of oxo-glutarate carrier antibody.

References

- [1] F. Palmieri, The mitochondrial transporter family (SLC25): physiological and pathological implications, *Eur. J. Physiol.* 447 (2004) 689–709.
- [2] D.J. Mangelsdorf, K. Umehara, R.M. Evans, The retinoid receptors, in: M.B. Sporn, A.B. Roberts, D.S. Goodman (Eds.), *The Retinoids: Biology, Chemistry, and Medicine*, Raven Press, New York, 1994, pp. 319–349.
- [3] P. Chambon, A decade of molecular biology of retinoid receptors, *FASEB J.* 10 (1996) 940–954.
- [4] M.B. Rogers, Life and death decisions influenced by retinoids, *Curr. Top. Dev. Biol.* 35 (1997) 1–46.
- [5] J.C. Saari, Retinoids in photosensitive system, in: M.B. Sporn, A.B. Roberts, D.S. Goodman (Eds.), *The Retinoids: Biology, Chemistry, and Medicine*, Raven Press, New York, 1994, pp. 351–385.
- [6] D.M. Wellik, D.H. Norback, H.F. DeLuca, Retinol is specifically required during mid gestation for neonatal survival, *Am. J. Physiol.* 272 (1997) E25–E29.
- [7] J. Buck, F. Derguini, E. Levi, K. Nakanishi, U. Hammerling, Intracellular signaling by 14-hydroxy-4,14-retroretinol, *Science* 254 (1991) 1654–1656.
- [8] S.D. Bolmer, G. Wolf, Retinoids and phorbol esters alter release of fibronectin from enucleated cells, *Proc. Natl. Acad. Sci. U. S. A.* 79 (1982) 6541–6545.
- [9] B. Notario, M. Zamora, O. Vinas, T. Mampel, All-*trans*-retinoic acid binds to and inhibits adenine nucleotide translocase and induces mitochondrial permeability transition, *Mol. Pharmacol.* 63 (2003) 224–231.
- [10] N. Takahashi, T.R. Breitman, Retinoic acid (retinoylation) of a nuclear protein in the human acute myeloid leukemia cell line HL60, *J. Biol. Chem.* 264 (1989) 5159–5163.
- [11] N. Takahashi, T.R. Breitman, Retinoic acid acylation: retinoylation, *Methods Enzymol.* 189 (1990) 233–239.
- [12] N. Takahashi, T.R. Breitman, Retinoylation of proteins in mammalian cells, in: R. Blomhoff (Ed.), *Vitamin A in Health and Disease*, Marcel Dekker, New York, 1994, pp. 257–273.
- [13] S. Tournier, F. Raynaud, P. Gerbaud, S.M. Lohmann, W.B. Anderson, D. Evain-Brion, Retinoylation of the type II cAMP-binding regulatory subunit of cAMP-dependent protein kinase is increased in psoriatic human fibroblasts, *J. Cell Physiol.* 167 (1996) 196–203.
- [14] A.M. Myhre, N. Takahashi, R. Blomhof, T.R. Breitman, K.R. Norum, Retinoylation of proteins in rat liver, kidney, and lung *in vivo*, *J. Lipid Res.* 37 (1996) 1971–1977.
- [15] B. Renstrom, H.F. DeLuca, Incorporation of retinoic acid into proteins via retinoyl-CoA, *Biochim. Biophys. Acta* 998 (1996) 69–74.
- [16] A.M. Myhre, E. Hagen, R. Blomhoff, K.R. Norum, Retinoylation of proteins in a macrophage tumor cell line J774, following uptake of chylomicron remnant retinyl ester, *J. Nutr. Biochem.* 9 (1998) 705–711.
- [17] G. Genchi, J.A. Olson, Retinoylation of proteins in cell-free fractions of rat tissues *in vitro*, *Biochim. Biophys. Acta* 1530 (2001) 146–154.
- [18] E. Cione, G. Genchi, Characterization of rat testes mitochondrial retinoylating system and its partial purification, *J. Bioenerg. Biomembr.* 36 (2004) 211–217.
- [19] E. Cione, P. Tucci, A. Chimento, V. Pezzi, G. Genchi, Retinoylation reaction of proteins in Leydig (TM-3) cells, *J. Bioenerg. Biomembr.* 37 (2005) 43–48.
- [20] P. Tucci, E. Cione, G. Genchi, Retinoic acid-induced testosterone production and retinoylation reaction are concomitant and exhibit a positive correlation in Leydig (TM-3) cells, *J. Bioenerg. Biomembr.* (in press), doi:10.1007/s10863-008-9156.
- [21] O.H. Lowry, N.J. Rosebrough, R.J. Randall, Protein measurement with the Folin phenol reagent, *J. Biol. Chem.* 193 (1951) 265–275.
- [22] F. Palmieri, M. Klingenberg, Direct methods for measuring metabolite transport and distribution in mitochondria, *Methods Enzymol.* 56 (1979) 279–301.
- [23] F. Bisaccia, C. Indiveri, F. Palmieri, Purification and reconstitution of two anion carriers from rat liver mitochondria: the dicarboxylate and the 2-oxoglutarate carrier, *Biochim. Biophys. Acta* 993 (1998) 229–240.
- [24] N. Takahashi, T.R. Breitman, Retinoylation of HL-60 Proteins, *J. Biol. Chem.* 266 (1990) 19158–19162.
- [25] R. Bolli, K.A. Nalecz, A. Azzi, Monocarboxylate and α -ketoglutarate carriers from bovine heart mitochondria. Purification by affinity chromatography on immobilized 2-cyano-4-hydroxycinnamate, *J. Biol. Chem.* 263 (1989) 18024–18030.
- [26] A.M. Schultz, L.E. Henderson, S. Oroszlan, Fatty acylation of proteins, *Annu. Rev. Cell Biol.* 4 (1988) 611–647.
- [27] M. Wada, T. Fukui, Y. Kubo, N. Takahashi, Formation of retinoyl-CoA in rat tissues, *J. Biochem.* 130 (2001) 457–463.
- [28] D.M. Stocco, Tracking the role of a star in the sky of the new millennium, *Mol. Endocrinol.* 15 (2001) 1245–1254.
- [29] M.A. Kane, A.E. Folias, C. Wang, J.L. Napoli, Quantitative profiling of endogenous retinoic acid *in vivo* and *in vitro* by tandem mass spectrometry, *Anal. Chem.* 80 (2008) 1702–1708.
- [30] E. Rial, M. González-Barroso, C. Fleury, S. Iturrizaga, D. Sanchis, J. Jiménez-Jiménez, D. Ricquier, M. Goubern, F. Bouillaud, Retinoids activate proton transport by the uncoupling proteins UCP1 and UCP2, *EMBO J.* 18 (1999) 5827–5833.
- [31] A. Radominska-Pandya, G. Chen, P.J. Czernik, J.M. Little, V.M. Samokyszyn, C.A. Carter, G. Nowak, Direct interaction of all-*trans*-retinoic acid with protein kinase C (PKC). Implications for PKC signaling and cancer therapy, *J. Biol. Chem.* 275 (2000) 22324–22330.
- [32] S.B. Wolbach, P.R. Howe, Nutrition classics: tissue changes following deprivation of fat soluble A vitamin, *J. Exp. Med.* 42 (1925) 753–777.
- [33] D.R. Appling, F. Chytil, Evidence of a role for retinoic acid (vitamin A-acid) in the maintenance of testosterone production in male rats, *Endocrinology* 108 (1981) 2120–2124.
- [34] S.J. Ruff, D.E. Ong, Cellular retinoic acid binding protein is associated with mitochondria, *FEBS Lett.* 487 (2000) 282–286.
- [35] P.S. Bernstein, S.-Y. Choi, Y.-C. Ho, R.R. Rando, Photoaffinity labeling of retinoic acid-binding proteins, *Proc. Natl. Acad. Sci. U. S. A.* 92 (1995) 654–658.



Stearyl ferulate-based solid lipid nanoparticles for the encapsulation and stabilization of β -carotene and α -tocopherol

Sonia Trombino^{a,*}, Roberta Cassano^a, Rita Muzzalupo^a, Attilio Pingitore^b, Erika Cione^b, Nevio Picci^a

^a Department of Pharmaceutical Sciences, University of Calabria, 87036 Arcavacata di Rende, Cosenza, Italy

^b Department of Pharmaco-Biology, University of Calabria, 87036 Arcavacata di Rende, Cosenza, Italy

ARTICLE INFO

Article history:

Received 26 November 2008

Received in revised form 4 March 2009

Accepted 31 March 2009

Available online 8 April 2009

Keywords:

Ferulic acid

β -Carotene

α -Tocopherol

Solid lipid nanoparticles (SLN)

Antioxidants

ABSTRACT

UVA exposure induces DNA damage that could result in skin carcinogenesis. Antioxidants are usually employed as protective agents to avoid this problem: in particular, both β -carotene and α -tocopherol can protect the skin against UVA-induced damage. It is well known that the photochemical instability of these compounds has been a limiting factor for their applications to protect skin. In this study, stearyl ferulate-based solid lipid nanoparticles (SF-SLNs), as vehicles for β -carotene and α -tocopherol, were formulated to improve the stability of these compounds. The SF-SLNs were characterized for entrapment efficiency, size and shape together with their cytotoxicity and capability to inhibit lipid peroxidation. After treatment with a pro-oxidant and/or exposition to sunlight the antioxidants entrapped in SF-SLNs were extremely stable. The results highlighted how SF-SLNs represent a suitable vehicle for β -carotene and α -tocopherol stabilizing and protecting them from degradation. A dermatological formulation in order to prevent skin damages is, therefore, suggested.

© 2009 Elsevier B.V. All rights reserved.

1. Introduction

UVA exposure induces DNA damage resulting in both acute and chronic lesions to human skin. These include sunburn, skin cancer, oxidative stress and photo ageing. They are strictly dependent on the form, amount and intensity of UV radiation as well as on the type of the individual exposed [1,2]. DNA does not absorb UVA radiation directly and the damage is mediated by the production of reactive oxygen species [3]. There is strong evidence suggesting that antioxidants can be employed as protective agents against the DNA damaging effects of UV exposure. In particular, β -carotene, a free radical scavenging antioxidant, has been shown to protect against photoimmunosuppression and sunlight-induced erythema in human skin [4–7] and α -tocopherol, a chain-breaking antioxidant, has been shown to protect against cell damage induced by UVA exposure [8]. Moreover, both β -carotene and α -tocopherol can inhibit lipid peroxidation by preventing free radical production, and/or by reducing malondialdehyde amount [9–11]. In spite of a wide range of biological and pharmacological effects, the dermatological application of these compounds is still limited due to their photochemical instability. In fact, the chemical structure of these vitamins comprises conjugated double-bond systems that

make them susceptible to oxidative cleavage and isomerization by oxygen, light and heat [12].

Therefore formulations that increase the chemical stability of β -carotene and α -tocopherol and enhance their penetration through the stratum corneum, are essential to improve their efficacy as topical agents.

During the last years, increasing attention has been given to alternative nanoparticles made from solid lipids, called solid lipid nanoparticles (SLNs). These are spherical particles, in the nanometer range, which are dispersed in water or in aqueous surfactant solutions [13,14]. They represent an alternative drug delivery system to colloidal carriers such as lipid emulsions, liposomes and polymeric nanoparticles and an excellent candidate for the encapsulation of drugs with poor water solubility. SLNs combine the advantages of different colloidal drug delivery systems, avoiding some of their disadvantages [15]. SLNs formulations have been developed for various pharmacological administration routes, such as parenteral, oral, ocular, pulmonary and rectal ones [16–19]. Recently, they have been considered advantageous for topical administration of active cosmetic ingredients, especially concerning antioxidants and sunscreens [20–22]. The incorporation of chemically labile active ingredients into the solid lipid matrix has been shown to protect them against degradation [23,24] giving new perspectives to the use of cosmetic ingredients that suffer chemical instability in traditional formulations [25]. Furthermore, the occlusive effect of SLNs leads to an increase in skin hydration and, thus,

* Corresponding author. Tel.: +39 0984493151; fax: +39 0984493163.
E-mail address: sonia.trombino@unical.it (S. Trombino).

Table 1
Composition of FA-SLNs and SA-SLNs.

Formulation	Lipid	Components				Drug
SF-SLNs	Stearic acid (g)	Tween 20 (ml)	Butanol (ml)	Sodium taurocholate (g)	Water (ml)	β -Carotene α -tocopherol (g)
	0.5	0.62	0.25	0.32	2.5	
SA-SLNs	Stearyl ferulate (g)	Tween 20 (ml)	Butanol (ml)	Sodium taurocholate (g)	Water (ml)	β -Carotene α -tocopherol (g)
	0.5	0.39	0.16	0.18	1.6	

to wrinkle smoothing, enhancing the penetration of compounds in specific skin layers [26] that is a fundamental requirement for the efficacy of cosmetic treatments.

In the present work, we have developed and characterized stearyl ferulate-based solid lipid nanoparticles (SF-SLNs), as vehicle for both β -carotene and α -tocopherol, with the aim of increasing the photochemical stability of these compounds. It is worth noting that ferulic acid is a potent antioxidant having synergistic effects with other antioxidants and it is able to protect and stabilize them from degradation [27,28]. For such reasons, we decided to link ferulic acid to stearyl alcohol that differs from the essential component of traditional SLNs, stearic acid, in the functional group. The obtained nanoparticles, SF-SLNs, were characterized for entrapment efficiency, size and shape, and compared to traditional stearic acid SLNs (SA-SLNs). We also investigated in rat liver microsomal membranes the antioxidant activity of either SF-SLNs or SA-SLNs, entrapping α -tocopherol and β -carotene, in inhibiting the lipid peroxidation induced by two different sources of free radicals, 2,2'-azobis (2-amidinopropane) (AAPH), which exogenously produces peroxy radicals by thermal decomposition, and *tert*-butyl hydroperoxide (*tert*-BOOH), which endogenously produces alkoxyl radicals by Fenton reactions. Moreover, the cytotoxicity of the SF-SLNs or SA-SLNs drug free was tested on RAT-1 immortalized fibroblasts. In addition all the obtained SLNs (SF-SLNs and SA-SLNs) were submitted to stability studies.

2. Materials and methods

2.1. Materials

β -Carotene, α -tocopherol, ferulic acid (FA), toluene, *p*-toluenesulfonic acid were used as received without further purification; stearyl alcohol (SA) taurocholic acid sodium salt (TC), Tween 20, potassium chloride (KCl), ethylenediaminetetraacetic acid (EDTA), sucrose, 4,2-hydroxyethyl-1-piperazineethanesulfonic acid (HEPES), trichloroacetic acid (TCA), hydrochloric acid, butylated hydroxytoluene (BHT), *tert*-butyl hydroperoxide (*tert*-BOOH), 2,2'-Azobis (2-amidinopropane) (AAPH) and 2-thiobarbituric acid (TBA) were supplied by Sigma (Sigma Chemical Co, St. Louis, MO), and used as received. Methanol, chloroform, butanol, toluene, dihydrogen sodium phosphate, phosphoric acid, ethyl acetate, acetonitrile and *n*-hexane were purchased from Fluka Chemika-Biochemika (Buchs, Switzerland), and Carlo Erba Reagents (Milan, Italy), and used as received. Water from a Millipore Milli-Q[®] ultrapure water purification unit was used. MEM medium, fetal calf serum and glutamine were purchased from Gibco (Invitrogen Life Technologies, Italy).

2.2. Methods

2.2.1. Synthesis of stearyl ferulate

Stearyl ferulate was synthesized according to the procedure described in the literature [29]. Ferulic acid (1.0 g, 5.15 mmol), *p*-

toluenesulfonic acid (0.07 g, 0.34 mmol) and stearyl alcohol (0.7 g, 5.4 mmol) were added to 10 ml dry toluene under stirring and N₂ at room temperature. When addition was complete, the solution was stirred under N₂ for 12 h at 110 °C. After cooling at room temperature, the solvent was evaporated under reduced pressure, the residue was treated with 15 ml water and the aqueous phase was extracted with chloroform (4 × 15 ml). The combined organic phases were collected, dried (Na₂SO₄) and the solvent was removed by rotary evaporation to give yellow-colored stearyl ferulate and purified by Merck silica gel (60–230 mesh) column chromatography, using ethyl acetate/*n*-hexane 85/15 (v/v) as eluent. The solvent of eluted ester was evaporated under reduced pressure. The stearyl ferulate was obtained with a yield of 80–90% and identified by TLC, UV and NMR analyses [29–31].

2.2.2. Preparation of SF-SLNs and SA-SLNs

SF-SLNs and SA-SLNs were prepared by a microemulsion technique at moderate temperature according to Gasco [32] as shown in Table 1. Briefly, stearyl ferulate or stearic acid in the absence and/or in the presence of β -carotene or α -tocopherol were melted at 70–75 °C. A warm water solution of sodium taurocholate, butanol and Tween 20 was then added to obtain an optically transparent system. The warm microemulsion was immediately dispersed in cold water (~2 °C) under high-speed homogenation (Model SL2, Silverson, Chesham Bucks, England) at 8000 rpm for 15 min. The volume ratio of warm microemulsion to cold water was 1:20. The SF-SLNs and SA-SLNs dispersions were washed two times using an Amicon TCF2A ultrafiltration system (Amicon Grace, Beverly, MA USA; membrane Amicon Diaflo YM 100).

2.2.3. Size distribution analysis

The size of the particles was determined by dynamic light scattering (DLS) using a 90 Plus Particle Size Analyzer (Brookhaven Instruments Corporation, New York, USA) at 25 °C by measuring the autocorrelation function at 90° scattering angle. Cells were filled with 100 μ l of sample solution and diluted to 4 ml with filtered (0.22 μ m) water. The polydispersity index (PI) indicating the measure of the distribution of nanoparticle population [33] was also determined. Six separate measurements were made to derive the average. Data were fitted by the method of inverse "Laplace transformation" and Contin [34,35].

2.2.4. Transmission electron microscopy (TEM)

The morphology of the hydrated niosomal dispersions was examined using TEM. A drop of niosomal dispersion was applied to a carbon-coated copper grid and left for 1 min to allow some of the particles to adhere to the carbon substrate. The excess of dispersion was removed by adsorbing the drop with a piece of filter paper. A drop of 1% phosphotungstic acid solution was applied and again excess of solution was removed by adsorbing the liquid with the tip of a filter paper and the sample was air-dried. The sample was then observed under a ZEISS EM 900 electron microscope at an accelerating voltage of 80 kV.

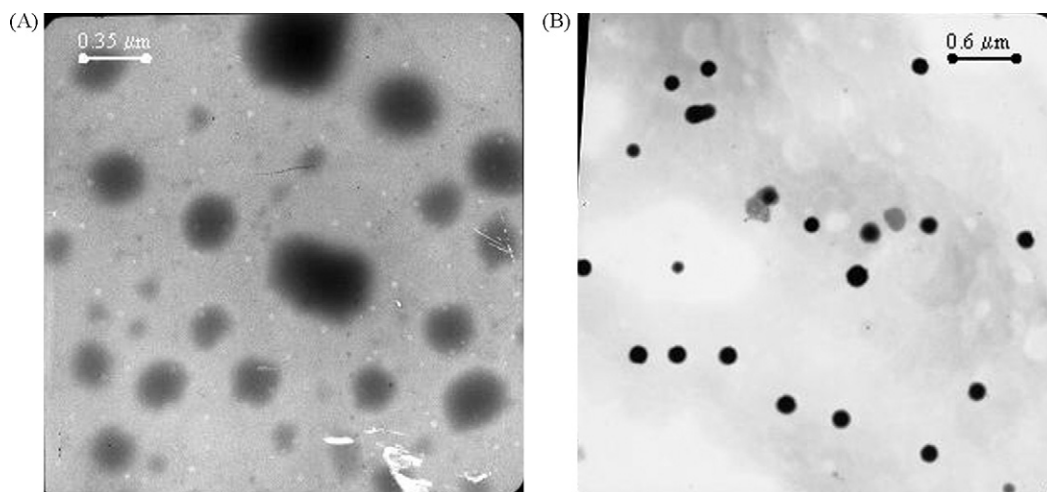


Fig. 1. Photomicrographs of SF-SLNs, containing α -tocopherol (A) and β -carotene (B), visualized by TEM (transmission electronic microscopy).

2.2.5. Percentage of drug incorporated into solid lipid nanoparticles

SLNs formulation (1 ml) was diluted to 10 ml with methanol and, to evaluate α -tocopherol and β -carotene content, was analyzed by reverse-phase HPLC with spectrophotometric detection at wavelengths of 280 nm and 450 nm, respectively, on a Jasco UV-2075 detector. The column was packed with Alltech C18 Adsorbosphere HS material, 3 μ m particle size, in a 15 cm \times 0.46 cm cartridge format (Alltech Associates, Deerfield, IL). A 1-cm cartridge precolumn, containing 5- μ m C18 Adsorbosphere packing was used. The mobile phases were: 60% acetonitrile/10% methanol/30% isopropanol, at a flow rate of 1 ml/min, for β -carotene; 0.01 M dihydrogen sodium phosphate/0.01 M phosphoric acid with acetonitrile (88:12, v/v) pH 2.3, at a flow rate of 0.5 ml/min, for α -tocopherol.

2.2.6. Microsomal suspensions preparation

Liver microsomes were prepared from Wistar rats by tissue homogenization with 5 volumes of ice-cold 0.25 M sucrose containing 5 mM Hepes, 0.5 mM EDTA, pH 7.5 in a Potter-Elvehjem homogenizer [36]. Microsomal membranes were isolated by the removal of the nuclear fraction at 8000 \times g for 10 min, and the removal of the mitochondrial fraction at 18,000 \times g for 10 min. The microsomal fraction was sedimented at 10,5000 \times g for 60 min, and the fraction was washed once in 0.15 M KCl, and collected again at 10,5000 \times g for 30 min [37]. The membranes, suspended in 0.1 M potassium phosphate buffer, pH 7.5, were stored at -80°C . Microsomal proteins were determined by the Bio-Rad method [38].

2.2.6.1. Addition of loaded SF-SLNs and SA-SLNs to microsomes.

Aliquots of loaded SF-SLNs and SA-SLNs (0.5 v/v) were added to the microsomes. Control microsomes received amounts of H_2O equal to those present in SLNs-treated microsomes. The microsomes were gently suspended by a Dounce homogenizer, and then the suspensions were incubated at 37°C in a shaking bath under air in the dark

in the absence and in the presence of *tert*-BOOH or AAPH.

2.2.7. Malondialdehyde formation

Malondialdehyde (MDA) was extracted, and analyzed as indicated by Hagerman et al. [39]. Briefly, aliquots of 1 ml of microsomal suspension (0.5 mg proteins) were mixed with 3 ml 0.5% TCA and 0.5 ml of TBA solution (two parts 0.4% TBA in 0.2 M HCl and one part distilled water), and 0.07 ml of 0.2% BHT in 95% ethanol. Samples were then incubated in a 90°C bath for 45 min. After incubation, the TBA-MDA complex was extracted with 3 ml of isobutyl alcohol. The absorbances of the extracts were measured by UV spectrophotometry at 535 nm, and the results were expressed as mmol per mg of protein, using an extinction coefficient of $1.56 \times 10^5 \text{ l mmol}^{-1} \text{ cm}^{-1}$.

2.2.8. Stability studies of SF-SLNs and SA-SLNs entrapping α -tocopherol and β -carotene

SF-SLNs and SA-SLNs entrapping α -tocopherol and β -carotene were stored at room temperature ($28\text{--}30^\circ\text{C}$) and exposed to sunlight for 3 months. An aliquot was taken, once a month, to examine the particle size and, after the third month, to evaluate the drug content. The mean particle size was determined by light scattering as described in Section 2.2.3. The entrapment efficiency was determined by reverse phase HPLC as described in Section 2.2.5.

2.2.9. Pro-oxidant test

Only one of the two loaded antioxidants was used for the pro-oxidant experiment. In particular SF-SLNs and SA-SLNs entrapping α -tocopherol (1 ml) were soaked, in the presence of 500 μl of a *tert*-BOOH ($0.25 \times 10^{-3} \text{ M}$) aqueous solution, in 5 ml 0.1 M potassium phosphate buffer, for 2 h at room temperature, and under magnetic stirring. After diafiltration, freezing and lyophilization, dried α -tocopherol-loaded SF-SLNs or SA-SLNs were divided into two portions. An aliquot (10 mg) was dissolved in 10 ml methanol. The pro-oxidant effect was evaluated, by CG/MS (Hewlett Packard GC-MSD 5972, UV-VIS spectrophotometer V-530 JASCO), as reported

Table 2
Mean particle size and PI index of SF-SLNs and SA-SLNs. Overall $^*P < 0.05$.

Formulation	Drug	Size (nm)	Polydispersity index
SF-SLNs	Drug-free	159.3 \pm 6.1	0.118 \pm 0.068
	α -Tocopherol	175.7 \pm 3.4	0.121 \pm 0.046
	β -Carotene	169.8 \pm 4.8	0.115 \pm 0.053
SA-SLNs	Drug-free	176.3 \pm 3.2	0.127 \pm 0.062
	α -Tocopherol	195.3 \pm 8.2	0.131 \pm 0.049
	β -Carotene	187.4 \pm 3.8	0.125 \pm 0.039

in our previous study [40]. Then a second aliquot of α -tocopherol loaded SF-SLNs or SA-SLNs was used to test the antioxidant activity, after pro-oxidation, following the procedures described in Sections 2.2.6.1 and 2.2.7.

2.2.10. Cell culture

RAT-1 immortalized fibroblasts (American Type Culture Collection, Rockville, MD, USA) were grown in MEM medium without antibiotics, supplemented with 10% fetal calf serum and 2 mM glutamine. Cells were maintained in log phase by seeding twice a week at a density of 3×10^5 cells/ml at 37 °C in a humidified atmosphere at 5% CO₂ in air. Cell number was estimated with a Burker camera. Drug-free SA-SLNs and SF-SLNs were dissolved in water and then diluted in cell culture media.

2.2.10.1. In vitro evaluation of toxicity. The cytotoxic effects of drug-free SA-SLNs and SF-SLNs on RAT-1 cells were evaluated with the trypan blue dye exclusion assay (cell mortality) and the MTT dye test (cell viability). RAT-1 were seeded at a density of 3×10^4 cells/ml in 12-well plastic culture dishes for the trypan blue dye exclusion test and at a density of 2×10^4 cells/ml in 12-well tissue culture plates for the MTT test. After 24 h incubation, the culture medium was replaced with serum-free medium and SA-SLNs or SF-SLNs were added at final scalar dilutions (0–50 μ M). The toxicity experiments were carried out at different incubation times from 3 h to 24 h. Untreated RAT-1 cells were used as control and blank sample in various experiments, respectively. To perform the trypan blue dye exclusion assay, RAT-1 were harvested using trypsin/EDTA (1 \times) solution (2 ml), washed twice with phosphate buffer solution (2 ml) and transferred to plastic centrifuge tubes with 4 ml. Samples were then centrifuged with an ALC PK 120R at 1200 rpm at room temperature for 5 min. The supernatant was discarded and the pellet was suspended in 200 μ l trypan blue buffer, for 30 s and the amount of dead cells (blue stained cells) was observed and counted using a Burker camera under an optical microscope (Olympus CKX31). The percentage of cell mortality was calculated using the following equation

$$\% \text{Mortality} = \frac{C_D}{C_T} \times 100$$

where C_D is the number of dead cells and C_T the total number of cells. The cell viability assay was carried out using the MTT dye test. RAT-1 cells were seeded at a density of 2×10^4 cells/ml in 12-well culture plates for 24 h at 37 °C and 5% CO₂ to allow the adhesion of the cells. After 24 h incubation, the culture medium was removed and substituted with serum-free fresh medium, RAT-1 immortalized fibroblasts were then treated with SA-SLNs and SF-SLNs. At the end of the incubation time 50 μ L of MTT tetrazolium salt (5 mg/ml dissolved in PBS buffer) were added to each well and RAT-1 cells were incubated for additional 3 h, to allow the formation of violet formazan crystals. A solution of 0.04 N HCl in isopropanol (1 ml) was added to solubilize the formazan crystals in the cells. The absorbance was measured with the Ultrospec 2100 pro spectrophotometer (Amersham-Biosciences) at a test wavelength of 570 nm with a reference wavelength of 690 nm. The effect of drug treatment on the percentage of viable cells, directly proportional to the amount of formazan crystals formed, was calculated using the following equation

$$\% \text{Cell viability} = \frac{\text{Abs}_T}{\text{Abs}_U} \times 100$$

where Abs_T is the absorbance of treated cells and Abs_U is the absorbance of untreated cells. Values of cell mortality and cell viability are expressed as the mean of six different experiments \pm SEM.

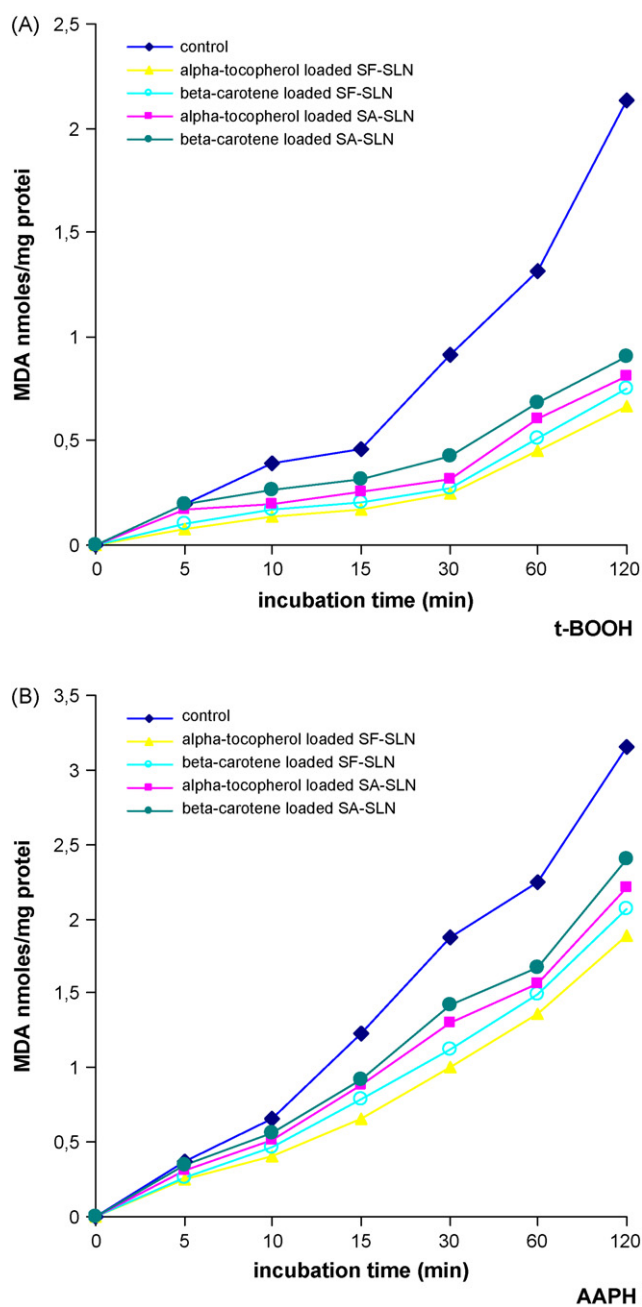


Fig. 2. Effects of SF-SLNs and SA-SLNs, α -tocopherol and β -carotene loaded, on malondialdehyde (MDA) production induced by *tert*-BOOH (A) and AAPH (B) in rat-liver microsomal membranes. The microsomal membranes were incubated with 0.25×10^{-3} M *tert*-BOOH or 25×10^{-3} M AAPH at 37 °C under air in the dark. Results represent the mean \pm SEM of six separate experiments. Overall $^{**} P < 0.01$.

2.3. Statistical analysis

Statistical differences were determined by one-way analysis of variance (ANOVA). The results were expressed as mean \pm SEM of n independent experiments.

3. Results and discussion

3.1. Morphology

SF-SLNs and SA-SLNs entrapping α -tocopherol and β -carotene were successfully prepared by microemulsion technique at the 70–75 °C temperature range.

Table 3Effect of time of storage (at room temperature and sunlight) on particle size of SF-SLNs and SA-SLNs. Overall ** $P < 0.01$.

Formulation	Drug	Size (nm), zero days	Size (nm), 1 month	Size (nm), 2 month	Size (nm), 3 month
SF-SLNs	α -Tocopherol	175.7 \pm 3.4	180.9 \pm 3.7	187.2 \pm 7.8	196.5 \pm 6.7
	β -Carotene	169.8 \pm 4.8	174.1 \pm 6.4	180.5 \pm 6.3	188.4 \pm 3.2
SA-SLNs	α -Tocopherol	195.3 \pm 8.2	205.6 \pm 8.9	219.1 \pm 2.3	241.2 \pm 4.8
	β -Carotene	187.4 \pm 3.8	200.2 \pm 3.4	224.4 \pm 4.9	235.4 \pm 3.2

Table 4Effect of time of storage (at room temperature and sunlight) on entrapment efficiency of SF-SLNs and SA-SLNs. Overall ** $P < 0.01$.

Formulation	Drug	Entrapment efficiency (EE%), zero days	Entrapment efficiency (EE%), 3 month
SF-SLNs	α -Tocopherol	58.7 \pm 0.32	57.3 \pm 0.41
	β -Carotene	49.2 \pm 0.26	48.4 \pm 0.31
SA-SLNs	α -Tocopherol	19.4 \pm 0.15	15.3 \pm 0.15
	β -Carotene	15.3 \pm 0.21	11.2 \pm 0.27

An oil-in-water microemulsion was spontaneously obtained as recognized by a clear solution after adding the heated water phase into the oil phase of the same temperature. The SLNs were obtained immediately when dispersing the warm microemulsion into cold water with the aid of a homogenizer. The cold water facilitated rapid lipid crystallization and prevented lipid aggregation [41]. Photomicrographs of SF-SLNs, containing α -tocopherol and β -carotene, visualized by TEM, are shown in Fig. 1(A and B) and revealed that the nanoparticles are spherical in shape, the particle size ranging approximately from 159 nm to 176 nm. However, a more accurate investigation into the size distribution was performed as described into the next section.

3.2. Particle sizes

The mean particle size of obtained formulations showed (Table 2), according to Dingler et al. [23], an increase of the particle size after incorporation of both antioxidants into the solid matrix of SLNs. In particular, the mean diameter was respectively 159.3 nm for the SF-SLNs drug free, 175.7 nm for SF-SLNs loaded with α -tocopherol and 169.8 nm for SF-SLNs entrapping β -carotene. On the other hand the SA-SLNs, both drug free and loaded with the two antioxidants, were characterized by a higher mean diameter.

PI values, as shown in Table 2, were lower than 0.2 for all formulations indicating a relatively narrow size distribution especially in the case of SF-SLNs.

3.3. Antioxidant properties of loaded SF-SLNs and SA-SLNs

The ability of loaded SF-SLNs and SA-SLNs to protect against lipid peroxidation induced by two different sources, of free radicals such as *tert*-BOOH and AAPH, was examined in rat-liver microsomal membranes during an incubation period of 120 min [27]. The effects of SF-SLNs and SA-SLNs on lipid peroxidation were time-dependent and effected as the MDA production (in nmol mg⁻¹ protein) (Fig. 2). Both SF-SLNs and SA-SLNs were stronger antioxidants in protecting the membranes from *tert*-BOOH- than from AAPH-induced lipid peroxidation showing a preservation of antioxidant activity up to 2 h, SF-SLNs exhibiting a higher antioxidant efficiency.

3.4. Stability data

In order to verify the ability to maintain the stability of entrapped antioxidants, SF-SLNs and SA-SLNs were stored at room temperature and exposed to sunlight for 3 months. α -tocopherol and β -carotene, in fact, are well-known light and oxygen sensitive substances; consequently, it is very important to protect them during storage. The results of stability studies are shown in

Tables 3 and 4. The mean particle size of SF-SLNs after preparation and after 3-months storage changed from 175.7 nm to 196.5 nm for SF-SLNs entrapping α -tocopherol and from 169.8 nm to 188.4 nm for SF-SLNs containing β -carotene. In the same period the SA-SLNs showed a major increase in size (Table 3). Also the content of the two antioxidants in SF-SLNs was similar after 3-months storage whereas the SA-SLNs showed a lower entrapment efficiency (Table 4).

3.5. Pro-oxidant test

We exposed SF-SLNs and SA-SLNs, entrapping α -tocopherol, to *tert*-BOOH, a free radicals generator. The antioxidant activity of both loaded SF-SLNs and SA-SLNs was evaluated after their pro-oxidation. The results suggest that, after this treatment, SF-SLNs exhibit an antioxidant activity higher than SA-SLNs (Fig. 3) confirming that the stearyl ferulate protected α -tocopherol during the pro-oxidation. In fact, CG/MS analysis of the drug, loaded in SF-SLNs, confirmed its integrity. On the contrary, only a small amount of α -tocopherol and some products of its degradation in SA-SLNs, under the same experimental conditions, were found (data not shown).

3.6. Effect of SA-SLNs and SF-SLNs on vitality of RAT-1 cells

In order to examine the cytotoxic effect of stearic acid and stearyl ferulate SLNs, RAT-1 cells were exposed to SA-SLNs and SF-SLNs in a concentration range from 0 μ M to 50 μ M for 24 h as described in Section 2.2.10.1, and MTT assay was carried out with cells cultured in SA-SLNs and SF-SLNs-free media as control. No significant change in viability was observed in RAT-1 cells treated with SA-SLNs in the range of 0–5 μ M, while no change was appreciated in

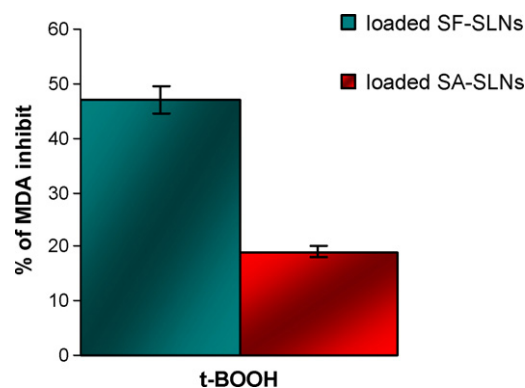


Fig. 3. Antioxidant activities of α -tocopherol-loaded SF-SLNs and SA-SLNs after pro-oxidant test Results represent the mean \pm SEM of six separate experiments. Overall ** $P < 0.01$.

Table 5
Influence of different concentrations of SA-SLNs and SF-SLNs on cell viability.

SA-SLNS (μM)	Vitality (%)	SF-SLNS(μM)	Vitality (%)
Control	100.0 \pm 4.2	Control	100.0 \pm 4.2
0.005	107.1 \pm 2.1	0.005	104.5 \pm 4.3
0.025	104.3 \pm 0.6	0.025	107.0 \pm 4.6
0.05	108.6 \pm 4.3	0.05	106.5 \pm 6.2
0.5	110.1 \pm 7.1	0.5	104.8 \pm 2.0
5	103.4 \pm 3.1	5	95.0 \pm 2.2
50	81.5 \pm 2.8	50	58.1 \pm 6.4

RAT-1 cells were harvested and treated with SA-SLNs and SF-SLNs in a dilution of 0–50 μM . After 24 h treatment, cells viability was assayed via MTT as described in Section 2. Results are expressed as Mean \pm SEM of three independent experiments. Overall ** $P < 0.01$.

cell viability for SF-SLNs in the concentration range of 0–0.5 μM (Table 5). On the contrary, a 20% reduction of vitality was found in the cells incubated with SA-SLNs at 50 μM and a 35% reduction of vitality was found in the cells incubated with SF-SLNs at 5 μM concentration. As shown in Fig. 4A, the cell viability was less than 80% after exposure to 50 μM SA-SLNs and less than 65% after exposure to 5 μM SF-SLNs for 24 h. The effect of both formulations on cell viability was also time-dependent, since the cell survival declined

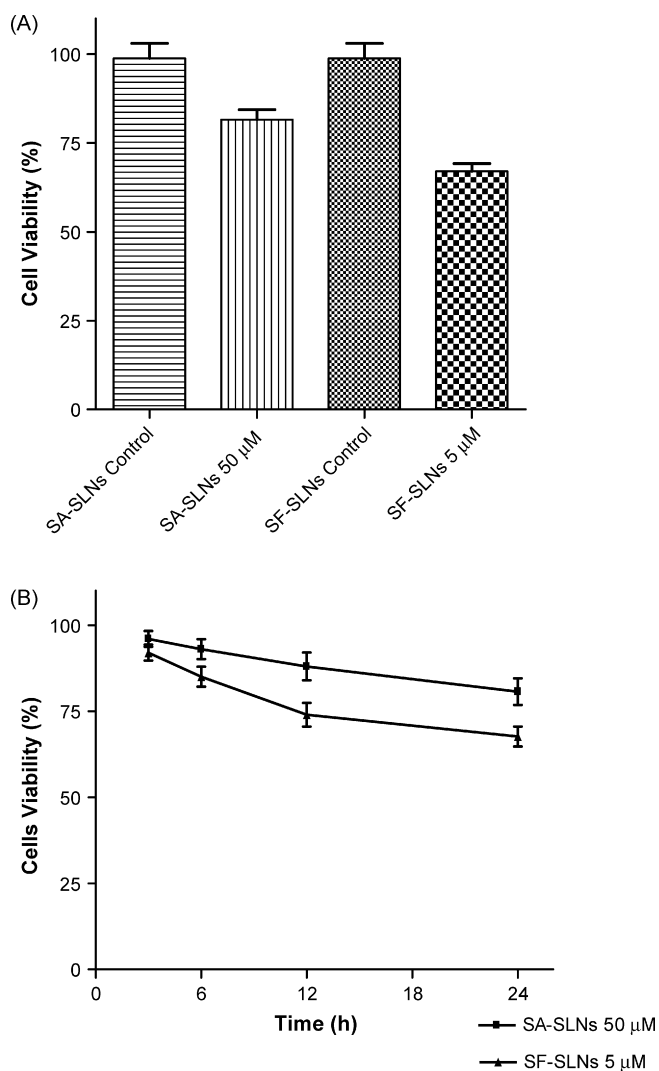


Fig. 4. Cells were incubated with SA-SLNs and SF-SLNs, 50 μM and 5 μM , respectively as described in Section 2.2.10. At 24 h post-exposure cell viability was assayed via MTT (A). A composite of 24 h treatment is shown in (B). Results represent the mean \pm SEM of six separate experiments. Overall ** $P < 0.01$.

drastically by increasing the treatment time from 3 h to 24 h in the cells incubated with 50 μM SA-SLNs or 5 μM SF-SLNs (Fig. 4B). The present results show that very high doses of SA-SLNs and high doses of SF-SLNs exert a cytotoxic effect on RAT-1 cells in a concentration- and time-dependent manner (Fig. 4A,B).

4. Conclusions

Stearyl ferulate was synthesized linking ferulic acid to stearyl alcohol and then SF-SLNs were successfully prepared by a microemulsion technique at moderate temperature. Then these nanoparticles entrapping two known antioxidants, β -carotene and α -tocopherol, were submitted to stability, antioxidant and cytotoxicity studies, characterized for entrapment efficiency, size, shape and compared to SLNs prepared with stearic acid. Our results demonstrate that SF-SLNs provide a good vehicle for β -carotene and α -tocopherol as they are able to stabilize them, preventing the oxidation and the degradation of both compounds. The cytotoxicity studies suggest that SF-SLNs are well tolerated at concentrations up to 5 μM , lower than SA-SLNs, in the formulation for short time exposure (no more than 6 h). However, it is interesting to note that SF-SLNs display a better efficiency of encapsulation (about 50% of β -carotene and α -tocopherol) with respect to SA-SLNs and for this reason they could even foster the release of the drugs. In this latter concern, further studies are needed. Therefore, SF-SLNs could be an interesting carrier for chemically labile active ingredients, in particular for what concerns topical application when they are used for all those formulations, either cosmetical or pharmaceutical, that are suitable with the low micromolar range of SF-SLNs or simply employed, at higher doses, to store photosensitive compounds before being used for chemical purposes.

Acknowledgements

This work was financially supported by University Funds.

References

- [1] M. Ichihashi, M. Ueda, A. Budiyanoto, T. Bito, M. Oka, M. Fukunaga, K. Tsuru, T. Horikawa, *Toxicology* 189 (2003) 21.
- [2] V.O. Melnikova, H.N. Ananthaswamy, *Mutat. Res.* 571 (2005) 91.
- [3] J.L. Ravanat, T. Douki, J. Cadet, *J. Photochem. Photobiol. B* 63 (2001) 88.
- [4] C.J. Fuller, H. Faulkner, A. Bendich, R.S. Parker, D.A. Roe, *Am. J. Clin. Nutr.* 56 (1992) 684.
- [5] L.A. Herraiz, W.C. Hsieh, R.S. Parker, J.E. Swanson, A. Bendich, D.A. Roe, *J. Am. Coll. Nutr.* 17 (1998) 617.
- [6] H.P.M. Gollnick, W. Hopfenmueller, C. Hemmes, S.C. Chun, C. Schmid, K. Kundermeier, H.K. Biesalski, *Eur. J. Dermatol.* 6 (1996) 200.
- [7] H.K. Biesalski, U.C. Obermuller-Jevic, *Arch. Biochem. Biophys.* 389 (2001) 1.
- [8] F. Bohm, R. Edge, L. Lange, T.G. Truscott, *J. Photochem. Photobiol. B* 44 (1998) 211.
- [9] M.G. Traber, J. Atkinson, *Free Radic. Biol. Med.* 43 (2007) 4.
- [10] P. Palozza, S. Moualla, N.I. Krinsky, *Free Radic. Biol. Med.* 13 (1992) 127.
- [11] P. Palozza, N.I. Krinsky, *Arch. Biochem. Biophys.* 297 (1992) 184.
- [12] A.P. De Leenheer, W.E. Lambert, in: H.J. Nelis (Ed.), *Modern Chromatographic Analysis of Vitamins*, second ed., Marcel Dekker Inc., NY, 1992.
- [13] M.R. Gasco, US Patent 5250236 (1993).
- [14] R.H. Müller, J.S. Lucks, EP 0605497 (1996).
- [15] R.H. Müller, *Adv. Drug Deliv. Rev.* 59 (2007) 375.
- [16] J.F. Pinto, R.H. Müller, *Pharmazie* 54 (1999) 506.
- [17] R. Cavalli, M.R. Gasco, P. Chetoni, S. Burchalassi, M.F. Saettone, *Int. J. Pharm.* 238 (2002) 241.
- [18] M.A. Videira, A.J. Almeida, M.F. Botelho, A.C. Santos, C. Gomes, J.J.P. De Lima, *Eur. J. Nucl. Med.* 26 (1999) 1168.
- [19] M. Sznitowska, M. Gajewska, S. Janicki, A. Radwanska, G. Lukowski, *Eur. J. Pharm. Biopharm.* 52 (2001) 159.
- [20] J. Jun-Pil, L. Soo-Jeong, P. Jeong-Sook, K. Chong-Kook, *Eur. J. Pharm. Biopharm.* 63 (2006) 134.
- [21] S.A. Wissing, R.H. Müller, *Int. J. Cosmet. Sci.* 23 (2001) 233.
- [22] S.A. Wissing, R.H. Müller, *J. Contr. Rel.* 81 (2002) 225.
- [23] A. Dingler, R.P. Blum, H. Niehus, R.H. Müller, S. Gohla, *J. Microencapsul.* 16 (1999) 751.
- [24] V. Jennings, S. Gohla, *J. Microencapsul.* 18 (2001) 149.
- [25] I.P. Kaur, M. Kapila, R. Agrawal, *Ageing Res. Rev.* 6 (2007) 271.

- [26] M. Uner, *Pharmazie* 61 (2006) 375.
- [27] S. Trombino, S. Serini, F. Di Nicuolo, L. Celleno, S. Andò, N. Picci, G. Calviello, P. Palozza, *J. Agric. Food Chem.* 52 (2004) 2411.
- [28] F.H. Lin, J.H. Lin, R.D. Gupta, J.A. Tournas, J.A. Burch, M.A. Selim, N.A. Monteiro-Riviere, J.M. Grichnik, J. Zielinski, R.S. Pinnel, *J. Invest. Dermatol.* 125 (2005) 826.
- [29] H. Taniguchi, E. Nomura, T. Tsuno, S. Minami, *Eur. Patent Appl.* (1998), 0681 825 A2.
- [30] M.A. Bernards, N.G. Lewis, *Phytochemistry* 31 (1992) 3409.
- [31] K. Kawanishi, J. Yasufuku, A. Ishikawa, Y. Ashimoto, *J. Agric. Food Chem.* 38 (1990) 105.
- [32] M.R. Gasco, *Pharm. Technol. Eur.* 9 (1997) 52.
- [33] D.E. Koppel, *J. Chem. Phys.* 57 (1972) 94814.
- [34] S.W. Provencher, *Comput. Phys. Commun.* 27 (1982) 213.
- [35] S.W. Provencher, *Comput. Phys. Commun.* 27 (1982) 229.
- [36] V.L. Tatum, C. Changoit, C.K. Chow, *Lipids* 25 (1990) 226.
- [37] T. Ohta, T. Nakano, Y. Egashira, H. Sanada, *Biosci. Biotechnol. Biochem.* 61 (1997) 1942.
- [38] M.M. Bradford, *Anal. Biochem.* 72 (1976) 248.
- [39] A.E. Hagerman, K.M. Riedl, G.A. Jones, K.N. Sovik, N.T. Ritchard, T.W. Hartzfeld, T.L. Riechel, *J. Agric. Food Chem.* 46 (1998) 1887.
- [40] R. Cassano, S. Trombino, R. Muzzalupo, L. Tavano, N. Picci, *Eur. J. Pharm. Biopharm.* 72 (2009) 232.
- [41] W. Mehnert, K. Mäder, *Adv. Drug Del. Rev.* 47 (2001) 165.